

REFERENCES

- Angeli, A. (1916) Synthesis of pyrrole blacks and relation to melanins. Gazzetta Chimica italiana, 46, 279.
- Aparecido, A.C. and Robert, G.R. (1996) A new method for extending the range of conductive polymer sensors for contact force. International Journal of Industrial Ergonomics, 17, 285-290.
- Blackwood, D. and Josowicz, M. (1991) Work function and spectroscopic studies of interactions between conducting polymers and organic vapors. Journal of Physical Chemistry, 95, 493-502.
- Blanc, J.P., Derouiche, N., Hadri, A. El., Germain, J.P., Maleysson, C., and Robert, H. (1990) Study of the action of gases on a polypyrrole film. Sensors and Actuators, B: Chemical, B41 (1-6), 130-133.
- Bocchi, V. and Gardini, G.P. (1986) Chemical synthesis of conducting polypyrrole and some composites. Journal of the Chemical Society Chemical Communications, 2, 148.
- Brédas, J.L., Scott, J.C., Yakushi, K., and Street, G.B. (1984) Polaron and bipolaron in polypyrrole: Evolution of the band structure and optical spectrum upon doping. Physical Review B, 30(2), 1023-1025.
- Briggs, D. (1998) Surface Analysis of Polymers by XPS and Static SIMS. 1st ed. (pp. 49-51). Cambridge: Cambridge University Press.
- Buncick M.C., Thomas, D.E., McKinny, K.S., and Jahan, M.S. (2000) Structural changes of ultra-high molecular weight polyethylene exposed to X-ray flux in X-ray photoelectron spectroscopy detected by valence band and electron spin resonance spectroscopy. Applied Surface Science, 156, 97-109.
- Campbell, D. and White, J.R. (1991) Polymer characterization. 2nd ed. (p. 163). Cambridge: Great Britain at the University Press.
- Cao, Y., Andreatta, A., Heeger, A.J., and Smith, P. (1989) Influence of chemical polymerization conditions on the properties of polyaniline. Polymer, 30, 2305-2311.

- Cao, Y., Smith, P., and Heeger, A.J. (1992) Counterion induced processibility of conducting polyaniline and of conducting polyblends of polyaniline in bulk polymers. Synthetic Metals, 48(1), 91-97.
- Cassignol, C., Olivier, P., and Ricard, A. (1998) Influence of the dopant of the polypyrrole moisture content: Effects on conductivity and thermal stability. Journal of Applied Polymer Science, 70, 1567- 1577.
- Chan, H.S.O., Munro, H.S., Davies, C., and Kang, E.T. (1988) XPS studies of chemically synthesized polypyrrole-halogen charge transfer complexes. Synthetic Metals, 22(4), 365-370.
- Chang, H.P. and Thomas, J.H. (1982) An XPS study of X-ray-induced dehydrochlorination of oxygen-free PVC. Journal of Electron Spectroscopy, 26, 203-212.
- Chiu, H.-T., Lin, S.-J., and Huang, C.-M. (1992) Influence of dopant permeability on electrochromic performance of polypyrrole films. Journal of Applied Electrochemistry, 22, 358.
- Chou, J. (2000) Hazardous gas monitors. 1st ed. New York: McGraw-Hill book company.
- Clarke, T.C., Scott, J.C., and Street, G.B. (1983) Magic angle spinning NMR of conducting polymers. IBM Journal of Research and Development, 27 (4), 331-320.
- Dall'Olio, A., Dascola Y., and Gardini, G.P. (1969) Comptes Rendus Hebdomadaires des Seances de l' Academie des Sciences, 267, 4336.
- Davidson, R.G., Hammond, L.C., Turner, T.G., and Wilson A.R. (1996) An electron and X-ray diffraction study of conducting polypyrrole/dodecyl sulfate. Synthetic Metals, 81(1), 1-4.
- Deng, Z., Stone, D. C., and Thompson, M. (1997) Characterization of polymer films of pyrrole derivatives for chemical sensing by cyclic voltammetry, X-ray photoelectron spectroscopy and vapour sorption studies. Analyst, 122, 1129-1138.
- Diaz, A.F. and Hall, B. (1983) Mechanical properties of electrochemically prepared polypyrrole films. IBM Journal of Research and Development, 27 (4), 342-347.

- Diaz, A.F., Kanazawa, K.K., Gardini, G.P. (1979) Electrochemical polymerisation of pyrrole. Journal of the Chemical Society Chemical Communications, 14, 635-636.
- Erlandsson, R., Inganas, O., Lundstrom, I., and Salaneck, W.R. (1985) XPS and electrical characterization of BF_4^- -doped polypyrrole exposed to oxygen and water. Synthetic Metals, 10(5), 303-318.
- Gassner, F., Graf, S., and Merz, A. (1997) On the physical properties of conducting poly(3,4-dimethoxypyrrole) films. Synthetic Metals, 87(1), 75-79.
- Geiss, R.H., Street, G.B., Volksen, W., and Economy, J. (1983) Polymer structure determination using electron diffraction techniques. IBM Journal of Research and Development, 27 (4), 321-329.
- Gulke, E. A. (1989). Solubility parameter values. In J. Brandrup, & E.H. Immergut (Eds.). Polymer handbook. 3rd ed., (pp. VII/519 – 559). USA: Wiley-Interscience publication.
- Gustafsson, G. and Lundström, I. (1987) The effect of ammonia on the physical properties of polypyrrole. Synthetic Metals, 21(2), 203-208.
- Gustafsson, G., Lundström, I., Liedberg, B., Wu, C. R., Inganäs, O., and Wennerström, O. (1989) The interaction between ammonia and poly(pyrrole). Synthetic Metals, 31(2), 163-179.
- Gomez, G.T. and Romero, P.G. (1998) Conducting organic polymers with electroactive dopants. Synthesis and electrochemical properties of hexacyanoferrate-doped PPy (PPy/HCF). Synthetic Metals, 98(2), 95-102.
- Hanawa, T., Kuwabata, S., and Yoneyama, H. (1988) Gas sensitivity of polypyrrole films to NO_2 . Journal of The Chemical Society-Faraday Transactions I, 84 (5), 1587-1592.
- Hanawa, T. and Yoneyama, H. (1989) Gas sensitivities of polypyrrole films doped chemically in the gas phase. Synthetic Metals, 30(3), 341-350.
- Harris, D. P., Arnold, M.W., Andrews, K.M., and Partridge, C.A. (1997) Resistance characteristics of conducting polymer films used in gas sensors. Sensor and Actuators, B: Chemical, B42, 177-184.

- Heeger, A.J. and MacDiarmid, A.G. (1980) In L. Alcacer (ed), The physics and chemistry of low dimensional solids (pp. 353-391). Boston: D. Reidel Pub. Co.
- Hodgins, D. (1995) The development of an electronic 'nose' for industrial and environmental applications. Sensors and Actuators, B: Chemical, B26-27, 255-258.
- <http://www.crowcon.com>
- <http://www.nlectc.org/assistance/edx/html>
- Hwang, B.J., Yang, J.Y., and Lin C.W. (1999) A microscopic gas-sensing model for ethanol sensors based on conductive polymer composites from polypyrrole and poly(ethylene oxide). Journal of the Electrochemical Society, 146(3), 1231-1236.
- Josowicz, M., Janata, J., Ashley, K., and Pons, S. (1987) Electrochemical and ultraviolet visible spectroelectrochemical investigation of selectivity of potentiometric gas sensors based on polypyrrole. Analytical Chemistry, 59 (2), 253-258.
- Kanazawa, K.K., Diaz, A.F., Gill, W.D., Grant, P.M., Street, G. B., Gardini, G.P., and Kwak, J.F. (1979/1980) Polypyrrole: An electrochemically synthesized conducting organic polymer. Synthetic Metals, 1(3), 329-336.
- Kang, E.T., Neoh, K.G., Ong, Y.K., Tan, K.L., and Tan, B.T.G. (1990) XPS studies of proton modification and some anion exchange processes in polypyrrole. Synthetic Metals, 39(1), 69-80.
- Kang, E.T., Neoh, K.G., Ong, Y.K., Tan, K.L., and Tan, B.T.G. (1991) X-ray photoelectron spectroscopic studies of polypyrrole synthesized with oxidative Fe(III) salts. Macromolecules, 24, 2822-2828.
- Kang, H.C. and Geckeler, K.E. (2000) Enhanced Electrical Conductivity of Polypyrrole Prepared by Chemical Oxidative Polymerization: Effect of the Preparation Technique and Polymer Additive. Polymer, 41, 6931-6934.
- Khatua, S. and Hsieh, Y. (1997) Chlorine Degradation of Polyether-Based Polyurethane. Journal of Polymer Science Part A-Polymer Chemistry, 35, 3263-3273.

- Langmaier, J. and Janata, J. (1991) Organic semiconductors as selective layers for work function gas sensors. Polymeric Material Science and Engineering, Proceedings of the ACS Division of Polymeric Materials Science and Engineering, 64, 285.
- Liang, W., Lei, J., and Martin, C.R. (1992) Effect of synthesis temperature on the structure, doping level and charge-transport properties of polypyrrole. Synthetic Metals, 52(2), 227-239.
- Lim, V.W.L., Li, S., Kang, E.T., Neoh, K.G., and Tan, K.L. (1999) In situ XPS study of thermally deposited aluminium on chemically synthesized polypyrrole films. Synthetic Metals, 106(1), 1-11.
- Lin C.W., Hwang, B.J., and Lee, C.R. (1999) Sensing behaviors of the electrochemically co-deposited polypyrrole-poly(vinyl alcohol) thin film exposed to ammonia gas. Materials Chemistry and Physics, 58 (2), 114-120.
- Lin C.W., Yang, J.Y., Hwang, B.J., and Chin, J. (1999) Methanol sensors based on conductive polymer composites from polypyrrole and poly(ethylene oxide)-sensing properties (I). Journal of Chinese Institute of Chemical Engineers, 30 (6), 449-456.
- Lindsey, S.E. and Street, G.B. (1984) Conductive composites from polyvinyl-alcohol and polypyrrole. Synthetic Metals, 10(1), 67-69.
- Loughlin, C. (1993). Sensor for industrial inspection. 1st ed. West Yorkshire, U.K.: Ilkley.
- Malitesta, C. Losito, I. Sabbatini, L., and Zambonin, P. G. (1995) New findings on polypyrrole chemical structure by XPS coupled to chemical derivatization labelling. Journal of Electron Spectroscopy and Related Phenomena, 76, 629-634.
- Mathys, G.I. and Truong, V.-T. (1997) Spectroscopic Study of Thermo-Oxidative Degradation of Polypyrrole Powder by FT-IR. Synthetic Metals, 89(2), 103-109.
- Miasik, J. J., Hooper, A., and Tofield, B.C. (1986) Conducting polymer gas sensors. Journal Of The Chemical Society-Faraday Transactions I, 82(4), 1117.
- Milella, E., Musio, F., and Alba, B.M. (1996) Polypyrrole LB multilayer sensitive films for odorants. Thin Solid Films, 284-285, 908-910.

- Musio, F. and Ferrara, M.C., (1997) Low frequency a.c. response of polypyrrole gas sensors. Sensors and Actuators, B: Chemical, B41 (1-3), 97-103.
- Nigorikawa, K., Kunugi, Y., Harima, Y., and Yamashita, K. (1995) A selective gas sensor using a polypyrrole thin-film as a sensitive matrix on a piezoelectric crystal. Journal of Electroanalytical Chemistry, 396 (1-2), 563-567.
- Okuzaki, H., Kondo, T., and Kunugi, T. (1997) A polypyrrole rotor driven by sorption of water vapour. Polymer, 38, 5491-5492.
- Okuzaki, H., Kondo, T., and Kunugi, T. (1999) Characteristics of water in polypyrrole films. Polymer, 40, 995-1000.
- Omastová, M., Košina, S., Pionteck, J., Andreas, J., and Pavlinec, J. (1996) Electrical properties and stability of polypyrrole containing conducting polymer composites. Synthetic Metals, 81, 49-57.
- Partridge, A.C., Harris, P., and Andrews, M.K. (1996) High sensitivity conducting polymer sensors. Analyst, 121, 1349-1359.
- Philip, N.B. and Sim, K.L. (1989) Conducting polymer gas sensors. Part II: Response of polypyrrole to methanol vapour. Sensors and Actuators, 19, 141-150.
- Pijolat, C., Pupier, C., Sauvan, M., Tournier, G., and Lalauze, R. (1999) Gas detection for automotive pollution control. Sensors and Actuators, B: Chemical, B 59, 195-202.
- Pouchert, C. J. (1997) The Aldrich library of FT-IR spectra. 2nd ed., Milwaukee, Wisconsin: Aldrich.
- Prissanaroon, W., Ruangchuay, L., Sirivat, A., and Schwank, J. (2000) Electrical conductivity response of dodecylbenzene sulfonic acid-doped polypyrrole films to SO₂-N₂ mixtures. Synthetic Metals, 114(1), 65-72.
- Rodríguez, J., Grande, H.-J., and Otero, T.F.(1997) Polypyrroles: From basic research to technological applications. In H.S. Nalwa (Ed) Organic conductive molecules and polymers. Vol. 2, 1st ed. (p. 415). England: John Wiley & Sons.
- Rosner, R.B. and Rubner, M.F. (1994) Solid-state polymerization of pyrrole within a Langmuir-Blodgett film of ferric stearate. Chemistry of Materials, 6 (5), 581-586.

- Salaneck, W.R., Lundstrom, I., and Ranby, B. (1993) Conjugated polymers and related materials. 1st ed., New York: Oxford University Press.
- Seader, J.D., Siirola, J.J., and Barnicki, S.D. (1998). Distillation. In R. H. Perry and D. W. Green (Eds.). Perry's chemical engineering's handbook. 7th ed. (p 13-21) Australia: McGraw-Hill.
- Selampinar, F., Toppare, L., Akbulut, U., Yalcin, T., and Suzer, S. (1995) A conducting composite of polypyrrole II As a gas sensor. Synthetic Metals, 68(2), 109-116.
- Shen, Y.Q. and Wan, M.X. (1997) Soluble conductive polypyrrole synthesized by in situ doping with β -naphthalene sulphonic acid. Journal of Polymer Science Part A-Polymer Chemistry, 35, 3689-3695.
- Shen, Y.Q. and Wan, M.X. (1998) In situ doping polymerization of pyrrole with sulfonic acid as a dopant. Synthetic Metals, 96(2), 127-132.
- Shirakawa, H., Zhang, Y.-X., Okuda, T., Sakamaki, K., and Akagi, K. (1994) Various factors affecting the synthesis of highly conducting polyacetylene. Synthetic Metals, 65(2-3), 93-101.
- Slater, J.M. and Watt, E.J. (1992) Piezoelectric and conductivity measurements of poly(pyrrole) gas interactions. Analytical Proceedings, 29, 53-56.
- Sun, Y. and Ruckenstein, E. (1996) Surface conductive films via polymerization on a liquid surface. Synthetic Metals, 82(1), 35-40.
- Tezuka, Y., Aoki, K. and Shinozaki, K. (1989) Kinetics of oxidation of polypyrrole-coated transparent electrodes by in situ linear sweep voltammetry and spectroscopy. Synthetic Metals, 30(3), 369-379.
- Tian, B. and Zerbi, G. (1990) Lattice Dynamics and Vibrational Spectra of Pristine and Doped Polypyrrole: Effective Conjugation Coordinate. Journal of Chemical Physics, 92(6), 3886-3891.
- Topart, P. and Josowicz, M. (1992) Characterization of the interaction between polypyrrole films and methanol vapor. Journal of Physical Chemistry, 96(19), 7824-7830.
- Toshima, N. and Ihata, O. (1996) Catalytic Synthesis of Conductive Polypyrrole Using Iron (III) Catalyst & Molecular Oxygen. Synthetic Metals, 79(2), 165-172.

- Truong, V.T., Ennis, B.C., and Forsyth, M. (1995) Enhanced thermal properties and morphology of ion-exchanged polypyrrole films. Polymer, 36(10), 1933-1940.
- Truong, V.T., Ennis, B.C., Terrence, T.G., and Jenden, C.M. (1992) Thermal stability of polypyrroles. Polymer International, 27, 187-195.
- Wagner, C.D. (1989) NIST X-ray photoelectron spectroscopy database 1.0. USA: National Institute of Standards and Technology.
- Wang, Z.H., Jawadi, H.H.S., Ray, A., MacDiarmid, A.G., and Epstein, A.J. (1990) Electron localization in polyaniline derivatives. Physical Review B: Condensed Matter, 42, 5411-5414.
- Weast, R.C. and Astle, J. (Eds.). (1978) Handbook of Chemistry and Physics. 59th ed. (p F-255) Boca Raton, FL: CRC Press.
- Wernet, W., Monkenbusch, M., and Wegner, G. (1984) A new series of conducting polymers with layered structure: Polypyrrole N-alkylsulfates and N-alkylsulfonates. Makromolekulare Chemie-Rapid Communications, 5(3), 157-164.
- Yamaura, M., Hagiwara, T., and Iwata, K. (1988) Enhancement of electrical conductivity of poly-pyrrole film by stretching - counter ion effect. Synthetic Metals, 26(3), 209-224.
- Zaid ,B., Aeiyaeh, S., and Lacaze, P.C. (1994) Electropolymerization of pyrrole in propylene carbonate on zinc electrodes modified by heteropolyanions. Synthetic Metals, 65(1), 27-34.
- Zotti, G. (1997) Electrochemical synthesis of polyheterocycles and their applications. In H.S. Nalwa (Ed) Organic conductive molecules and polymers. Vol. 2, 1st ed. (p. 415) England: John Wiley & Sons.
- Zotti, G. and Schiavon, G. (1989) Spectroelectrochemical determination of polarons in polypyrrole and polyaniline. Synthetic Metals, 30, 151-158.

APPENDICES

Appendix A Polymerization Mechanism and Yield of PPy

There are two main synthesis methods for PPy: electrochemical and chemical polymerization. The advantages of the chemical polymerization are capability of mass production and low cost; whereas one of its disadvantages is a low conductivity of product. In this dissertation, the chemical polymerization was selected. Figure A1 shows scheme for coupling of Py to PPy. This corresponds to the relationship between amount of oxidant (APS) used and yield observed in our laboratory, as shown in Figure A2. The higher amount of oxidant, the higher yield obtained. Even though it provided the lowest yield, a APS:Py ratio of 1:5 was selected through out this work due to the high conductivity of PPy obtained (see Figure A3).

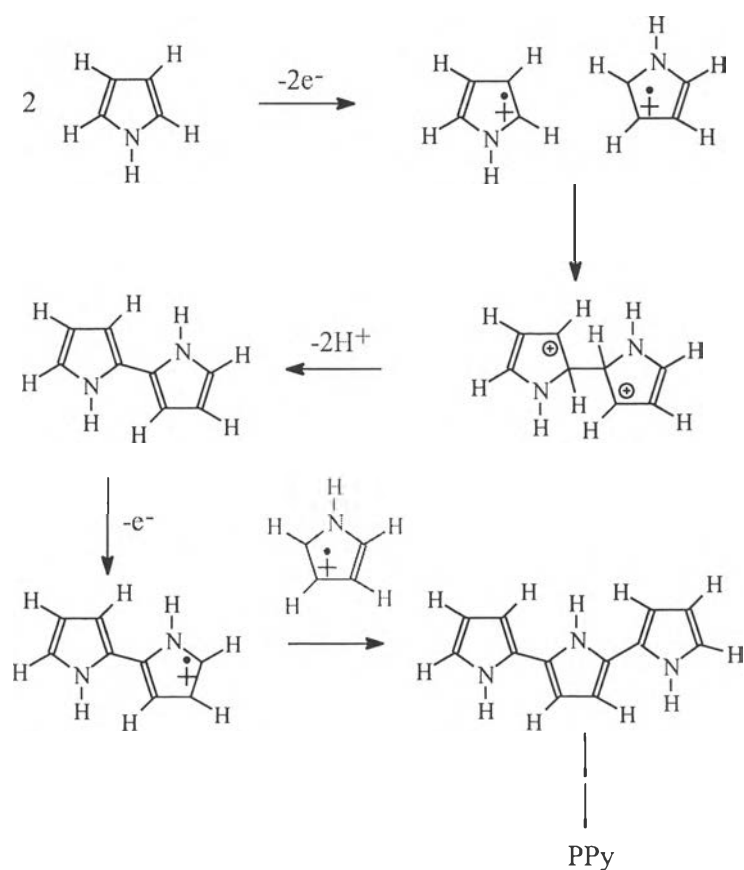


Figure A1 Oxidative coupling polymerization of Py to PPy (Zotti, 1997).

An optimum synthesis temperature of PPy was 0 – 5 °C in aqueous solution of ferric salts (Bocchi and Gardini, 1986). It was 0 °C for PPy/HCF (Gómez and Romero, 1998) but with a lessened yield as compared to high temperature synthesis. A study on chemical polymerization conditions of polyaniline (Cao *et al.*, 1989) indicated its optimum synthesis temperature of 0 –5 °C and claimed the precipitation of polyaniline at –10 °C. The proper low temperature seems to lower the reaction rate, resulting in less branching and enhanced conductivity. In this dissertation, the synthesis temperature was kept at 0 ± 0.5 °C. High APS:Py ratios could induce high reaction rate and hence low conductive PPy. Moreover, temperature was difficult to control during adding the concentrated APS solution.

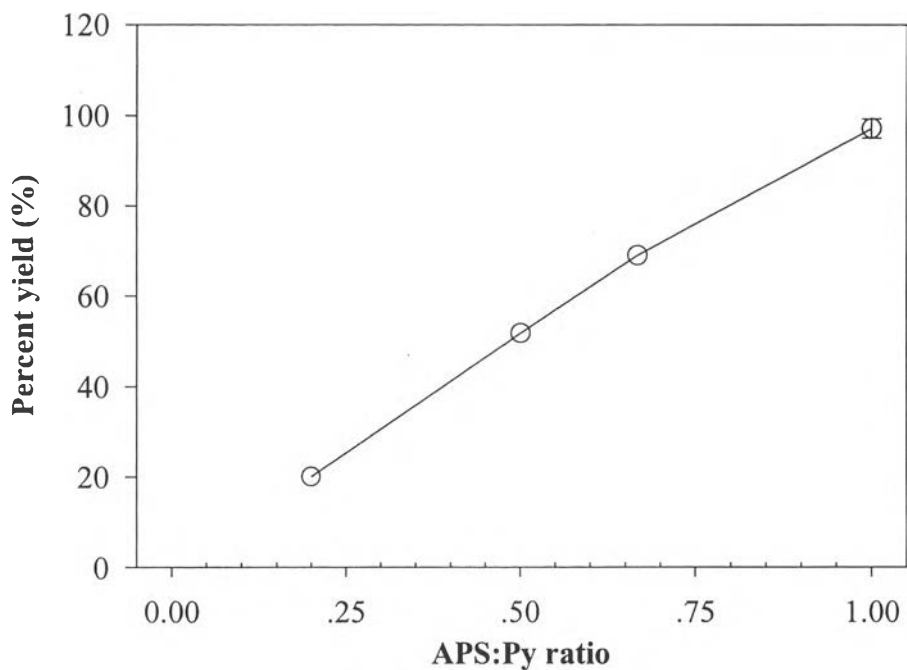


Figure A2 Effect of oxidant (APS):Py ratio on percent yield (normalized with the weight of loaded Py monomer).

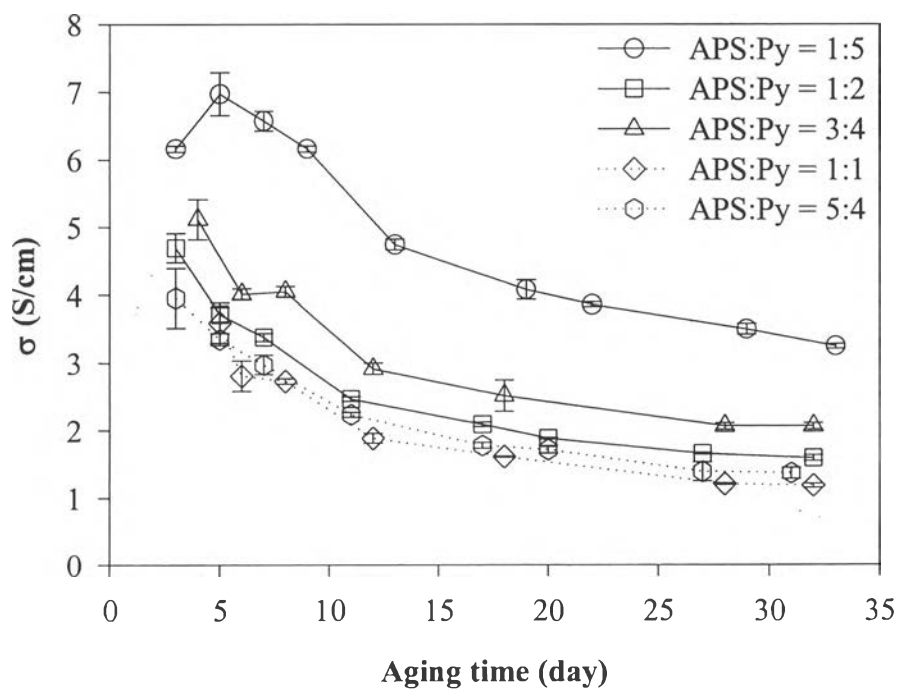


Figure A3 Effect of APS:Py ratio on conductivity and aging time.

Appendix B Determination of the Molecular Structure of Undoped and Doped PPy from an Elemental Analysis and a Thermogravimetric Analysis

Raw data obtained from the elemental analysis were weight percentages of N, C, S, and H whereas the data from the thermogravimetric analysis was weight percentage of water content which can be identified as the weight loss when sample was heated at 100 – 150 °C. These data were used to determine molecular structures of undoped and doped PPy under some assumptions as follows:

B.1 Undoped PPy

In the matrix of undoped PPy, there were not only PPy itself, but also water and co-dopants: HSO_4^- and SO_4^{2-} [1,2]. However, there has been no report indicating the proportion of these two species. The oxidation states of S atoms in these two species are the same, making distinguishing between the two states by XPS an impossible task. To simplify the calculation, we assume that the ratio of HSO_4^- : SO_4^{2-} is 1:1.

$$\begin{aligned} \text{Number of N atom} &= \text{weight percentage of N} / 14 \\ &= \text{N in Py ring} \end{aligned} \quad \text{.....(B.1)}$$

$$\begin{aligned} \text{Number of C atom} &= \text{weight percentage of C} / 12 \\ &= \text{C in Py ring} \end{aligned} \quad \text{.....(B.2)}$$

$$\begin{aligned} \text{Number of S atom} &= \text{weight percentage of S} / 32 \\ &= \text{S in } \text{HSO}_4^- + \text{S in } \text{SO}_4^{2-} \\ &= 2 \times \text{S in } \text{HSO}_4^- \end{aligned} \quad \text{.....(B.3)}$$

$$\begin{aligned} \text{Number of H atom} &= \text{weight percentage of H} / 1 \\ &= \text{H in Py ring} + \text{H in } \text{H}_2\text{O} + \text{H in } \text{HSO}_4^- \\ &= \text{H in Py ring} + 1/(2+16) \times \% \text{H}_2\text{O (from TGA)} + \text{S in } \text{HSO}_4^- \end{aligned} \quad \text{.....(B.4)}$$

$$\begin{aligned}
\text{Number of O atom} &= (100 - \text{weight percentage of N, C, S, H}) / 16 \\
&= \text{O in Py ring} + \text{O in H}_2\text{O} + \text{O in HSO}_4^- + \text{O in SO}_4^{2-} \\
&= \text{O in Py ring} + 16/(2+16) \times \% \text{H}_2\text{O (from TGA)} \\
&\quad + 4 \times \text{S in HSO}_4^- + 4 \times \text{S in SO}_4^{2-} \quad \dots\dots(\text{B.5})
\end{aligned}$$

Then, the calculated data were normalized with the number of N. The chemical structure of undoped PPy is shown in Table B1 along with the theoretical value without co-dopants. The theoretical value of H:N is 3.0. The excess amount is attributed to the presence of the saturated pyrrolidine rings which have H:N as high as 7:1 (Street *et al.*, 1982). Number of O existing in Py ring is attributed to C-O, C-OH, and C=O groups arising during polymerization and storage (Kang *et al.*, 1991).

B.2 Doped PPy

In doped PPy, there were: PPy itself; fed dopant, e.g. $\text{C}_{10}\text{H}_7\text{SO}_3^-$; water content; and co-dopants, HSO_4^- and SO_4^{2-} (Cassignol *et al.*, 1998 and Prissanaroon *et al.*, 2000). The assumptions used for calculation of chemical structures are: 1) $\text{HSO}_4^- : \text{SO}_4^{2-}$ is 1:1; and 2) C:N of Py ring is perfectly 4.0. The excess amount is attributed to the presence of dopant molecules. The following equations are for naphthalene sulfonate doped PPy.

$$\text{Number of N atom} = \text{N in Py ring} \quad \dots\dots(\text{B.6})$$

$$\begin{aligned}
\text{Number of C atom} &= \text{C in Py ring} + \text{C in Dopant} \\
&= 4 \times \text{N in Py ring} + \text{C in Dopant} \quad \dots\dots(\text{B.7})
\end{aligned}$$

$$\begin{aligned}
\text{Number of S atom} &= \text{S in dopant} + \text{S in HSO}_4^- \\
&= 1/10 \times \text{C in dopant} + \text{S in HSO}_4^- \quad \dots\dots(\text{B.8})
\end{aligned}$$

$$\begin{aligned}
\text{Number of H atom} &= \text{H in Py ring} + \text{H in dopant} + \text{H in H}_2\text{O} + \text{H in HSO}_4^- \\
&= \text{H in Py ring} + 7/10 \times \text{C in dopant} \\
&\quad + 1/(2+16) \times \% \text{H}_2\text{O (from TGA)} + \text{S in HSO}_4^- \quad \dots\dots(\text{B.9})
\end{aligned}$$

$$\begin{aligned}\text{Number of O atom} &= \text{O in Py ring} + \text{O in dopant} + \text{O in H}_2\text{O} + \text{O in HSO}_4^- \\ &= \text{O in Py ring} + 3/10 \times \text{C in dopant} \\ &\quad + 16/(2+16) \times \% \text{H}_2\text{O (from TGA)} + 4 \times \text{S in HSO}_4^- \dots (\text{B.10})\end{aligned}$$

For PPy doped with other dopants, the correlation between the numbers of S, H, and O to that of C in dopants is considered from particular dopant molecular structures. The calculated chemical structures of PPy/A and PPy/B with different dopant to monomer molar ratios are shown in Table B1.

Table B.1 Experimental data and calculated data for chemical structure determination from EA and TGA of PPy/U, PPy/A, and PPy/B with various D/M ratios

Material	D/M	Data from EA				Data from TGA	Chemical structure	Proportion of pyrrolidine ring	S/N
		%C	%H	%N	%S	% H ₂ O			
Ideal PPy	-	-	-	-	-	-	(C _{4.00} H _{3.00} N _{1.00})	-	-
PPy/U	0	27.76	4.66	11.81	2.98	4.86	(C _{2.74} H _{4.83} N _{1.00}) (HSO ₄ ⁻) _{0.06} (SO ₄ ²⁻) _{0.06} (H ₂ O) _{0.32}	0.46	0.11
PPy/U	0	36.42	4.32	12.48	3.01	4.86	(C _{3.40} H _{4.19} N _{1.00}) (HSO ₄ ⁻) _{0.05} (SO ₄ ²⁻) _{0.05} (H ₂ O) _{0.30}	0.30	0.11
PPy/A	1/12	59.61	5.06	12.40	6.93	3.95	(C _{4.00} H _{4.05} N _{1.00}) (HSO ₄ ⁻) _{0.04} (SO ₄ ²⁻) _{0.04} (C ₁₀ H ₇ SO ₃) _{0.16} (H ₂ O) _{0.45}	0.26	0.24
PPy/A	2/3	62.09	5.08	11.77	6.91	2.55	(C _{4.00} H _{4.18} N _{1.00}) (HSO ₄ ⁻) _{0.02} (SO ₄ ²⁻) _{0.02} (C ₁₀ H ₇ SO ₃) _{0.22} (H ₂ O) _{0.36}	0.29	0.26
PPy/B	1/24	57.72	4.87	13.20	6.51	4.49	(C _{4.00} H _{3.81} N _{1.00}) (HSO ₄ ⁻) _{0.05} (SO ₄ ²⁻) _{0.05} (C ₁₀ H ₇ SO ₃) _{0.11} (H ₂ O) _{0.20}	0.20	0.22
PPy/B	1/12	59.76	5.05	11.71	7.05	3.05	(C _{4.00} H _{4.23} N _{1.00}) (HSO ₄ ⁻) _{0.03} (SO ₄ ²⁻) _{0.03} (C ₁₀ H ₇ SO ₃) _{0.20} (H ₂ O) _{0.22}	0.31	0.26
PPy/B	1/12	58.91	5.10	11.80	7.06	3.05	(C _{4.00} H _{4.33} N _{1.00}) (HSO ₄ ⁻) _{0.04} (SO ₄ ²⁻) _{0.04} (C ₁₀ H ₇ SO ₃) _{0.18} (H ₂ O) _{0.18}	0.33	0.26
PPy/B	1/6	60.29	5.00	12.44	7.00	3.47	(C _{4.00} H _{3.99} N _{1.00}) (HSO ₄ ⁻) _{0.04} (SO ₄ ²⁻) _{0.04} (C ₁₀ H ₇ SO ₃) _{0.17} (H ₂ O) _{0.19}	0.25	0.25
PPy/B	1/2	61.82	5.12	10.70	7.50	2.61	(C _{4.00} H _{4.39} N _{1.00}) (HSO ₄ ⁻) _{0.02} (SO ₄ ²⁻) _{0.02} (C ₁₀ H ₇ SO ₃) _{0.27} (H ₂ O) _{0.10}	0.35	0.31
PPy/B	2/3	60.62	4.45	10.08	6.77	1.34	(C _{4.00} H _{3.87} N _{1.00}) (HSO ₄ ⁻) _{0.00} (SO ₄ ²⁻) _{0.00} (C ₁₀ H ₇ SO ₃) _{0.30} (H ₂ O) _{0.17}	0.22	0.29
PPy/B	2/3	62.85	4.99	11.49	7.38	2.56	(C _{4.00} H _{4.04} N _{1.00}) (HSO ₄ ⁻) _{0.02} (SO ₄ ²⁻) _{0.02} (C ₁₀ H ₇ SO ₃) _{0.24} (H ₂ O) _{0.09}	0.26	0.28
PPy/B	1/1	64.81	5.36	11.70	7.78	2.91	(C _{4.00} H _{4.28} N _{1.00}) (HSO ₄ ⁻) _{0.02} (SO ₄ ²⁻) _{0.02} (C ₁₀ H ₇ SO ₃) _{0.25} (H ₂ O) _{0.19}	0.32	0.29

Appendix C Determination of the Functional Groups in PPy by a Fourier transform Infrared Spectroscopy

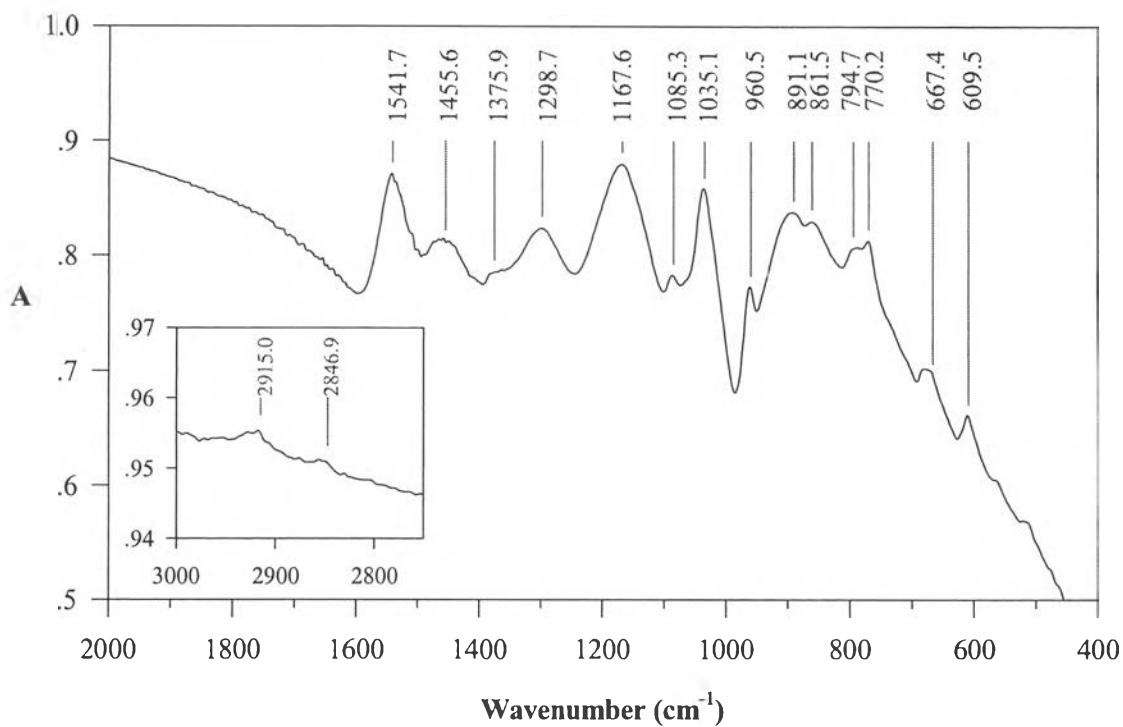


Figure C1 FT-IR spectrum of PPy/A at D/M of 1/12 with peak positions.

Table C1 Peak positions in FT-IR spectra of PPy/De, PPy/U, and PPy doped with various dopants (excluding data of PPy/A which are shown in Table C2).

Material Assignment	Ref	PPy/De	PPy/U (1)	PPy/U (2)	PPy/B	PPy/C	PPy/D (1)	PPy/D (2)	PPy/E (1)	PPy/E (2)	PPy/P (1)	PPy/P (2)	PPy/AB
ν N-H [†]	3527	-	-	-	-	-	-	-	-	-	-	-	-
ν_{as} CH ₂ [§]	2917	-	2918	-	2923	2919	2913	-	-	-	-	-	-
ν_{as} CH ₂ ^κ	2954	-	2918	-	2923	2919	2913	-	-	-	-	-	-
ν_s CH ₂ [§]	2851	2847	2857	2846	-	-	2847	2847	-	-	-	-	-
ν_s CH ₂ ^κ	2852	2847	2857	2846	-	-	2847	2847	-	-	-	-	-
C=O ^φ	1720	-	-	-	-	-	-	-	-	-	-	-	1701
ν C=C [#]	1550	1562	1545	1542	1542	1543	1549	1549	1549	1542	1542	1542	1561
ν C=C [†]	1546	1562	1545	1542	1542	1543	1549	1549	1549	1542	1542	1542	1561
ν C=C [#]	1480	1481	1468	1457	-	1459	1482	1475	1459	1457	1459	1458	1482
ν C=C [†]	1470	1481	1468	1457	-	1459	1482	1475	1459	1457	1459	1458	1482
N/A	-	-	-	-	1448	1450	-	1449	-	-	-	-	-
ν C-C & C-N [†]	1391	1393	-	-	-	-	-	-	-	-	-	-	-
ν C-N [#]	1380	-	-	-	-	-	1380	-	-	-	-	-	-
N/A	-	1362	1357	1353	-	-	-	1371	-	1356	-	-	1368
Deformation vib. [#]	1300	-	-	-	-	-	-	-	-	-	-	-	-
C-H&N-H def. [†]	1295	1297	1293	1280	1298	1294	1282	1282	1296	1286	1295	1291	-
ν C-C ^ε	1290	1297	1293	1280	1298	1294	1282	1282	1296	1286	1295	1291	-
C-H&N-H def. [†]	1242	1241	-	-	-	-	-	-	-	-	-	-	-
ν C-N ^ε	1190	1199	-	-	-	-	1206	1205	-	-	-	-	-
ν S=O ^ψ	1180	-	1174	-	-	1170	1171	1178	1178	-	1175	-	-
ν of Py ring ^ε	1167	-	-	1166	1165	-	-	1161	-	1169	-	1164	-
ν C-C & C-N [†]	1148	-	-	-	-	-	-	-	-	-	-	-	-
N/A	-	-	-	-	-	-	1120	1119	-	1126	-	-	1111
N/A	-	1091	1095	1085	-	-	-	-	-	1104	-	-	-
C-H def. [†]	1050	-	-	-	-	-	-	-	-	-	-	-	-
ν of Py ring ^ε	1045	1040	1037	1032	1034	1037	1035	1031	1039	1034	1037	1034	1045
in-plane N-H [‡]	1029	1040	1037	1032	1034	1037	1035	1031	1039	1034	1037	1034	1045
ν of Py ring ^ε	968	954	962	960	-	963	-	951	963	960	962	959	964
ν of Py ring ^ε	922	925	-	-	-	-	-	-	-	-	-	-	922
out-of-plane C-H [‡]	908	-	898	887	885	890	909	908	-	896	889	883	-
N/A	-	-	-	856	860	-	865	864	-	859	-	-	792
out-of-plane C-H [‡]	767	779	782	771	-	779	785	780	783	777	775	773	-
-SO ₃ ⁻ group ^λ	670	-	-	669	-	-	-	662	-	668	-	660	-
ν S-O ^ω	620	-	-	597	-	615	-	579	616	615	615	612	617

[†] Tian and Zerbi, 1990

[‡] Zaid *et al.*, 1994

[§] Rosner and Rubner, 1994

[#] Toshima and Ihata, 1996

^κ Khatua and Hsieh, 1997

^λ Weast and Astle, 1978

^ε Kang and Geckeler, 2000

^ε Shen *et al.*, 1998

^φ Mathys and Truong, 1997

^ψ Gassner *et al.*, 1997

^ω Pouchert, 1997

Table C2 Peak positions in FT-IR spectra of PPy/A at various D/M ratios.

Assignment \ D/M	Ref	1/96	1/12 (1)	1/12 (2)	1/12 (3)	1/12 (4)	1/6	1/3	1/2	1/1
ν N-H [†]	3527	-	-	-	-	-	-	-	-	-
ν_{as} CH ₂ [§]	2917	2907	2916	-	2909	2915	-	-	-	-
ν_{as} CH ₂ ^κ	2954									
ν_s CH ₂ [§]	2851	-	-	-	2840	2847	-	-	-	-
ν_s CH ₂ ^κ	2852									
ν C=C [#]	1550	1534	1543	1544	1542	1542	1540	1542	1543	1543
ν C=C [†]	1546									
ν C=C [#]	1480	1450	1454	1460	1447	1456	1450	1454	1454	1454
ν C=C [†]	1470									
ν C-N [#]	1380	1359	1364	-	1361	1375	1362	1369	1372	1362
Deformation vib. [#]	1300	1285	1300	1302	1292	1299	1294	1294	1291	1296
C-H&N-H def. [†]	1295									
ν C-C ^ε	1290									
ν of Py ring ^ε	1167	1155	1162	1164	1150	1168	1161	1169	1166	1166
N/A	-	1079	1085	1087	1084	1085	1085	1085	1084	1084
ν of Py ring ^ε	1045	1026	1031	1033	1030	1035	1034	1036	1035	1036
in-plane N-H [†]	1029									
ν of Py ring ^ε	968	959	960	961	959	961	961	962	961	962
out-of-plane C-H [†]	908	877	885	885	877	891	885	898	900	898
N/A	-	844	856	856	834	862	830	862	862	860
N/A	-	-	787	788	784	795	786	793	788	791
out-of-plane C-H [†]	767	764	-	-	768	770	769	772	770	772
-SO ₃ ⁻ group ^λ	670	665	669	-	667	668	675	682	680	680
ν S-O ^ω	620	601	614	617	603	610	608	611	610	610

Appendix D Determination of the water content and degradation temperature of PPy by a Thermogravimetric Analysis

In thermogravimetric analysis (TGA), a weight of 2-4 mg per sample is measured as a function of increasing temperature with a constant heating rate under N_2 atmosphere. The decrease in weight when the temperature is raised to 150 °C can be defined as the loss of small volatile molecules, which is mainly water. At higher temperature where the weight sharply declines, main chain degradation occurred. An on-set of degradation temperature is defined here as the temperature at which the sample starts to loss its weight at the rate (derivative) of $-0.5 \%Wt./^{\circ}C$. This transition has to cause more than a 50 %Wt. decrease. Thermogram of PPy/B at D/M of 1/12 is shown in Figure D1 with its derivative and labels of the described transitions. Water contents and an on-set of degradation temperatures of starting materials, PPy/De, PPy/U, and PPy doped with various dopants at D/M ratio of 1/12 are shown in Table D1 and D2, respectively. Water contents of PPy/A at various D/M ratios are shown in Table D3.

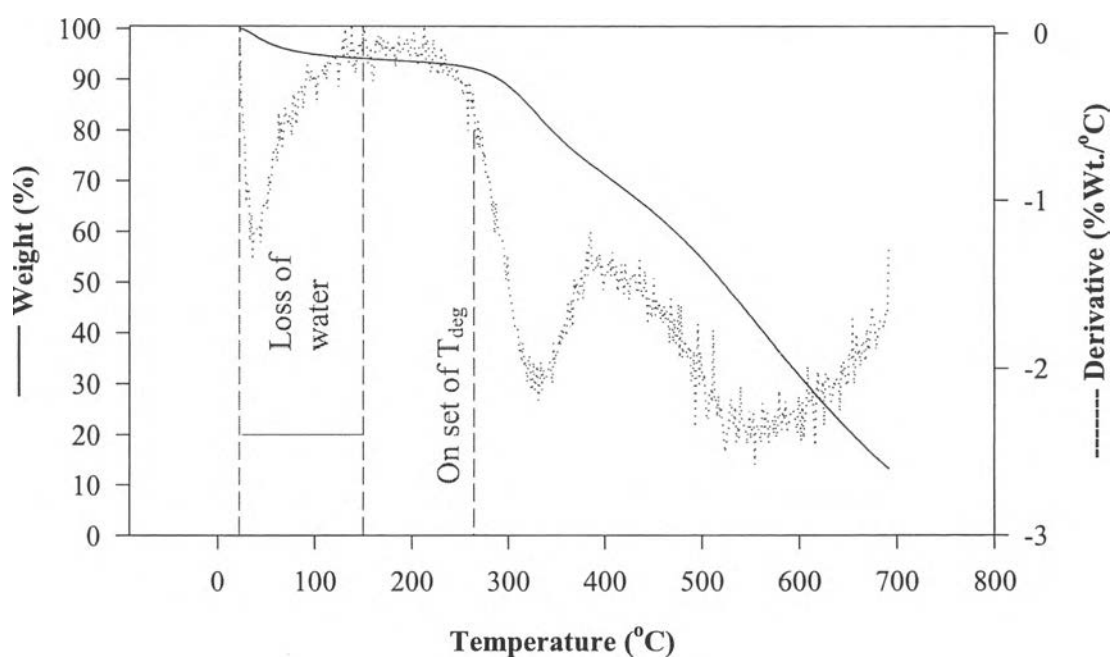


Figure D1 Thermogram of PPy/B at D/M of 1/12 with its derivative.

Table D1 Water content in starting materials and PPy/De, PPy/U, and PPy doped with various dopants at D/M ratio of 1/12.

Material \ Run #	Water content (%)								Average	SD
	1	2	3	4	5	6	7			
APS	2.3	-	-	-	-	-	-	-	2.33	-
α -NSA	3.2	-	-	-	-	-	-	-	3.3	-
β -NSA	0.3	-	-	-	-	-	-	-	0.3	-
CSA	4.1	-	-	-	-	-	-	-	4.1	-
DBSA	3.2	-	-	-	-	-	-	-	3.2	-
<i>p</i> -Aminobenzoate	0.7	-	-	-	-	-	-	-	0.7	-
PPy/De	10.1	-	-	-	-	-	-	-	10.1	-
PPy/U	5.2	4.1	5.1	4.5	4.8	5.0	5.4	4.9	0.4	
PPy/A	3.9	4.0	-	-	-	-	-	3.9	0.1	
PPy/B	3.3	2.7	2.9	2.8	2.6	3.4	3.5	3.0	0.4	
PPy/C	4.4	6.1	3.8	-	-	-	-	4.8	1.2	
PPy/D	0.9	0.8	1.0	-	-	-	-	0.9	0.1	
PPy/E	4.9	6.2	5.8	-	-	-	-	5.6	0.7	
PPy/P	5.4	5.4	-	-	-	-	-	5.4	0.0	
PPy/AB	5.1	5.3	3.4	-	-	-	-	4.6	1.0	

Table D2 On-set of degradation temperature of starting materials and PPy/De, PPy/U, and PPy doped with various dopants at D/M ratio of 1/12.

Material \ Run #	On-set of degradation temperature (°C)						
	1	2	3	4	5	Average	SD
α -NSA	459.0	-	-	-	-	459.0	-
β -NSA	526.4	-	-	-	-	526.4	-
CSA	196.3	-	-	-	-	196.3	-
DBSA	415.0	-	-	-	-	415.0	-
<i>p</i> -Aminobenzoate	171.0	-	-	-	-	171.0	-
PPy/De	175.1	-	-	-	-	175.1	-
PPy/U	226.9	223.6	227.9	208.4	224.7	222.3	8.0
PPy/A	249.0	250.0	-	-	-	249.5	0.7
PPy/B	268.1	264.4	231.4	268.1	269.0	260.2	16.2
PPy/C	200.0	200.0	208.7	-	-	202.9	5.0
PPy/D	274.4	275.6	262.8	-	-	270.9	7.1
PPy/E	206.0	219.0	219.4	-	-	214.8	7.6
PPy/P	233.6	230.0	-	-	-	231.8	2.5
PPy/AB	214.9	210.5	215.6	-	-	213.7	2.8

Table D3 Water content in PPy/A at various D/M ratios.

Run # \ D/M	Water content (%)							Average	SD
	1	2	3	4	5	6	7		
PPy/U	5.2	4.1	5.1	4.5	4.8	5.0	5.4	4.9	0.4
1/96	4.8	-	-	-	-	-	-	4.8	-
1/48	5.0	-	-	-	-	-	-	5.0	-
1/24	3.9	4.5	-	-	-	-	-	4.2	0.4
1/12	4.4	3.9	4.0	-	-	-	-	4.1	0.3
1/6	3.2	2.6	3.9	-	-	-	-	3.2	0.7
1/3	2.6	2.6	-	-	-	-	-	2.6	0.0
1/2	2.7	2.5	2.9	-	-	-	-	2.7	0.2
2/3	2.4	2.3	-	-	-	-	-	2.4	0.1
1/1	1.4	0.3	2.0	-	-	-	-	1.2	0.8

Appendix E Determination of the Order Aggregation in PPy by an X-Ray Diffractometer

From the well-known Bragg law (Campbell and White, 1991), a crystal lattice spacing, d , in a material can be calculated from a scattering angle, θ , in an X-ray diffraction pattern, where $\lambda = 1.542 \text{ \AA}$ for CuK_α radiation:

$$1 / d = (2 \sin \theta) / \lambda \quad \dots\dots(E.1)$$

For PPy, the X-ray diffraction pattern contained no maxima and hence no structure present (Geiss *et al.*, 1983). The presence of other bonding in PPy, besides a dominant α, α' -bond (Clarke *et al.*, 1983; Diaz and Hall, 1983), leads to its structural disorder. Geiss *et al.* (1983) observed the diffuse electron diffraction pattern from PPy. It was thought to originate from a structure that consists of small crystalline regions separated by much larger amorphous regions.

One of the source of line broadening in X-ray diffraction pattern is the small crystal size effect: the crystal is oriented close to, but not exactly at, the Bragg position. This small crystalline region is referred as 'order aggregation' in this dissertation. The correlation of the extent of order aggregation and the breadth of X-ray diffraction peak can be described by Scherrer equation (Campbell and White, 1991):

$$t = \frac{K\lambda}{B \cos \theta} \quad \dots\dots(E.2)$$

where

t	=	extent of order aggregation,
B	=	breadth at half the peak height in radians,
θ	=	Bragg angle, and
K	=	coefficient depending on the shape of the crystals, it is normally close to 0.9.

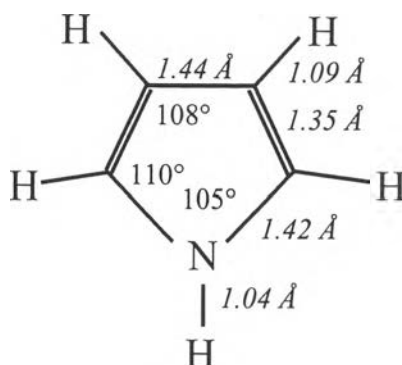


Figure E1 Bond lengths and bond angles in pyrrole ring (Geiss *et al.*, 1983).

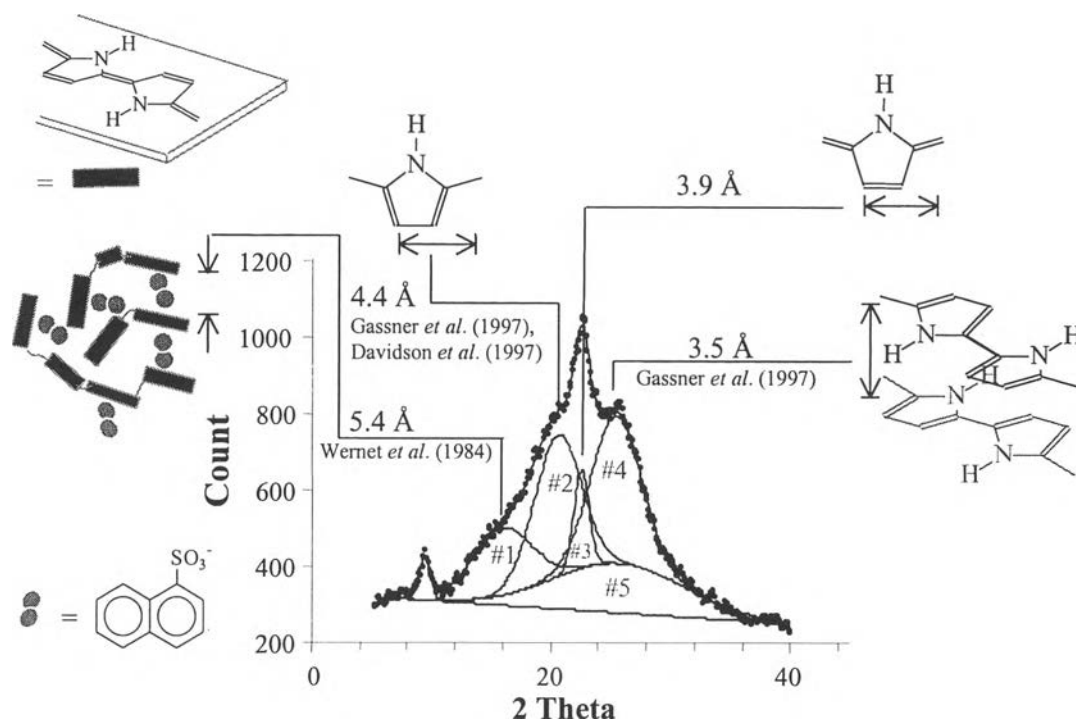


Figure E2 The X-ray diffraction pattern of PPy/A (D/M = 1/12) and its deconvoluted results attributed to its order aggregations.

The X-ray diffraction pattern of PPy/A is shown in Figure E2 along with its deconvoluted results attributed to order aggregations in PPy/A, as described in Chapter II. The X-ray diffraction patterns of PPy/De, PP/U and PPy doped with other dopants are shown in Figure E3 whereas the 2θ , d-spacing, t , and percentage of each deconvoluted scatters are shown in Table E1. Effect of D/M ratio used during the synthesis of PPy/A on PPy ordering was not dominantly observed. Their 2θ , d-spacing, t , and percentage of each deconvoluted scatters are shown in Table E2.

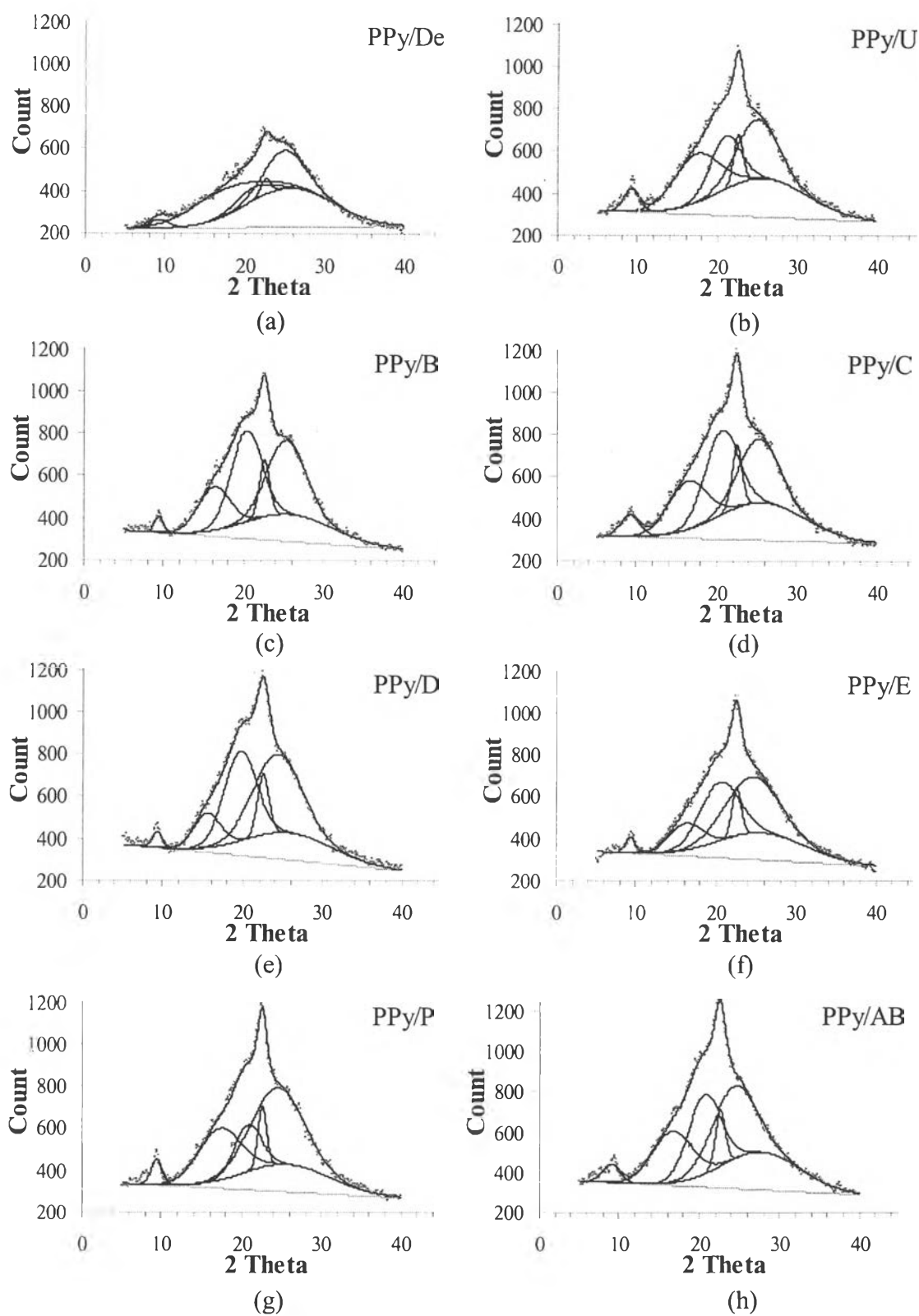


Figure E2 The X-ray diffraction patterns with deconvoluted results underneath of: a) PPy/De; b) PPy/U; c) PPy/B; d) PPy/C; e) PPy/D; f) PPy/E; g) PPy/P; and h) PPy/AB.

Table E1 The deconvoluted results from X-ray diffractograms of PPy/De, PPy/U, and doped PPys with various dopants.

Material	Line-broadening #1				Line-broadening #2				Line-broadening #3				Line-broadening #4				Line-broadening #5			
	2 θ (deg)	d (Å)	t (Å)	%	2 θ (deg)	d (Å)	t (Å)	%	2 θ (deg)	d (Å)	t (Å)	%	2 θ (deg)	d (Å)	t (Å)	%	2 θ (deg)	d (Å)	t (Å)	%
PPy/De	17.3	5.1	16.0	24.6	21.0	4.2	31.7	6.1	22.6	3.9	110.6	2.1	24.9	3.6	28.2	20.3	25.7	3.5	13.1	44.7
PPy/U (1)	17.3	5.1	25.0	21.1	21.0	4.2	37.6	15.3	22.6	3.9	119.4	4.5	24.9	3.6	27.8	23.2	25.7	3.5	13.1	32.7
PPy/U (2)	16.9	5.2	25.7	20.3	20.3	4.4	41.9	12.0	22.5	3.9	90.6	7.9	24.3	3.7	23.1	26.4	25.7	3.5	13.1	29.9
PPy/A (1)	15.9	5.6	28.1	15.2	20.6	4.3	36.1	24.9	22.6	3.9	110.1	5.7	25.5	3.5	33.5	28.2	25.7	3.5	13.1	24.1
PPy/A (2)	16.8	5.3	24.2	21.6	20.4	4.3	43.0	14.8	22.5	3.9	98.1	6.3	25.2	3.5	28.4	32.9	25.7	3.5	13.1	21.6
PPy/A (3)	16.2	5.5	29.5	16.9	20.2	4.4	39.9	18.6	22.6	3.9	92.7	7.5	25.1	3.5	28.2	33.6	25.7	3.5	13.1	21.6
PPy/B	16.3	5.4	35.0	13.6	20.3	4.4	36.5	27.6	22.6	3.9	105.7	6.0	25.3	3.5	29.4	28.0	25.7	3.5	13.1	23.4
PPy/C (1)	16.3	5.5	29.4	16.7	20.8	4.3	31.3	32.1	22.6	3.9	109.9	5.6	25.5	3.5	31.8	17.9	27.0	3.3	16.8	24.1
PPy/C (2)	16.4	5.4	27.9	16.2	20.7	4.3	39.8	24.1	22.6	3.9	88.6	5.6	25.3	3.5	35.4	22.2	25.7	3.5	13.1	28.5
PPy/D (1)	15.6	5.7	41.9	8.5	19.7	4.5	34.8	26.8	22.6	3.9	96.4	6.6	24.3	3.7	23.7	34.6	25.7	3.5	13.1	22.1
PPy/D (2)	15.8	5.6	41.6	10.0	20.3	4.4	28.8	41.3	22.8	3.9	105.4	7.8	24.4	3.6	27.0	13.2	25.2	3.5	11.8	26.3
PPy/E (1)	16.2	5.5	34.0	9.8	20.5	4.3	29.2	24.8	22.6	3.9	120.3	5.0	24.5	3.6	21.5	32.6	25.7	3.5	13.1	26.1
PPy/E (2)	16.3	5.4	26.8	15.6	20.3	4.4	32.3	22.6	22.6	3.9	95.2	7.1	25.3	3.5	24.1	28.6	25.7	3.5	13.1	22.7
PPy/P	17.2	5.1	26.5	20.5	20.8	4.3	41.5	11.8	22.6	3.9	124.6	5.2	24.4	3.6	21.7	37.7	25.7	3.5	13.1	22.3
PPy/AB	16.7	5.3	28.2	17.7	20.7	4.3	35.0	22.1	22.7	3.9	113.1	4.9	24.4	3.7	26.4	27.0	27.8	3.2	14.6	25.6

Table E2 The deconvoluted results from X-ray diffractograms of PPy/A with various D/M ratios.

D/M	Line-broadening #1				Line-broadening #2				Line-broadening #3				Line-broadening #4				Line-broadening #5			
	2 θ (deg)	d (Å)	t (Å)	%	2 θ (deg)	d (Å)	t (Å)	%	2 θ (deg)	d (Å)	t (Å)	%	2 θ (deg)	d (Å)	t (Å)	%	2 θ (deg)	d (Å)	t (Å)	%
PPy/U (1)	17.3	5.1	25.0	21.1	21.0	4.2	37.6	15.3	22.6	3.9	119.4	4.5	24.9	3.6	27.8	23.2	25.7	3.5	13.1	32.7
PPy/U (2)	16.9	5.2	25.7	20.3	20.3	4.4	41.9	12.0	22.5	3.9	90.6	7.9	24.3	3.7	23.1	26.4	25.7	3.5	13.1	29.9
1/48	16.4	5.4	26.5	18.0	20.3	4.4	40.4	17.9	22.5	4.0	94.2	7.1	25.2	3.5	26.8	33.3	25.7	3.5	13.1	21.1
1/24	15.9	5.6	24.9	18.3	20.6	4.3	31.5	24.7	22.6	3.9	108.2	5.0	25.5	3.5	28.5	25.7	25.7	3.5	13.1	24.5
1/12 (1)	15.9	5.6	28.1	15.2	20.6	4.3	36.1	24.9	22.6	3.9	110.1	5.7	25.5	3.5	33.5	28.2	25.7	3.5	13.1	24.1
1/12 (2)	16.8	5.3	24.2	21.6	20.4	4.3	43.0	14.8	22.5	3.9	98.1	6.3	25.2	3.5	28.4	32.9	25.7	3.5	13.1	21.6
1/12 (3)	16.2	5.5	29.5	16.9	20.2	4.4	39.9	18.6	22.6	3.9	92.7	7.5	25.1	3.5	28.2	33.6	25.7	3.5	13.1	21.6
1/6	16.6	5.4	25.7	20.6	20.8	4.3	37.5	20.9	22.6	3.9	114.3	5.0	25.0	3.6	30.2	28.1	25.7	3.5	13.1	24.0
1/2 (1)	16.7	5.3	26.1	19.8	20.9	4.2	34.6	18.3	22.6	3.9	118.9	3.8	24.8	3.6	26.4	32.4	25.7	3.5	13.1	24.4
1/2 (2)	15.9	5.6	25.9	23.4	20.0	4.4	34.7	19.0	22.1	4.0	123.0	3.6	24.1	3.7	27.9	27.5	25.7	3.5	13.1	24.4
2/3	16.2	5.5	28.0	18.7	20.5	4.3	38.0	18.2	22.6	3.9	116.1	5.9	24.5	3.6	25.5	34.0	25.7	3.5	13.1	21.8
1/1	16.9	5.2	25.1	21.6	20.7	4.3	41.1	16.1	22.6	3.9	99.2	5.2	25.0	3.6	30.1	31.2	25.7	3.5	13.1	24.6

Appendix F Determination of the Morphology of PPy and Its Blends by a Scanning Electron Microscope

The scanning electron micrographs of PPy/U and PPy doped with various dopants with D/M ratio of 1/12 are shown in Figure F1; whereas, those of PPy/A5 blends are shown in Figure F2 (see additional pictures in Chapter IV).

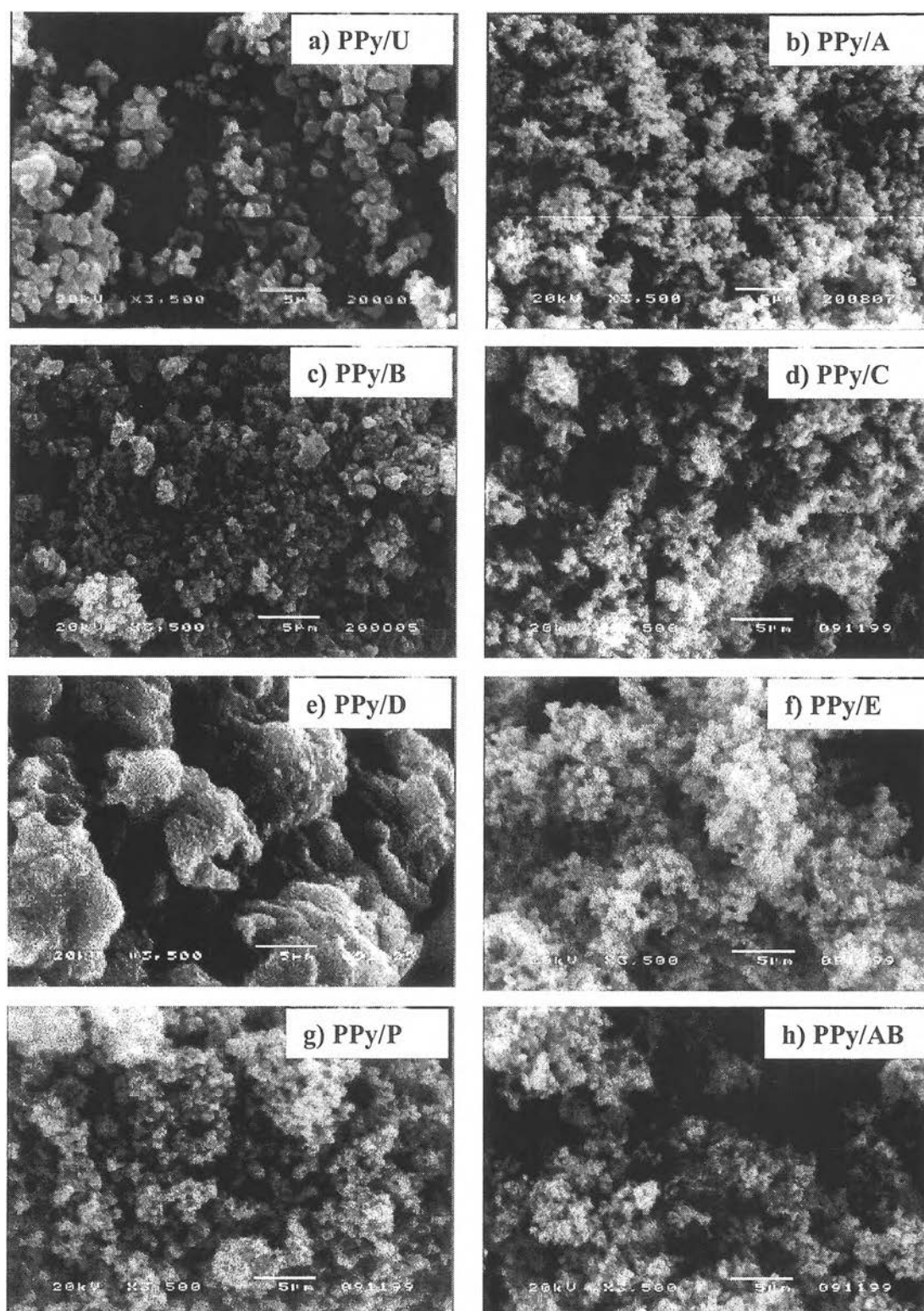


Figure F1 The scanning electron micrographs of: a) PPy/U; b) PPy/A; c) PPy/B; d) PPy/C; e) PPy/D; f) PPy/E; g) PPy/P; and h) PPy/AB with D/M ratio of 1/12, taken at 20 kV and 3,500 times magnification.

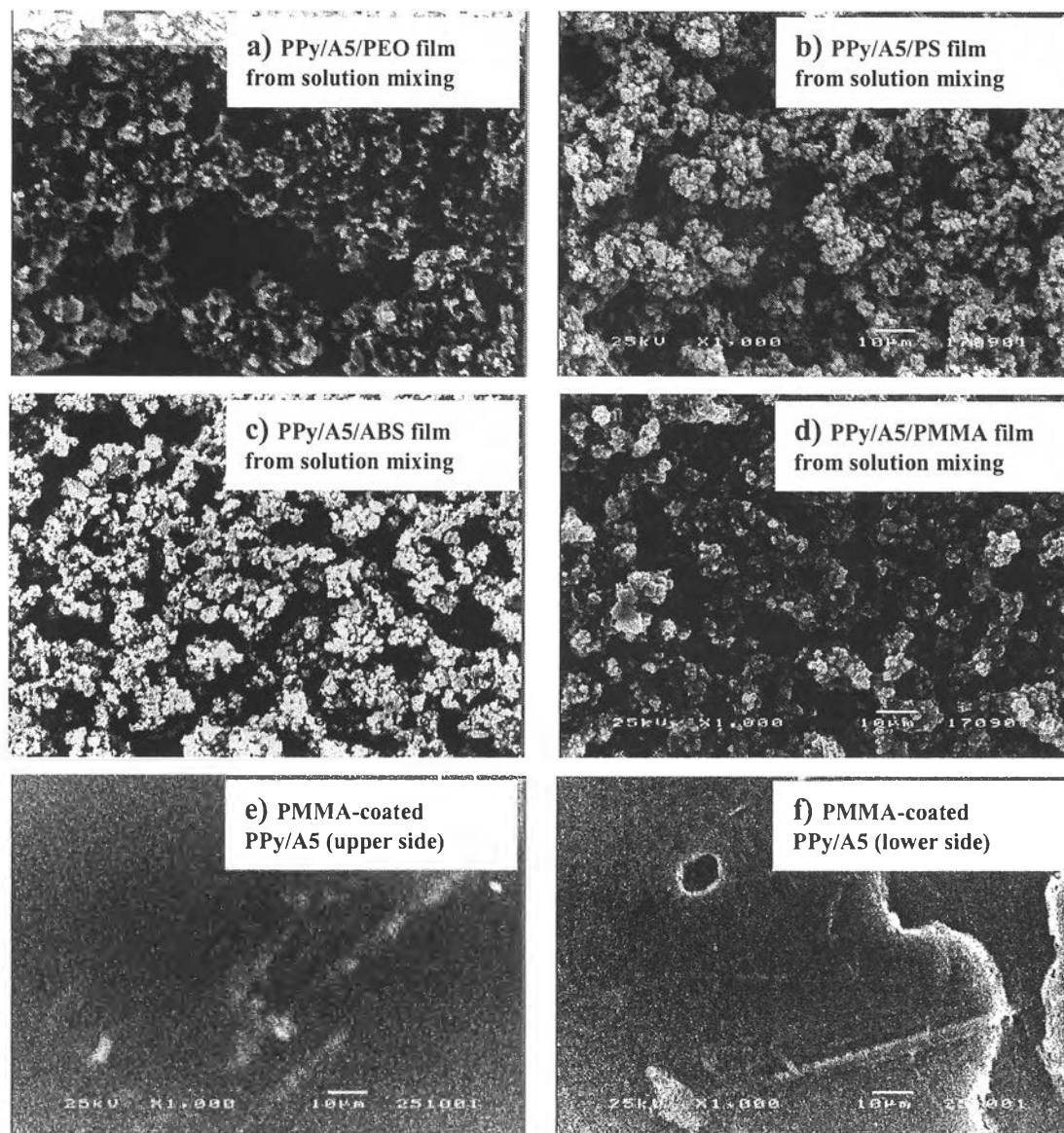


Figure F2 The scanning electron micrographs of: a) PPy/A5/PEO film; b) PPy/A5/PS film; c) PPy/A5/ABS film; d) PPy/A5/PMMA film from solution mixing; e) PMMA-coated PPy/A5 (upper side); and d) PMMA-coated PPy/A5 (lower side); taken at 25 kV and 1,500 times magnification.

Appendix G Determination of the Doping Level by a Scanning Electron Microscope in an Energy Dispersive Mode

An energy-dispersive X-ray analyzer is an accessory of a scanning electron microscope (SEM/EDS) with a capability for elemental analysis. The electron beam in an SEM (5 – 20 keV) can dislodge many atomic electrons from the sample with a penetration depth about 1 μm (<http://www.nlectc.org/assistance/edx/html>). The atom is then immediately neutralized by other electron from higher energy level. In this neutralization process, an X-ray with energy which is a characteristic of the atom is emitted. Figure G1 shows the EDS spectrum of PPy/P at D/M of 1/12 with the labels showing atoms from where X-ray is emitted. Note that two Cu peaks are derived from a copper sample holder. Determination of doping level in term of atomic ratio of PPy doped with various dopants is described in Chapter II. The results are shown in Table G1.

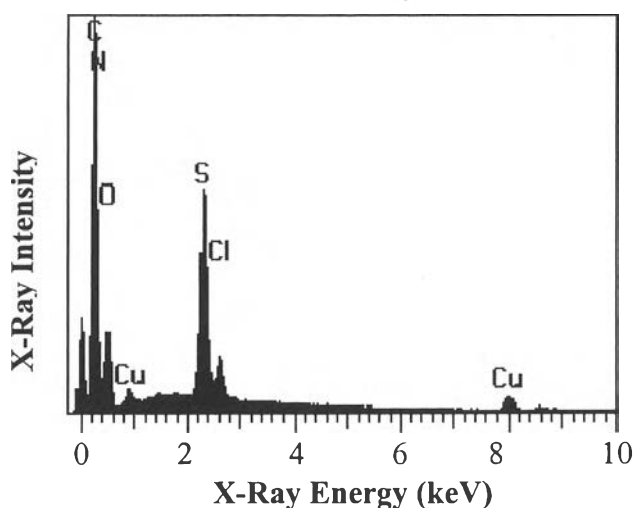


Figure G1 EDS spectrum of PPy/P at D/M of 1/12.

Table G1 Doping level of PPy/De, PPy/U and PPy doped with various dopants D/M ratio of 1/12 as determined by SEM/EDS.

Run # Material	Doping level (atomic ratio)									
	1	2	3	4	5	6	7	8	Average	SD
PPy/De	0.019	0.006	0.004	0.003	0.005	-	-	-	0.007	0.007
PPy/U	0.103	0.117	-	-	-	-	-	-	0.110	0.010
PPy/A	0.303	0.299	0.204	0.192	0.174	0.215	-	-	0.231	0.056
PPy/B	0.223	0.276	0.206	0.261	0.218	0.226	0.226	0.244	0.235	0.024
PPy/C	0.105	0.165	0.182	-	-	-	-	-	0.151	0.040
PPy/D	0.246	0.296	0.192	-	-	-	-	-	0.245	0.052
PPy/E	0.083	0.104	0.167	0.195	0.149	0.072	0.111	-	0.126	0.045
PPy/P	0.175	0.131	-	-	-	-	-	-	0.153	0.031
PPy/AB	0.257	0.225	-	-	-	-	-	-	0.241	0.023

Appendix H Determination of the Charge Carrier Species by an Ultraviolet-Visible Spectroscopy

The electron holes in the positively charged PPy that discontinue electron mobility manifest themselves as mid-gap states. The polaron state of the p-type doped PPy contains one electron and one electron hole, whereas the bipolaron state contains two empty electron holes. Figure H1 shows the energy, ω (eV) that electron needs for transitions in the neutral state and states containing polaron and bipolaron of PPy under the irradiation of ultraviolet or visible light (Blackwood and Josowicz, 1991). Since polaron is formed by removal of only one electron from the valence band of the neutral state, we can assume that $\omega_3 \approx \omega'_3$.

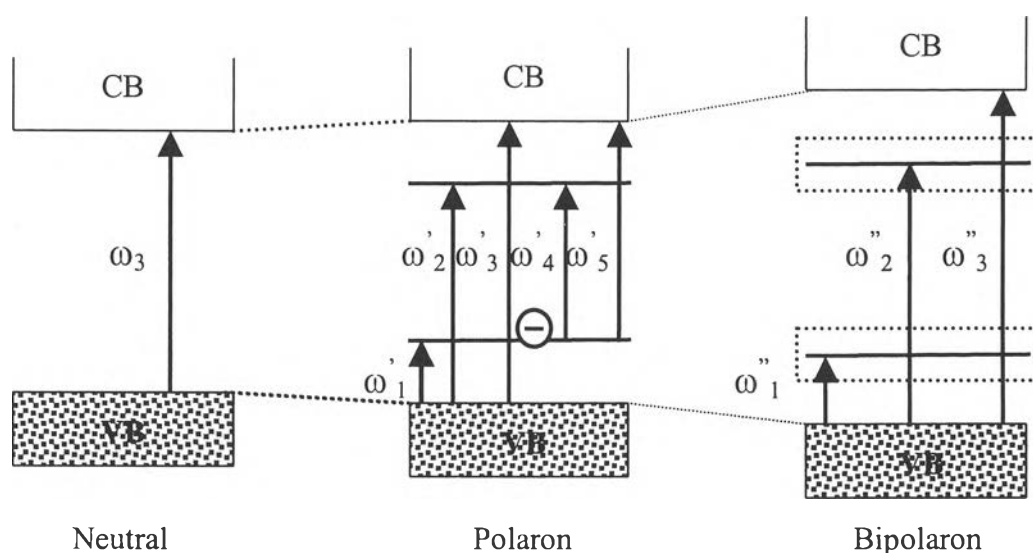


Figure H1 Electronic structure of the bandgap of p-type doped PPy in its neutral, polaron and bipolaron states: CB = conducting band; VB = valence band.

The energy that the molecule needs for electron transition, E , is interrelated to the maximum absorption wavelength, λ_{\max} observed from UV-Vis spectroscopy, as clarified by the Einstein equation:

$$E = hc / \lambda, \quad \dots\dots(H.1)$$

where E = energy for transition (eV)
 h = Plank's constant (4.14×10^{-15} eV · s)
 c = light velocity (2.998×10^{17} nm · s)
 λ = wavelength of the irradiation light (nm).

Energies for electron transition that were appeared in literatures are listed in Table H1. Note that some of them were reported in terms of λ_{\max} with no type of transition specified. The transition energies observed in some soluble PPys from our laboratory are shown in Table H2.

Table H1 Absorption peaks or transition energies for PPy reported in literatures.

Description Sample	Neutral		Polaron					Bipolaron				
	λ_{\max} (nm)	ω_3 (eV)	λ_{\max} (nm)	ω'_1 (eV)	ω'_2 (eV)	ω'_3 (eV)	ω'_4 (eV)	ω'_5 (eV)	λ_{\max} (nm)	ω''_1 (eV)	ω''_2 (eV)	ω''_3 (eV)
Almost neutral PPy*	-	-	-	0.7	2.1	-	1.4	-	-	-	-	3.16
PPy/Perchlorate (doping level = 33 %)*	-	-	-	-	-	-	-	-	-	0.76	2.47- 2.86	3.56
Electrochemically synthesized PPy†	-	2.53	-	0.86	-	-	-	-	-	-	-	2.53
Neutral PPy‡	400 (3.1 eV)	-	-	-	-	-	-	-	-	-	-	-
PPy/TEATos‡	-	-	540 (2.3 eV)	-	-	-	-	-	-	-	-	-
Fully oxidized PPy/TEATos‡	-	-	-	-	-	-	-	-	900 (1.38 eV)	-	-	-
PPy/TCNQ film§	-	~3.2	-	~0.5	~2.3	~3.2	~1.8	~2.3	-	>0.5	~2.3	~3.6
Electrochemically synthesized PPy/DBSA¶	-	-	-	-	-	-	-	-	461 (2.7 eV)	-	-	-
Chemically synthesized PPy/DBSA¶	-	-	-	-	-	-	-	-	430 (2.9 eV)	-	-	-
PPy/NSA in m-cresol#	415 (3.0 eV)	-	655 (1.9 eV)	-	-	-	-	-	965 (1.3 eV)	-	-	-

*Brédas *et al.*, 1984

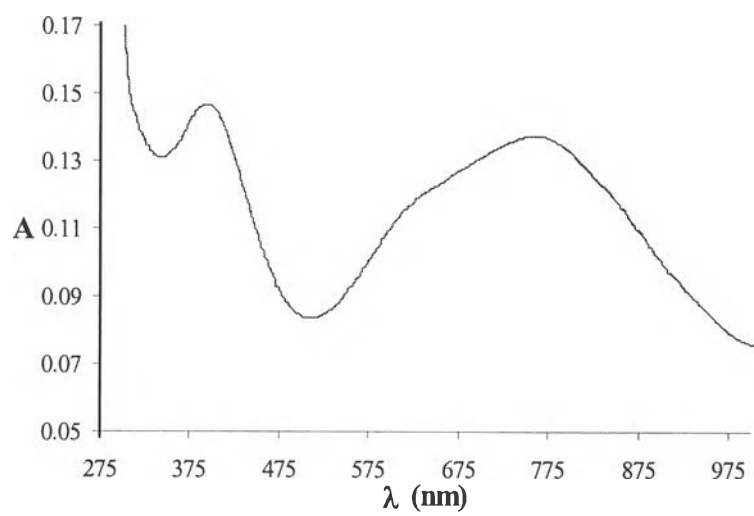
†Tezuka and Aoki, 1989

‡Zotti and Schiavon, 1989

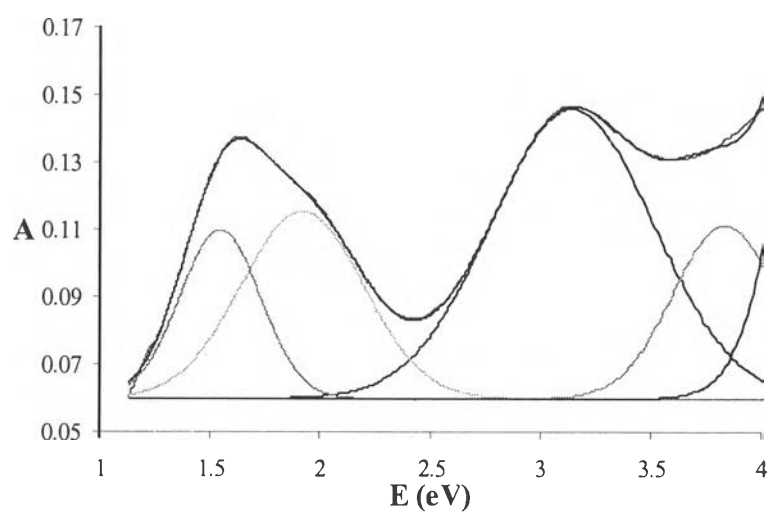
§Blackwood and Josowicz, 1991

¶Kim *et al.*, 1995

Shen and Wan, 1997



(a)



(b)

Figure H2 a) The visible spectrum of PPy/B in NMP solution; and b) its converted data with deconvoluted results.

Table H2 Transition energies in soluble PPy's synthesized in our laboratory, along with their percentages.

Sample \ Transition	ω_3 or ω'_3		ω'_4		ω''_1		ω''_3	
	(eV)	(%)	(eV)	(%)	(eV)	(%)	(eV)	(%)
PPy/A film from m-cresol solution	2.8	13.2	-	-	1.4	49.2	3.5	37.6
PPy B in NMP solution	3.1 (0.04)	41.8 (5.84)	1.9 (0.06)	20.5 (4.55)	1.6 (0.03)	19.1 (5.12)	3.8 (0.09)	18.6 (2.78)
PPy/B film from m-cresol solution	2.5 (0.00)	18.3 (1.48)	2.0 (0.01)	11.0 (1.02)	1.4 (0.02)	2.4 (0.54)	3.0 (0.00)	68.3 (1.00)
PPy/D film from m-cresol solution	3.0	10.8	-	-	1.7	63.8	3.4	25.4

Absorbance, A of the sample depends on the molar absorptivity, ϵ as described by Beer's law:

$$A = \epsilon b c \quad \dots\dots(H.2)$$

Where

- A = Absorbance (arbitrary unit)
- ϵ = molar absorptivity ($M^{-1} \text{ cm}^{-1}$)
- b = path length of the light through the sample (cm)
- c = sample concentration (M)

Since ϵ depends on both the electron concentration of occupied sites and that of unoccupied sites available, we can expect that:

$$\epsilon \text{ of } \omega_3 > \epsilon \text{ of } \omega'_3 \approx \epsilon \text{ of } \omega''_3 \quad \text{and} \quad \dots\dots(H.3)$$

$$\epsilon \text{ of } \omega'_1, \omega'_2, \omega'_3 > \epsilon \text{ of } \omega'_4, \omega'_5. \quad \dots\dots(H.4)$$

ϵ values of each transitions found in our samples were determined by measuring A values of PPy/B solution in NMP with different concentrations whereas b was fixed at 1 cm. The slopes of the plots of A values vs. PPy concentrations (in g/L), as shown in Figure H3, imply ϵ values in $(\text{g/L})^{-1} \text{ cm}^{-1}$: they are listed in Table H3.

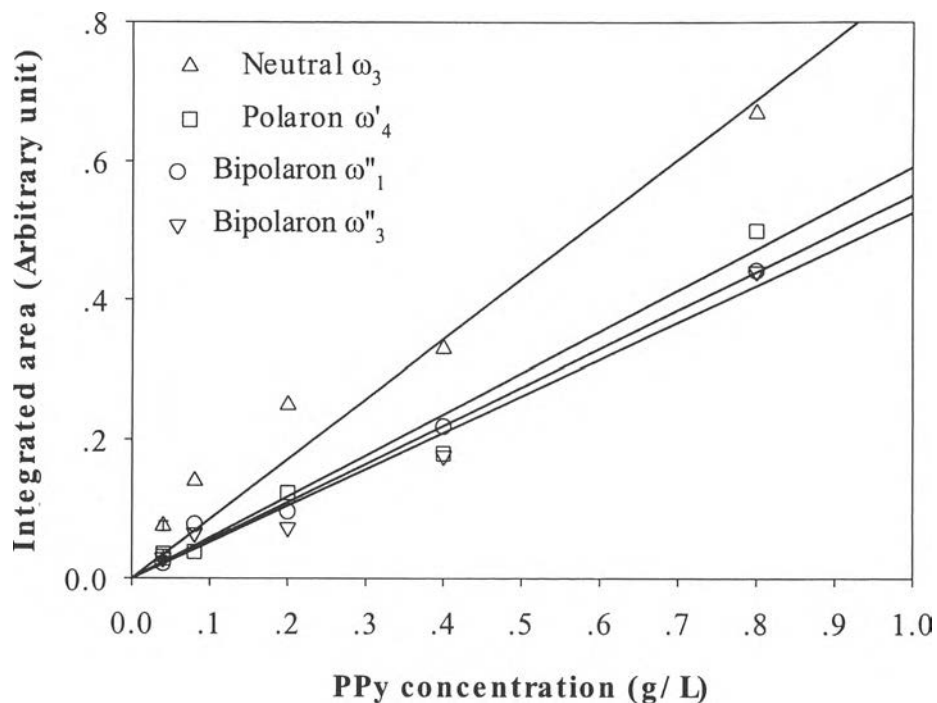


Figure H3 Calibration curves from PPy/B samples in NMP solution.

Table H3 ϵ values of all transitions found in PPy/B in NMP solution and their fit goodness, R^2 .

Transition	ϵ values (g/L) ⁻¹ cm ⁻¹	R^2
ω_3 or ω'_3	0.86	0.91
ω'_4	0.59	0.96
ω''_1	0.55	0.98
ω''_3	0.53	0.97

Appendix I Determination of the Surface Compositions of PPy by an X-ray Photoelectron Spectroscopy

Table II Binding energy (BE) of PPy components from literaturess.

Reference	Internal standard	BE (eV)	Description as written in reference	Description used in this book
Liang <i>et al.</i> ,1992	C 1s = 284.6 eV	283.80	α ring carbon	C α
		284.90	β ring carbon	C β
		286.50	carbon atoms which are adjacent to a positively charged N atom and carbon atoms which are sigma bonded to oxygen	C-N ⁺ & C-O
		288.00	carbonyl carbon	C=O
		397.50	imine-like nitrogen	=N-
		401.50	positively charged pyrrolylium nitrogen cations	N ⁺
		531.50	carbonyl oxygen	O=C
Kang <i>et al.</i> ,1990	C 1s = 284.6 eV	168.50	characteristic of the sulfate species (S(2p _{3/2}))	S VI
		166.50	imine-like nitrogen	=N-
		399.70	pyrrolylium nitrogen (-NH-)	-NH-
Gustafsson <i>et al.</i> ,1989	N/A	288.00	carbonyl carbon	C=O
		399.80	-NH-	-NH-
Chan <i>et al.</i> , 1988	C 1s = 285.0 eV	397.50	deprotonated, uncharged nitrogen atoms having three bonds to carbon	=N-
		399.50	uncharged nitrogen	-NH-
		401.40	nitrogen atom associated with a unit positive charge in PPy-I ₂	N ⁺
		401.60	nitrogen atom associated with a unit positive charge in PPy-Br ₂	N ⁺
		402.60	nitrogen atom associated with a unit positive charge in PPy-I ₃	N ⁺
		403.50	nitrogen atom associated with a unit positive charge in PPy-Br ₂	N ⁺
Erlandsson <i>et al.</i> , 1985	N/A	397.70	imine-like nitrogen	=N-
		400.00	-NH-	-NH-
Lim <i>et al.</i> , 1999	C 1s = 284.6 eV	167.70	S 2p _{3/2}	S
		398.10	imine-like nitrogen	=N-
		399.70	amine-like nitrogen	-NH-
		400.00	positively charged nitrogen	N ⁺

Table I1 Binding energy of PPy components from literatures (continued).

Reference	Internal standard	BE (eV)	Description as written in reference	Description used in this book
Malitesta <i>et al.</i> , 1995	N 1s = 399.6 eV	283.83 ±0.05	Cβ	Cβ
		284.81 ±0.03	Cα, cont. C	Cα & contaminate C
		286.29 ±0.06	C-OH, C=N, C-N ⁺	C-OH, C=N, C-N ⁺
		287.83 ±0.11	C=O, C=N ⁺	C=O, C=N ⁺
		289.70 ±0.20	shake-up 1	-
		291.50 ±0.40	shake-up 2	-
		397.68 ±0.12	C=N	C=N
		399.60	-NH-	-NH-
		401.11 ±0.09	C-N ⁺	C-N ⁺
		402.71 ±0.17	C=N ⁺	C=N ⁺
		531.53 ±0.10	O=C	O=C
		533.18 ±0.11	OH-C	OH-C

Table I2 Nitrogen compositions of PPy/De, PPy/U, and PPy doped with various dopants at D/M ratio of 1/12.

Material	FWHM* (eV)	-N= (imine-like N)		-NH- (neutral N)		-NH ⁺ - (polaron)		=NH ⁺ - (bipolaron)	
		BE (eV)	%	BE (eV)	%	BE (eV)	%	BE (eV)	%
PPy/De (1)	1.80	397.2	12.98	399.0	74.56	401.0	12.46	-	-
PPy/De (1)	1.61	397.9	11.66	399.6	77.55	401.1	10.79	-	-
PPy/De (2)	2.53	397.0	40.16	398.7	47.09	400.9	12.75	-	-
PPy/U (1)	1.63	397.6	3.56	399.3	73.44	401.1	23.00	-	0.00
PPy/U (1)	1.58	397.4	3.17	399.3	65.21	401.0	31.62	-	0.00
PPy/U (2)	1.58	398.1	1.68	399.4	72.63	400.9	25.69	-	0.00
PPy/A (1)	1.49	397.1	1.47	399.3	70.97	400.8	21.24	402.4	6.33
PPy/A (1)	1.50	397.4	1.85	399.3	70.50	400.8	21.19	402.4	6.46
PPy/A (2)	1.47	397.4	3.62	399.2	68.93	400.7	21.31	402.3	6.13
PPy/A (2)	1.54	397.2	3.69	399.3	68.87	400.8	21.26	402.4	6.18
PPy/A (3)	1.52	397.2	1.87	399.3	70.27	400.8	21.19	402.4	6.67
PPy/A (4)	1.48	397.4	0.81	399.3	72.87	400.8	20.03	402.4	6.29
PPy/A (4)	1.56	397.4	2.00	399.2	69.33	400.8	22.36	402.4	6.31
PPy/B (1)	1.47	-	0.00	399.3	68.17	400.8	25.97	402.4	5.87
PPy/B (2)	1.50	397.4	0.93	399.3	71.05	400.8	28.01	-	0.00

* Full width at half-maximum, FWHM

Table I2 Nitrogen compositions of PPy/De, PPy/U, and PPy doped with various dopants at D/M ratio of 1/12 (continued).

Material	FWHM (eV)	-N= (imine-like N)		-NH- (neutral N)		-NH ⁺ - (polaron)		=NH ⁺ - (bipolaron)	
		BE (eV)	%	BE (eV)	%	BE (eV)	%	BE (eV)	%
PPy/B (3)	1.47	397.4	3.43	399.3	64.72	400.8	25.99	402.4	5.85
PPy/C (1)	1.61	397.7	4.74	399.3	71.62	400.8	19.71	402.4	3.92
PPy/C (2)	1.59	397.7	18.46	399.3	58.15	400.8	19.86	402.4	3.53
PPy/D (1)	1.57	397.7	8.98	399.5	71.35	401.0	19.68	-	0.00
PPy/D (2)	1.56	397.7	8.75	399.5	68.67	401.0	18.01	402.6	4.57
PPy/D (3)	1.57	397.7	7.12	399.5	72.24	401.0	20.36	402.6	0.28
PPy/D (3)	1.56	397.7	5.47	399.5	70.68	401.0	19.30	402.6	4.55
PPy/E (1)	1.67	-	0.00	399.3	79.52	400.8	20.48	-	0.00
PPy/E (1)	1.68	-	0.00	399.3	76.54	400.8	19.28	402.4	4.18
PPy/E (2)	1.41	397.7	4.47	399.3	65.60	400.8	22.09	402.4	7.85
PPy/E (2)	1.36	397.7	4.92	399.3	63.80	400.7	22.33	402.2	8.95
PPy/P	2.11	397.4	19.67	399.1	58.57	400.6	21.76	-	0.00
AB (1)	1.63	397.5	16.04	399.4	75.08	401.0	8.89	-	0.00
AB (1)	1.63	397.5	15.99	399.4	74.37	401.0	9.64	-	0.00
AB (2)	1.66	397.5	14.76	399.4	74.89	401.0	10.35	-	0.00
AB (2)	1.66	397.5	16.57	399.4	71.75	401.0	11.68	-	0.00

Table I3 Nitrogen compositions of PPy/A at various D/M ratios.

D/M	FWHM (eV)	-N= (imine-like N)		-NH- (neutral N)		-NH ⁺ (polaron)		=NH ⁺ (bipolaron)	
		BE (eV)	%	BE (eV)	%	BE (eV)	%	BE (eV)	%
1/96 (1)	1.30	398.2	7.76	399.4	61.72	400.5	23.88	402.0	6.64
1/96 (1)	1.27	397.8	5.15	399.2	60.65	400.3	25.04	401.6	9.15
1/96 (2)	1.57	397.8	3.30	399.4	75.58	401.0	17.78	402.6	3.34
1/48 (1)	1.57	397.4	11.13	399.2	62.90	400.8	18.36	402.2	7.60
1/48 (2)	1.52	397.4	11.19	399.2	60.67	400.7	19.42	402.3	8.72
1/24	1.50	397.4	5.30	399.3	68.28	400.8	20.04	402.4	6.38
1/12 (1)	1.44	397.2	0.00	399.3	70.30	400.6	20.46	402.1	9.24
1/12 (2)	1.50	397.2	0.00	399.3	73.78	400.8	18.76	402.4	7.46
1/6 (1)	1.48	397.2	0.00	399.2	71.47	400.7	21.18	402.3	7.35
1/6 (2)	1.48	397.3	2.94	399.3	72.17	400.8	19.69	402.4	5.20
1/3 (1)	1.50	397.4	2.65	399.3	71.48	400.9	20.33	402.5	5.54
1/3 (2)	1.56	397.2	2.56	399.4	73.92	401.1	19.68	402.9	3.85
1/2 (1)	1.69	397.2	3.67	399.3	73.35	400.8	21.70	402.4	1.29
1/2 (2)	1.68	397.1	2.94	399.3	68.21	400.8	20.41	402.4	8.45
2/3 (1)	1.50	397.2	0.00	399.4	72.92	400.9	20.99	402.5	6.08
2/3 (1)	1.43	397.2	0.00	399.3	69.50	400.7	23.10	402.3	7.39
2/3 (2)	1.52	397.2	0.00	399.3	74.03	400.9	19.78	402.5	6.19
2/3 (2)	1.50	397.2	0.00	399.3	73.04	400.8	20.22	402.4	6.74
1/1 (1)	1.51	397.2	0.00	399.3	71.54	400.8	23.36	402.4	5.10
1/1 (2)	1.47	397.2	0.00	399.3	69.64	400.7	23.66	402.1	6.70

Table I4 Sulfur compositions of PPy/A at various D/M ratios.

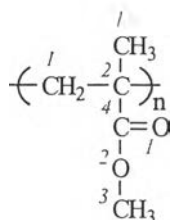
D/M	FWHM (eV)	S IV / N [†]						S VI / N [‡]					
		BE* (eV)	Run #					BE (eV)	Run #				
			1	2	3	4	5		1	2	3	4	5
α -NSA	1.37	167.8	-	-	-	-	-	-	-	-	-	-	-
0	2.32	-	0.00	-	-	-	-	167.2	0.12	-	-	-	-
1/96	2.43	166.4	0.14	0.11	0.11	0.20	-	167.9	0.01	0.01	0.01	0.02	-
1/48	1.77	166.8	0.17	0.16	0.19	-	-	169.6	0.02	0.02	0.02	-	-
1/24	1.78	166.8	0.17	0.17	0.17	-	-	168.7	0.06	0.06	0.06	-	-
1/12	1.64	166.6	0.19	0.18	0.20	0.20	0.20	168.5	0.05	0.06	0.04	0.05	0.06
1/6	1.69	166.7	0.22	0.24	0.20	-	-	168.6	0.09	0.11	0.06	-	-
1/3	2.07	167.9	0.18	0.14	0.21	-	-	169.8	0.15	0.19	0.12	-	-
1/2	1.74	166.6	0.21	0.16	0.20	0.23	0.23	168.5	0.11	0.16	0.12	0.09	0.06
2/3	1.66	166.6	0.19	0.14	0.20	0.23	-	168.5	0.14	0.19	0.13	0.10	-
1/1	1.73	166.5	0.26	0.25	0.26	-	-	167.8	0.09	0.10	0.09	-	-

* Represents BEs of S 2p 1/2; whereas those of 2p 3/2 are ~1.28 eV (SD = 0.6 eV) lower

† Represents areas of S 2p in S IV (S 2p 1/2 and 2p 3/2)

‡ Represents areas of S 2p in S VI (S 2p 1/2 and 2p 3/2)

Appendix J Determination of the Surface Compositions of PPy Blends by an X-Ray Photoelectron Spectroscopy



Scheme J1 Chemical structure of PMMA with labels on C and O atoms (italic letters).

Table J1 Parameters in XP spectra of PMMA (Wagner, 1989).

Orbital Parameter	C 1s				O 1s	
	1	2	3	4	1	2
BE* (eV)	285	285.72	286.79	289.03	532.21	533.77
FWHM† (eV)	1.15	1.06	1.28	0.99	1.27	1.39
Area (%)	42	21	21	17	51	49

* Binding energy, BE

† Full width at half-maximum, FWHM

The fractions of PMMA (derived from the XPS peak area ratios, as described in Chapter IV) at the surfaces of PPy/A5/PMMA obtained from dry mixing, of PPy/A5/PMMA films obtained from solution mixing, and of PMMA-coated PPy are shown in Table J2. The fractions of PMMA at the surfaces of PPy/A/PMMA obtained from solution mixing with various fed PMMA/PPy ratios, as reported in Chapter V, are shown in Table J3.

Table J2 PMMA fraction at surface of PPy/A5 blends from three different mixing methods.

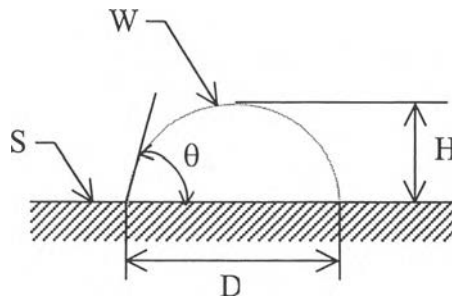
Material	Fed PMMA/PPy	PMMA fraction at surface			
		Run # 1	Run # 2	Average	SD
PPy/A5/PMMA from dry mixing	1/1	0.21	-	0.21	-
PPy/A5/PMMA from solution mixing	1/1	0.34	0.38	0.36	0.03
PMMA-coated PPy/A5	2.2/1	0.68	-	0.68	-

Table J3 PMMA fraction at surface of PPy/A blends from solution mixing with various fed PMMA/PPy ratios.

Material	Fed PMMA/PPy	PMMA/PPy at surface			
		Run # 1	Run # 2	Average	SD
PPy/A/PMMA from solution mixing	1/1	0.38	-	0.38	-
PPy/A/PMMA from solution mixing	2/1	0.46	0.42	0.44	0.03
PPy/A/PMMA from solution mixing	3/1	0.50	0.39	0.44	0.08
PPy/A/PMMA from solution mixing	4/1	0.41	0.32	0.37	0.07

Appendix K Determination of the Contact Angle of Water on PPy and Its Blends

As 5 μL of water was dropped onto sample surface, contact angle, θ , was directly measured visually, whereas the remaining water volume on the surface was calculated from the observed parameters as shown in Scheme K.1.

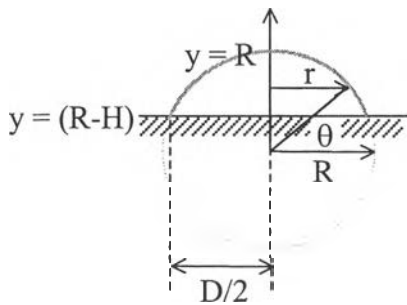


Scheme K.1 Profile of water droplet on specimen surface: W = water droplet; S = specimen; D = diameter of the surface of contact of the droplet; H = height of the droplet; and θ = contact angle.

K.1 Determination of water volume on specimen surface

If the specimen is absorbent, the decrease of water volume at the surface as the functions of time is worth determining. The volume was calculated from the droplet profile, assuming the droplet on the surface is a part of a symmetric sphere.

K.1.1 When $H < D/2$ and $\theta < 90$

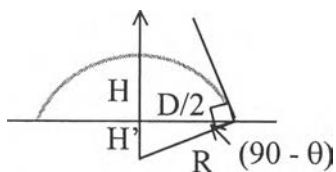


$$\text{Vol.} = \int_{y=R-H}^{y=R} \pi r^2 dy$$

$$= \int_{y=R-H}^{y=R} \pi (\sqrt{R^2 - y^2})^2 dy$$

$$= \int_{y=R-H}^{y=R} \pi R^2 dy$$

$$- \int_{y=R-H}^{y=R} \pi y^2 dy$$

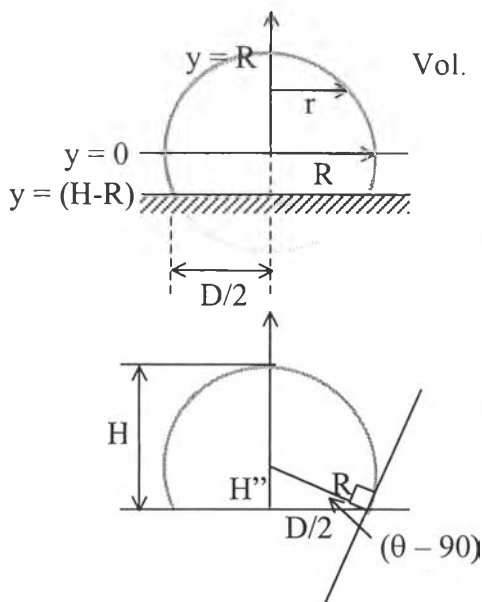


$$\begin{aligned}
 &= \pi R^2 y \Big|_{R-H}^R - \frac{\pi}{3} y^3 \Big|_{R-H}^R \\
 &= \pi R^2 R - \pi R^2 (R - H) - \frac{\pi}{3} R^3 + \frac{\pi}{3} (R - H)^3 \quad \dots\dots(K.1)
 \end{aligned}$$

When $R = H + H'$

$$= H + \frac{D}{2} \tan (90 - \theta) \quad \dots\dots(K.2)$$

K.1.2 When $H > D/2$ and $\theta > 90$



$$\begin{aligned}
 \text{Vol.} &= \frac{1}{2} \times \frac{4}{3} \pi R^3 + \int_{y=0}^{y=(H-R)} \pi r^2 dy \\
 &= \frac{2}{3} \pi R^3 + \pi R^2 y \Big|_0^{H-R} - \frac{\pi}{3} y^3 \Big|_0^{H-R} \\
 &= \frac{2}{3} \pi R^3 + \pi R^2 (H - R) - 0 - \frac{\pi}{3} (H - R)^3 + 0 \quad \dots\dots(K.3)
 \end{aligned}$$

When $R = H - H''$

$$= H - \frac{D}{2} \tan (\theta - 90) \quad \dots\dots(K.4)$$

Experimental data from contact angle measurement between water and the surfaces of PPy/A5, its blends, and PMMA sheet are shown in Tables K1 – K5.

Table K1 Experimental data from the contact angle measurement between water and the surface of PPy/A5.

Time (sec)	D (cm)	H (cm)	Vol. (cm ³)	Contact angle (degree)		Time (sec)	D (cm)	H (cm)	Vol. (cm ³)	Contact angle (degree)	
				Left	Right					Left	Right
41	0.262	0.130	4.6E-03	90	90	370	0.244	0.065	1.5E-03	-	60
91	0.262	0.118	4.5E-03	-	80	405	0.240	0.049	1.3E-03	-	40
117	0.260	0.114	4.5E-03	-	75	449	0.236	0.035	6.3E-04	-	40
150	0.274	0.106	4.3E-03	70	70	477	0.234	0.026	3.3E-04	-	40
264	0.268	0.087	2.9E-03	-	65	493	0.232	0.020	2.7E-04	-	30
284	0.262	0.078	2.2E-03	-	65	510	0.230	0.015	1.4E-04	-	30
307	0.256	0.076	2.3E-03	-	60	530	0.228	0.010	6.4E-05	-	30
326	0.250	0.073	2.0E-03	-	60	553	0.226	0.000	0.0E+00	-	0

Table K2 Experimental data from the contact angle measurement between water and the surface of PPy/A5/PMMA as obtained from dry mixing.

Time (sec)	D (cm)	H (cm)	Vol. (cm ³)	Contact angle (degree)		Time (sec)	D (cm)	H (cm)	Vol. (cm ³)	Contact angle (degree)	
				Left	Right					Left	Right
8	0.312	0.104	5.1E-03	55	70	297	0.300	0.044	1.6E-03	30	35
29	0.312	0.090	4.6E-03	45	60	335	0.290	0.038	1.3E-03	-	30
55	0.310	0.077	3.4E-03	-	50	365	0.280	0.030	1.1E-03	-	20
113	0.308	0.070	3.1E-03	45	45	404	-	0.020	-	-	10
170	0.306	0.064	2.9E-03	40	-	440	-	0.014	-	15	5
218	0.304	0.058	2.3E-03	-	40	495	-	0.010	-	-	-
248	0.302	0.052	1.8E-03	-	40						

Table K3 Experimental data from the contact angle measurement between water and the surface of PPy/A5/PMMA as obtained from solution mixing.

Time (sec)	D (cm)	H (cm)	Vol. (cm ³)	Contact angle (degree)		Time (sec)	D (cm)	H (cm)	Vol. (cm ³)	Contact angle (degree)	
				Left	Right					Left	Right
10	0.178	0.174	3.9E-03	130	130	527	-	0.096	-	95	-
38	0.178	0.174	3.9E-03	130	-	580	0.165	0.084	1.1E-03	95	95
47	0.178	0.170	3.5E-03	130	-	640	-	0.070	-	85	85
87	0.177	0.166	3.2E-03	130	-	700	0.161	0.057	6.9E-04	70	70
139	0.176	0.160	3.6E-03	125	-	720	0.160	0.044	4.6E-04	60	60
168	0.175	0.157	3.4E-03	125	-	760	0.160	0.036	3.3E-04	-	55
240	0.174	0.147	3.2E-03	120	120	787	0.148	0.030	2.0E-04	55	-
330	0.172	0.130	2.9E-03	110	-	820	0.112	0.010	2.3E-05	40	40
410	0.171	0.119	2.9E-03	100	100	840	0.000	0.000	0.0E+00	20	20
492	0.171	0.104	1.8E-03	100	-						

Table K4 Experimental data from the contact angle measurement between water and the surface of PMMA-coated PPy/A5.

Time (sec)	D (cm)	H (cm)	Vol. (cm ³)	Contact angle (degree)		Time (sec)	D (cm)	H (cm)	Vol. (cm ³)	Contact angle (degree)	
				Left	Right					Left	Right
10	0.258	0.126	5.3E-03	-	80	360	0.236	0.073	1.7E-03	-	65
60	0.254	0.120	4.6E-03	-	80	420	0.227	0.061	1.1E-03	-	65
90	0.250	0.115	4.1E-03	-	80	480	0.218	0.051	1.2E-03	-	45
120	0.250	0.110	3.6E-03	-	80	540	0.205	0.040	7.5E-04	-	40
180	0.250	0.102	2.9E-03	-	80	600	0.175	0.028	4.2E-04	-	30
240	0.244	0.093	2.3E-03	-	80	660	0.124	0.013	9.5E-05	-	20
300	0.240	0.083	1.9E-03	-	75						

Table K5 Experimental data from the contact angle measurement between water and the surface of PMMA sheet.

Time (sec)	D (cm)	H (cm)	Vol. (cm ³)	Contact angle (degree)		Time (sec)	D (cm)	H (cm)	Vol. (cm ³)	Contact angle (degree)	
				Left	Right					Left	Right
15	0.305	0.116	4.7E-03	75	80	300	0.302	0.075	2.9E-03	45	60
45	0.305	0.112	4.8E-03	75	70	360	0.302	0.066	2.9E-03	45	40
90	0.305	0.103	4.1E-03	-	70	420	0.300	0.056	2.3E-03	40	35
120	0.305	0.101	4.4E-03	-	65	480	0.295	0.048	2.1E-03	30	30
165	0.305	0.094	3.7E-03	-	65	540	0.290	0.038	1.9E-03	20	20
180	0.305	0.093	3.6E-03	-	65	600	0.279	0.029	1.1E-03	15	25
210	0.305	0.089	3.2E-03	-	65	660	0.269	0.018	5.2E-04	20	10
240	0.305	0.084	3.2E-03	-	60	690	0.251	0.014	2.9E-04	15	15
270	0.305	0.076	2.9E-03	50	60						

Appendix L Effect of Contact Force of Probe on the Specific Conductivity of PPy

L.1 Introduction

Aparecido *et al.* (1996) pointed out the significant influence of force on the conductivity of conductive polymers. The force of more than 30 N may cause bending to polymer. As the applied force increases, the conductivity increases nonlinearly, along with the increasing of measurement errors. In this work, this phenomenon has been carefully considered before building a four-point probe. The custom-made four-point probe was fabricated by fixing the stainless steel bar on the upper piece of probe (see Figure L1). The suitable weight, which is sufficiently high to give the precise conductivity values but not so high as can destroy the sample, was investigated by the following procedure.

L.2 Experiment

Stainless steel bars with different weights were attached onto the upper piece of probe (Figure L1). The specific conductivity of a sample was measured. The PPy sample used can be any. In this experiment, the pellet of PPy/A at D/M of 1/60 and at APS/M of 1/1 was used.

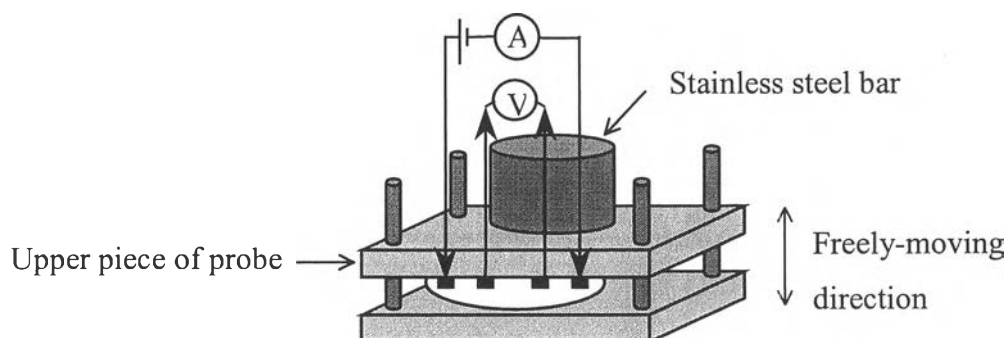


Figure L1 Geometry of the custom-made four-point probe.

L.3 Result and Discussion

When the loading weight was varied from 57.9 – 384.3 g, the specific conductivity of the sample remained constant at 0.29 S/cm with the standard deviation of only 0.014 S/cm. This means all of the weights studied here are suitable. The experimental results are shown in Table L1.

Table L1 The specific conductivity of PPy/A at D/M ratio of 1/60 and at APS/M of 1/1 at different loading weights on the upper piece of the custom-made four-point probe, thickness of pellet = 0.008 cm and K of probe = 1.65.

Loading Weight (g)	σ (S/cm)	
	Run #1	Run #2
57.9	2.9E-01	-
114.7	2.7E-01	2.9E-01
173.7	2.8E-01	-
327.0	3.0E-01	3.1E-01
384.3	3.1E-01	-
average σ (S/cm)	2.9E-01	
SD (S/cm)	1.4E-02	

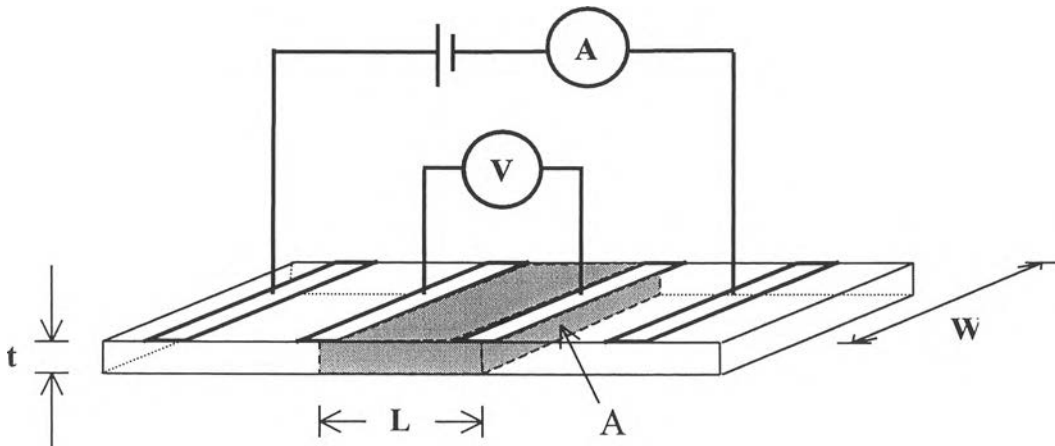
L.4 Conclusion

The specific conductivity of the sample does not depend on the loading weight on the top of the probe in the range of study. So, any of stainless steel bars can be selected for the further experiment and it was the bar with the weight of 327.0 g.

L.5 Reference

1. Aparecido, A.C., Robert, G.R. (1996) A new method for extending the range of conductive polymer sensors for contact force. International Journal of Industrial Ergonomics, 17, 285-290.

Appendix M Determination of the Geometric Correction Factor of the Custom-Made Four-Point Probe



Scheme M.1 Dimensions of probes and sample: W = width of probes; t = thickness of sample; L = distance between two inner probes; and A = cross-sectional area where electron flux flows.

A geometric correction factor, K of a four-point probe is a ratio of probe width, W , to the distance between two inner probes, L . This factor can be obtained practically by measuring the specific conductivity of standard semiconductor sheets with known resistivity values. K is then simply defined as a ratio of a specific resistivity of the standard obtained from text book or measured by another reliable probe, $\rho_{\text{std, text}}$, to a resistance times thickness of the standard sample measured in our laboratory, $(R_{\text{std, mea}} \cdot t)$, as derived from these following correlation:

$$\begin{aligned}
 \sigma_{\text{std, text}} &= 1 / \rho_{\text{std, text}} \\
 &= L / (R_{\text{std, mea}} \cdot A) \\
 &= L / (R_{\text{std, mea}} \cdot t \cdot W) \quad \dots\dots(M.1)
 \end{aligned}$$

$$L / W = \sigma_{\text{std, text}} (R_{\text{std, mea}} \cdot t). \quad \dots\dots(M.2)$$

By definition,

$$K = W / L,$$

then

$$K = 1 / [\sigma_{\text{std, text}} (R_{\text{std, mea}} \cdot t)],$$

or

$$K = \rho_{\text{std, text}} / (R_{\text{std, mea}} \cdot t). \quad \dots\dots(M.3)$$

For other samples

$$K = 1 / [\sigma_{\text{real}} (R_{\text{mea}} \cdot t)],$$

then

$$\sigma_{\text{real}} = 1 / R_{\text{mea}} / t / K \quad \dots\dots(M.4)$$

In this work, K values were determined from Si and SiO₂ wafers with known specific resistivity values. The results are shown in Tables M1 and M2 for the custom-built four-point probes having linear array geometry (for gas exposure) and in Table M3 for the one having square array geometry (for liquid exposure).

Table M1 Experimental data of K determination for the custom-built four-point probe #1 (linear array for gas exposure), measured at 25 ± 1 °C, 50 ± 10 %RH.

Material	ρ (Ω cm)	Thickness (cm)	Applied I (mA)	Volt drop (mV)	K
Si_A1	9.1E-03	7.2E-02	60.6	4.1	1.87E+00
Si_A1	9.1E-03	7.2E-02	82.6	5.6	1.87E+00
Si_A1	9.1E-03	7.2E-02	115.9	7.8	1.88E+00
Si_A1	9.1E-03	7.2E-02	153.4	10.2	1.90E+00
Si_A1	9.1E-03	7.2E-02	195.0	13.7	1.80E+00
Average					1.87E+00
Si_A2	9.3E-03	7.2E-02	69.4	5.6	1.61E+00
Si_A2	9.3E-03	7.2E-02	88.6	7.1	1.62E+00
Si_A2	9.3E-03	7.2E-02	109.5	8.8	1.62E+00
Si_A2	9.3E-03	7.2E-02	133.9	11.1	1.57E+00
Si_A2	9.3E-03	7.2E-02	173.1	14.4	1.56E+00
Average					1.59E+00
Si_A3	9.3E-03	7.2E-02	66.9	6.1	1.42E+00
Si_A3	9.3E-03	7.2E-02	97.1	8.4	1.50E+00
Si_A3	9.3E-03	7.2E-02	122.7	10.5	1.52E+00
Si_A3	9.3E-03	7.2E-02	166.0	14.8	1.46E+00
Si_A3	9.3E-03	7.2E-02	187.4	16.4	1.48E+00
Average					1.48E+00
Si_B1	1.2E+00	5.4E-02	0.6960	7.5	2.10E+00
Si_B1	1.2E+00	5.4E-02	0.7150	8.0	2.02E+00
Si_B1	1.2E+00	5.4E-02	0.8020	8.7	2.08E+00
Si_B1	1.2E+00	5.4E-02	0.8160	9.4	1.96E+00
Average					2.04E+00
Si_C1	3.6E+01	5.3E-02	0.0510	24.5	1.42E+00
Si_C1	3.6E+01	5.3E-02	0.0655	33.4	1.34E+00
Si_C1	3.6E+01	5.3E-02	0.0689	34.6	1.36E+00
Si_C1	3.6E+01	5.3E-02	0.0707	30.7	1.57E+00
Si_C1	3.6E+01	5.3E-02	0.0752	35.4	1.45E+00
Average					1.43E+00

Average K 1.68E+00
SD 2.63E-01

Table M2 Experimental data of K determination for the custom-built four-point probe #2 (linear array for gas exposure), measured at 25 ± 1 °C, 50 ± 10 %RH.

Material	ρ (Ω cm)	Thickness (cm)	Applied I (mA)	Volt drop (mV)	K
Si_A1	9.1E-03	7.2E-02	54.7	3.8	1.82E+00
Si_A1	9.1E-03	7.2E-02	70.7	4.7	1.90E+00
Si_A1	9.1E-03	7.2E-02	82.7	6.2	1.69E+00
Si_A1	9.1E-03	7.2E-02	104.4	7.8	1.69E+00
Si_A1	9.1E-03	7.2E-02	125.0	9.8	1.62E+00
Si_A1	9.1E-03	7.2E-02	180.5	14.1	1.62E+00
Average					1.72E+00
Si_A2	9.3E-03	7.2E-02	166.6	14.6	1.48E+00
Si_A2	9.3E-03	7.2E-02	80.5	6.9	1.52E+00
Si_A2	9.3E-03	7.2E-02	80.8	6.7	1.57E+00
Si_A2	9.3E-03	7.2E-02	107.3	9.2	1.51E+00
Si_A2	9.3E-03	7.2E-02	131.8	10.2	1.68E+00
Si_A2	9.3E-03	7.2E-02	133.1	10.8	1.60E+00
Average					1.56E+00
Si_A4	9.1E-03	7.2E-02	142.6	10.0	1.81E+00
Si_A4	9.1E-03	7.2E-02	154.3	11.2	1.74E+00
Si_A4	9.1E-03	7.2E-02	160.2	11.0	1.84E+00
Si_A4	9.1E-03	7.2E-02	157.0	11.0	1.82E+00
Si_A4	9.1E-03	7.2E-02	159.5	11.0	1.84E+00
Average					1.81E+00
Si_B1	1.2E+00	5.4E-02	0.5900	7.5	1.78E+00
Si_B1	1.2E+00	5.4E-02	0.7500	8.4	2.02E+00
Si_B1	1.2E+00	5.4E-02	0.8100	9.4	1.95E+00
Si_B1	1.2E+00	5.4E-02	0.8500	9.9	1.94E+00
Average					1.92E+00
Si_C1	3.6E+01	5.3E-02	0.0611	31.5	1.32E+00
Si_C1	3.6E+01	5.3E-02	0.0668	32.8	1.39E+00
Si_C1	3.6E+01	5.3E-02	0.0712	36.1	1.35E+00
Average					1.35E+00

Average K 1.67E+00
SD 2.23E-01

Table M3 Experimental data of K determination for the custom-built four-point probe (square array for liquid exposure), measured at 26 ± 1 °C, 55 ± 5 %RH.

Material	ρ (Ω cm)	Thickness (cm)	Applied I (mA)	Volt drop (mV)	K
SiO ₂ _A1	2.9E-01	5.3E-02	80.9	74.5	5.96E+00
SiO ₂ _A1	2.9E-01	5.3E-02	91.5	84.5	5.94E+00
SiO ₂ _A1	2.9E-01	5.3E-02	107.5	98.0	6.02E+00
SiO ₂ _A1	2.9E-01	5.3E-02	122.2	110.5	6.07E+00
SiO ₂ _A1	2.9E-01	5.3E-02	137.1	124.0	6.07E+00
SiO ₂ _A1	2.9E-01	5.3E-02	147.1	132.0	6.11E+00
Average					6.03E+00
SiO ₂ _B1	2.1E+00	7.2E-02	56.9	445.5	3.67E+00
SiO ₂ _B1	2.1E+00	7.2E-02	73.7	545.5	3.88E+00
SiO ₂ _B1	2.1E+00	7.2E-02	85.3	607.5	4.03E+00
SiO ₂ _B1	2.1E+00	7.2E-02	94.0	625.5	4.31E+00
SiO ₂ _B1	2.1E+00	7.2E-02	100.6	836.5	3.45E+00
Average					3.87E+00
Si_C2	3.5E+01	5.2E-02	2.93	830.5	2.35E+00
Si_C2	3.5E+01	5.2E-02	2.95	857.5	2.29E+00
Si_C2	3.5E+01	5.2E-02	3.22	896.5	2.39E+00
Si_C2	3.5E+01	5.2E-02	3.07	890.5	2.29E+00
Average					2.33E+00

Average K 4.08E+00
SD 1.86E+00

Appendix N Determination of Chemical Vapor Concentration for the Flow System

The concentration of a chemical saturated vapor at a particular temperature can be determined from its constants: A, B, and C, by using an Antoine equation (Seader *et al.*, 1998) as shown in Eqs. N.1 and N.2.

$$\text{Vapor pressure} = 10^{A-(B/(C+T))} \text{ mmHg} \quad \dots(\text{N.1})$$

$$\text{Saturated concentration at } T \text{ }^\circ\text{C} = \text{Vapor pressure} / 760 \times 100 \text{ Vol.}\% \quad \dots(\text{N.2})$$

Table N1 Antoine parameters of chemical studied in this work.

Chemical	A	B	C	Saturated concentration at 25 °C (Vol.%)
Water*	N/A	N/A	N/A	23.56
Toluene†	6.95464	1344.80	219.482	3.74
Acetone†	7.23160	1277.03	237.230	30.26
Acetic-acid†	7.29960	1479.02	216.820	2.01

* Saturated concentration at 25 °C was calculated from saturated concentration of water at 20 °C (17.5 Vol.%: Chou, 2000)

† A, B, and C constants were obtained from Seader *et al.* (1998)

The concentration of chemical vapors in the flow system can be varied by changing the chemical volume (V_{liq}) in a chemical container, using this correlation:

$$\text{Vapor concentration (Vol.}\%) = \frac{V_{liq}(\text{cm}^3) \times 22,400 (\text{cm}^3/\text{mole}) \times \rho (\text{g}/\text{cm}^3) \times 100}{V_{tot} (\text{cm}^3) \times \text{Mw} (\text{g}/\text{mole})} \dots(\text{N.3})$$

Where:

- V_{liq} = volume of liquid chemical in container
- V_{tot} = volume of the whole flow system
- ρ = density of chemical (0.791 g/cm³ for acetone)
- Mw = molecular weight of chemical (58.08 g/mole for acetone)

Appendix O Experimental Data of Conductivity Measurement and Electrical Conductivity Response of PPy and Its Blends

Table O1 The experimental conditions and data of conductivity measurement and electrical conductivity response toward water liquid of PPy/A5 and its blends.

Material	Run #	T (°C)	% RH	t (cm)	Applied current (A)	Voltage drop (V)	σ (S/cm)	Water exposure			
								$\Delta\sigma$ (S/cm)	$\Delta\sigma/\sigma_i \times 100$ (%)	t_r^\dagger (s)	t_{eqb}^\ddagger (s)
PPy/A5	1	25	59	0.007	3.4E-02	2.0E-01	6.2E+00	2.4E+00	39.50	2	635
PPy/A5	2	25	59	0.007	3.7E-02	1.8E-01	7.5E+00	1.9E+00	25.00	1	628
<u>Blends from Dry mixing</u>											
PPy/A5/PEO	1	27	51	0.018	3.1E-02	9.6E-01	4.6E-01	-3.6E-02	-7.88	3	999
PPy/A5/PMMA	1	27	51	0.007	2.6E-02	2.0E+00	4.5E-01	1.8E-01	40.27	19	346
PPy/A5/PMMA	2	27	51	0.008	2.7E-02	1.7E+00	4.8E-01	2.1E-01	44.55	22	689
PPy/A5/HDPE	1	27	51	0.007	2.3E-02	2.5E+00	3.6E-01	1.1E-01	29.67	55	380
<u>Blends from solution mixing</u>											
PPy/A5/PEO	1	25	59	0.040	8.0E-04	5.6E+00	8.9E-04	-5.4E-04	-61.06	3	183
PPy/A5/PMA	-	-	-	-	-	-	-	-	-	-	-
PPy/A5/PMMA	1	25	59	0.010	5.5E-04	2.4E+00	5.7E-03	1.6E-05	0.29	30	400
PPy/A5/PS	1	25	59	0.011	2.3E-03	1.9E+00	2.7E-02	1.1E-03	4.09	unclear	356
PPy/A5/PS	2	25	59	0.011	3.0E-03	1.9E+00	3.6E-02	-8.4E-04	-2.33	unclear	489
PPy/A5/PS	3	25	59	0.011	1.9E-03	1.9E+00	2.3E-02	1.1E-04	0.49	unclear	787
PPy/A5/ABS	1	25	59	0.011	1.5E-03	1.9E+00	1.8E-02	-1.5E-03	-8.35	1	464
PPy/A5/ABS	2	25	59	0.010	2.6E-03	5.3E+00	1.2E-02	-9.0E-04	-7.19	2	799
<u>Polymer-coated PPy/A5</u>											
PMMA-coated PPy/A5	1	26	70	0.006	4.3E-05	5.1E+00	3.6E-04	-4.5E-06	-1.26	210	1614
PMMA-coated PPy/A5	2	25	69	0.006	2.2E-05	6.7E+00	1.4E-04	-3.3E-06	-2.44	unclear	3000

† the time at which sample conductivity started to change (response time, t_r)

‡ the time sample needed to reach an equilibrium change (equilibrium time, t_{eqb})

Table O2 The experimental conditions and data of conductivity measurement and electrical conductivity response toward toluene liquid of PPy/A5 and its blends.

Material	Run #	T (°C)	% RH	t (cm)	Applied current (A)	Voltage drop (V)	σ (S/cm)	Toluene exposure			
								$\Delta\sigma$ (S/cm)	$\Delta\sigma/\sigma_i \times 100$ (%)	t_r (s)	t_{eqb} (s)
PPy/A5	1	25	59	0.006	3.1E-02	2.1E-01	6.2E+00	7.5E-02	1.20	unclear	628
<u>Blends from solution mixing</u>											
PPy/A5/PMMA	1	25	59	0.010	1.2E-03	5.1E+00	5.6E-03	-4.2E-03	-74.43	1	233
PPy/A5/PS	1	28	77	0.011	4.0E-03	4.6E+00	1.9E-02	-1.2E-02	-64.13	1	796
PPy/A5/ABS	1	25	59	0.011	1.5E-03	6.5E+00	5.4E-03	-3.5E-03	-65.25	1	455
<u>Polymer-coated PPy/A5</u>											
PMMA-coated PPy/A5	1	25	69	0.006	3.5E-06	1.1E+00	1.3E-04	1.7E-04	132.16	150	2500
PMMA-coated PPy/A5	2	25	69	0.006	3.4E-06	1.0E+00	1.4E-04	2.0E-04	146.09	9	3530

Table O3 The experimental conditions and data of conductivity measurement and electrical conductivity response toward acetone liquid of PPy/A5 and its blends.

Material	Run #	T (°C)	% RH	t (cm)	Applied current (A)	Voltage drop (V)	σ (S/cm)	Acetone exposure			
								$\Delta\sigma$ (S/cm)	$\Delta\sigma/\sigma_i \times 100$ (%)	t_r (s)	t_{eqb} (s)
PPy/A5	1	25	59	0.006	3.4E-02	1.8E-01	7.8E+00	-1.8E+00	-23.65	1	719
PPy/A5	2	25	59	0.006	3.4E-02	1.9E-01	7.5E+00	-2.5E+00	-33.22	1	927
<u>Blends from solution mixing</u>											
PPy/A5/PMMA	1	25	59	0.010	9.2E-04	2.9E+00	7.9E-03	-7.7E-03	-98.27	2	281
PPy/A5/PMMA	2	28	77	0.011	1.2E-03	7.0E+00	3.8E-03	-3.7E-03	-98.16	1	357
PPy/A5/PS	1	28	77	0.011	3.7E-03	6.6E+00	1.3E-02	-1.3E-02	-99.48	1	153
PPy/A5/PS	2	28	77	0.011	3.4E-03	6.7E+00	1.1E-02	-1.1E-02	-99.49	1	94
PPy/A5/ABS	1	25	59	0.011	1.4E-03	3.5E+00	8.9E-03	-8.8E-03	-98.81	1	817
PPy/A5/ABS	2	28	58	0.010	2.5E-03	5.8E+00	1.1E-02	-1.0E-02	-97.11	1	395
<u>Polymer-coated PPy/A5</u>											
PMMA-coated PPy/A5	1	26	70	0.006	9.3E-05	5.1E+00	7.7E-04	-7.3E-04	-94.617	1144	1614

Table O4 The experimental conditions and data of conductivity measurement and electrical conductivity response toward glacial acetic acid liquid of PPy/A5 and its blends.

Material	Run #	T (°C)	% RH	t (cm)	Applied current (A)	Voltage drop (V)	σ (S/cm)	Acetic acid exposure			
								$\Delta\sigma$ (S/cm)	$\Delta\sigma/\sigma_i \times 100$ (%)	t_r (s)	t_{eqb} (s)
PPy/A5	1	25	59	0.006	3.1E-02	1.6E-01	7.8E+00	-4.4E-01	-27.21	1	614
<u>Blends from solution mixing</u>											
PPy/A5/PMMA	1	25	59	0.010	1.1E-03	6.1E+00	4.4E-03	-2.3E-03	-51.97	0	397
PPy/A5/PMMA	2	28	58	0.011	1.4E-03	5.2E+00	6.2E-03	-3.7E-03	-58.66	1	381
PPy/A5/PS	1	28	77	0.011	3.7E-03	7.1E+00	1.2E-02	-6.5E-03	-55.03	2	578
PPy/A5/PS	2	28	77	0.011	3.3E-03	4.6E+00	1.6E-02	-9.6E-03	-58.97	1	140
PPy/A5/ABS	1	25	59	0.011	1.1E-03	2.1E+00	1.2E-02	-4.8E-03	-38.72	1	177
PPy/A5/ABS	2	28	58	0.010	2.4E-03	6.2E+00	9.5E-03	-4.8E-03	-50.48	1	250
<u>Polymer-coated PPy/A5</u>											
PMMA-coated PPy/A5	1	28	67	0.006	4.8E-04	4.2E+00	4.3E-04	-3.3E-04	-76.26	885	3000

Table O5 The experimental conditions and data of reproducibility measurement in electrical conductivity response toward saturated acetone vapor in N₂ of PPy/A/PMMA from solution mixing at various PMMA:PPy weight ratios.

Material	PMMA/PPy ratio	n	T (°C)	%RH	t (cm)	Applied current (A)	Voltage drop (V)	σ (S/cm)	Acetone exposure		
									$\Delta\sigma$ (S/cm)	$\Delta\sigma/\sigma_1 \times 100$ (%)	σ_n/σ_1
PPy/A	0	1	26	43	0.006	2.52E-02	9.27E-02	2.77E+01	-4.32E-01	-1.57	1.00
		2	25	49		3.00E-03	1.07E-02	2.85E+01	-6.88E-01	-2.44	1.03
		3	26	48		3.18E-03	1.12E-02	2.89E+01	-6.55E-01	-2.29	1.04
		4	26	49		3.29E-03	1.15E-02	2.92E+01	-7.20E-01	-2.49	1.05
		5	26	59		3.50E-03	1.22E-02	2.93E+01	-7.10E-01	-2.16	1.06
1.0 PMMA/PPy/A	1	1	25	44	0.028	2.10E-03	2.73E+00	1.64E-02	-2.85E-03	-17.43	1.00
		2	24	54		1.57E-03	1.95E+00	1.72E-02	-3.22E-03	-16.55	1.05
		3	24	49		1.42E-03	1.72E+00	1.75E-02	-3.29E-03	-18.75	1.07
		4	25	47		1.52E-03	1.89E+00	1.71E-02	-	-	1.05
1.0 PMMA/PPy/A	1	1	25	44	0.027	1.53E-03	2.47E+00	1.35E-02	-1.87E-03	-13.88	1.00
		2	24	54		1.50E-03	1.90E+00	1.73E-02	-3.11E-03	-18.00	1.27
		3	24	49		1.83E-03	2.73E+00	1.47E-02	-2.71E-03	-18.42	1.09
		4	25	47		1.54E-03	2.31E+00	1.45E-02	-	-	1.07
2.0 PMMA/PPy/A	2	1	26	43	0.034	8.04E-04	2.14E+00	6.53E-03	-3.30E-03	-50.46	1.00
		2	25	49		7.79E-04	2.80E+00	4.84E-03	-1.39E-03	-28.80	0.74
		3	26	48		7.77E-04	2.82E+00	4.80E-03	-1.29E-03	-26.94	0.73
		4	26	49		8.04E-04	2.88E+00	4.84E-03	-1.22E-03	-25.21	0.74
		5	26	59		8.29E-04	2.94E+00	4.90E-03	-9.45E-04	-19.27	0.75
3.0 PMMA/PPy/A	3	1	25	54	0.020	1.30E-03	1.99E+00	1.95E-02	-1.32E-02	-67.76	1.00
		2	26	57		6.15E-04	2.15E+00	8.52E-03	-4.54E-03	-53.30	0.44
		3	25	52		3.95E-04	2.04E+00	5.79E-03	-1.02E-03	-17.67	0.30
		4	26	53		4.18E-04	2.05E+00	6.07E-03	-1.14E-03	-18.80	0.31
		5	26	52		4.26E-04	2.06E+00	6.17E-03	-	-	0.32
3.0 PMMA/PPy/A	3	1	25	54	0.018	3.86E-03	2.59E+00	4.95E-02	-3.60E-02	-72.73	1.00
		2	26	57		1.14E-04	2.09E-01	1.81E-02	-1.10E-02	-61.07	0.37
		3	25	52		1.72E-04	4.96E-01	1.15E-02	-2.69E-03	-23.34	0.23
		4	26	53		2.24E-04	6.09E-01	1.22E-02	-2.97E-03	-24.34	0.25
		5	26	52		1.99E-04	5.40E-01	1.22E-02	-	-	0.25

Table O5 The experimental conditions and data of reproducibility measurement in electrical conductivity response toward saturated acetone vapor in N₂ of PPy/A/PMMA from solution mixing at various PMMA:PPy weight ratios (continued).

Material	PMMA/PPy ratio	n	T (°C)	%RH	t (cm)	Applied current (A)	Voltage drop (V)	σ (S/cm)	Acetone exposure		
									$\Delta\sigma$ (S/cm)	$\Delta\sigma/\sigma_i \times 100$ (%)	σ_n/σ_1
4.0 PMMA/PPy/A	4	1	26	53	0.017	2.31E-04	3.33E+00	2.45E-03	-2.28E-03	-93.29	1.00
		2	26	43		3.55E-05	2.92E+00	4.29E-04	-1.89E-04	-44.06	0.18
		3	26	50		4.10E-05	3.03E+00	4.76E-04	-2.15E-04	-45.13	0.19
		4	25	44		5.40E-05	3.41E+00	5.58E-04	-4.63E-04	-82.81	0.23
		5	27	53		2.28E-02	2.67E+03	3.01E-04	-2.36E-05	-7.83	0.12
4.0 PMMA/PPy/A	4	1	26	53	0.018	3.04E-04	2.16E+00	4.67E-03	-4.22E-03	-90.39	1.00
		2	26	43		5.90E-05	3.34E+00	5.87E-04	-1.54E-04	-26.18	0.13
		3	26	50		5.90E-05	3.27E+00	5.98E-04	-2.43E-04	-40.65	0.13
		4	25	44		4.30E-05	3.94E+00	3.62E-04	-2.79E-04	-77.05	0.08
		5	27	53		2.28E-02	4.04E+03	1.87E-04	-3.06E-05	-16.39	0.04

Table O6 The experimental conditions and data of reproducibility measurement in electrical conductivity response toward saturated acetic acid vapor in N₂ of PPy/A/PMMA from solution mixing at various PMMA:PPy weight ratios.

Material	PMMA/PPy ratio	n	T (°C)	%RH	t (cm)	Applied current (A)	Voltage drop (V)	σ (S/cm)	Acetic acid exposure		
									$\Delta\sigma$ (S/cm)	$\Delta\sigma/\sigma_i \times 100$ (%)	σ_n/σ_1
PPy/A	0	1	26	59	0.006	3.45E-03	1.20E-02	2.90E+01	-6.24E-01	-2.15	1.00
		2	25	55		5.96E-03	2.05E-02	2.94E+01	-2.21E-01	-0.75	1.01
		3	26	44		9.16E-03	3.26E-02	2.83E+01	-4.19E-01	-1.48	0.98
		4	25	49		6.24E-03	2.13E-02	2.96E+01	-1.06E+00	-3.57	1.02
		5	26	49		8.67E-03	2.93E-02	2.99E+01	-1.24E+00	-4.15	1.03
1.0 PMMA/PPy/A	1	1	24	50	0.028	1.59E-03	1.97E+00	1.72E-02	-1.55E-03	-9.02	1.00
		2	25	49		1.69E-03	1.99E+00	1.80E-02	-3.41E-03	-18.91	1.05
		3	25	49		1.65E-03	1.97E+00	1.78E-02	-3.12E-03	-17.57	1.03
		4	25	49		1.69E-03	2.01E+00	1.79E-02	-3.09E-03	-17.32	1.04
		5	25	47		1.72E-03	2.08E+00	1.75E-02	-3.40E-03	-19.43	1.02

Table O6 The experimental conditions and data of reproducibility measurement in electrical conductivity response toward saturated acetic acid vapor in N₂ of PPy/A/PMMA from solution mixing at various PMMA:PPy weight ratios (continued).

Material	PMMA/PPy ratio	n	T (°C)	%RH	t (cm)	Applied current (A)	Voltage drop (V)	σ (S/cm)	Acetic acid exposure		
									$\Delta\sigma$ (S/cm)	$\Delta\sigma/\sigma_i \times 100$ (%)	σ_n/σ_1
1.0 PMMA/ PPy/A	1	1	24	50	0.027	1.28E-03	1.92E+00	1.46E-02	-8.40E-04	-5.74	1.00
		2	25	49		1.40E-03	2.00E+00	1.54E-02	-2.25E-03	-14.64	1.05
		3	25	49		1.65E-03	2.04E+00	1.78E-02	-3.02E-03	-17.03	1.21
		4	25	49		1.69E-03	2.08E+00	1.79E-02	-3.26E-03	-18.28	1.22
		5	25	47		1.30E-03	1.97E+00	1.45E-02	-2.12E-03	-14.56	0.99
2.0 PMMA/ PPy/A	2	1	26	59	0.034	8.29E-04	2.93E+00	4.90E-03	-9.45E-04	-19.27	1.00
		2	25	55		9.03E-04	3.04E+00	5.16E-03	-1.13E-03	-21.95	1.05
		3	26	44		7.93E-04	2.90E+00	4.74E-03	-3.00E-03	-63.20	0.97
		4	25	49		4.68E-04	2.90E+00	2.80E-03	-8.53E-04	-30.45	0.57
		5	26	49		1.38E-03	3.05E+00	7.87E-03	-3.43E-03	-43.59	1.60
3.0 PMMA/ PPy/A	3	1	26	47	0.014	5.20E-04	1.16E+01	1.95E-03	-5.12E-04	-26.21	1.00
		2	26	50		9.03E-04	2.19E+01	1.80E-03	-3.78E-04	-21.05	0.92
		3	27	61		1.27E-03	2.68E+01	2.06E-03	-2.97E-04	-14.40	1.06
		4	27	59		1.55E-03	3.20E+01	2.11E-03	-4.47E-04	-21.13	1.08
4.0 PMMA/ PPy/A	4	1	26	54	0.017	2.72E-04	2.75E+00	3.46E-03	-1.29E-03	-37.39	1.00
		2	25	45		2.53E-04	2.95E+00	3.00E-03	-8.30E-04	-27.64	0.87
		3	26	53		2.31E-04	3.31E+00	2.45E-03	-2.28E-03	-93.29	0.71
		4	26	43		3.55E-05	2.90E+00	4.29E-04	-	-	0.12
4.0 PMMA/ PPy/A	4	1	26	54	0.018	2.16E-04	2.00E+00	3.57E-03	-1.91E-03	-53.48	1.00
		2	25	45		4.81E-04	2.01E+00	7.91E-03	-3.84E-03	-48.54	2.22
		3	26	53		3.04E-04	2.16E+00	4.67E-03	-4.22E-03	-90.39	1.31
		4	26	43		5.90E-05	3.33E+00	5.87E-04	-	-	0.16

Table O7 The experimental conditions and data of a study of the effect of humidity on electrical conductivity response toward saturated acetone vapor in N₂ of PPy/A/PMMA from solution mixing at PMMA:PPy weight ratios of 3:1.

Sample #	T (°C)	%RH	t (cm)	Applied current (A)	Voltage drop (V)	σ (S/cm)	Acetone exposure		
							t_{cab} (sec)	$\Delta\sigma$ (S/cm)	$\Delta\sigma/\sigma_i \times 100$ (%)
1	26	20	0.026	2.25E-04	4.27E+00	1.21E-03	8	-9.90E-04	-81.59
2	26	20	0.040	1.96E-04	2.39E+00	1.22E-03	8	-1.05E-03	-86.19
3	26	31	0.026	3.63E-04	5.02E+00	1.66E-03	12	-9.33E-04	-56.13
4	26	31	0.026	3.35E-04	6.40E+00	1.20E-03	12	-7.54E-04	-62.81
5	24	48	0.020	1.44E-04	2.91E+00	1.47E-03	6	-1.02E-03	-68.98
6	26	48	0.017	8.04E-04	2.56E+00	1.11E-02	15	-5.58E-03	-50.46
7	25	48	0.020	1.30E-03	2.38E+00	1.95E-02	29	-1.38E-02	-70.83
8	25	48	0.018	3.86E-03	3.10E+00	4.73E-02	33	-3.44E-02	-72.73
9	26	70	0.026	2.95E-04	6.26E+00	1.08E-03	26	-6.49E-04	-59.85
10	26	70	0.026	2.01E-04	4.34E+00	1.07E-03	26	-5.93E-04	-55.62

Table O8 The experimental conditions and data of a study of effect of humidity on electrical conductivity response toward saturated acetic acid vapor in N₂ of PPy/A/PMMA from solution mixing at PMMA:PPy weight ratios of 3:1.

Sample #	T (°C)	%RH	t (cm)	Applied current (A)	Voltage drop (V)	σ (S/cm)	Acetic acid exposure		
							t_{cab} (sec)	$\Delta\sigma$ (S/cm)	$\Delta\sigma/\sigma_i \times 100$ (%)
1	26	20	0.020	5.23E-05	1.17E+00	1.34E-03	44	-3.50E-04	-26.19
2	26	20	0.020	9.03E-05	2.19E+00	1.23E-03	42	-2.62E-04	-21.31
3	25	47	0.020	1.35E-04	2.92E+00	1.38E-03	45	-2.94E-04	-21.40
4	25	47	0.018	1.99E-04	6.47E+00	1.02E-03	36	-3.08E-03	-30.14
5	27	70	0.014	1.22E-04	3.23E+00	1.65E-03	40	-3.62E-04	-21.93
6	27	70	0.016	1.24E-04	2.97E+00	1.56E-03	43	-1.94E-04	-12.45

Appendix P Experimental Data of Electrical Conductivity Measurement of PPy at Aging Time more than 1 Year

Table P1 Experimental conditions and data of electrical conductivity measurement of PPy/U and PPy doped with various dopants at D/M of 1/12 at aging time more than 1 year.

Material	Synthesis date (mm/dd/yy)	Age (day)	t (cm)	T (°C)	% RH	Applied voltage (V)	Applied current (mA)	Voltage drop (mV)	σ (S/cm)	Average σ (S/cm)
PPy/U (1)	03/21/00	612	7.18E-03 (1.85E-04)	25.5	58	12.0	3.30	1720	6.68E-02	6.87E-02 (1.68E-03)
						14.5	4.00	2070	6.73E-02	
						16.9	4.80	2420	6.91E-02	
						20.8	5.90	2950	6.97E-02	
						23.7	6.90	3390	7.09E-02	
PPy/U (2)	08/20/00	463	8.53E-03 (2.43E-04)	25.8	57	10.9	4.40	1695	7.61E-02	7.70E-02 (9.01E-04)
						13.7	5.50	2095	7.70E-02	
						18.7	7.60	2860	7.79E-02	
PPy/U (3)	08/22/00	461	7.79E-03 (3.90E-04)	25.8	57	7.5	1.00	1035	3.10E-02	3.26E-02 (8.87E-04)
						11.6	1.60	1565	3.28E-02	
						16.7	2.30	2240	3.30E-02	
						21.1	2.90	2825	3.30E-02	
						24.7	3.40	3290	3.32E-02	
PPy/A (1)	08/31/99	813	5.70E-03 (3.42E-04)	25	56	0.3	15.90	47	1.48E+01	1.62E+01 (7.26E-01)
						0.5	23.35	65	1.58E+01	
						0.7	28.35	78	1.59E+01	
						0.8	35.75	96	1.63E+01	
						1.0	42.45	113	1.65E+01	
						1.2	51.35	134	1.68E+01	
						1.4	60.35	156	1.70E+01	
PPy/A (2)	08/23/00	460	5.59E-03 (3.32E-04)	25.5	56	0.6	29.85	77	1.73E+01	1.77E+01 (3.49E-01)
						0.7	37.45	96	1.74E+01	
						0.9	43.85	110	1.78E+01	
						1.0	51.70	129	1.80E+01	
						1.2	59.25	146	1.81E+01	
PPy/B (1)	08/31/99	817	6.01E-03 (3.80E-04)	25.8	57	2.4	69.15	210	1.37E+01	1.39E+01 (1.63E-01)
						2.7	80.00	240	1.39E+01	
						3.0	94.90	282	1.40E+01	
PPy/B (2)	11/02/99	755	6.66E-03 (2.29E-03)	26.5	60	1.3	56.90	168	1.27E+01	1.31E+01 (2.88E-01)
						1.6	74.50	216	1.29E+01	
						2.1	97.00	275	1.32E+01	
						2.4	111.30	313	1.33E+01	

Table P1 Experimental data of electrical conductivity measurement of PPy doped with various dopants at D/M of 1/12 at aging time more than 1 year (continued).

Material	Synthesis date (mm/dd/yy)	Age (day)	t (cm)	T (°C)	% RH	Applied voltage (V)	Applied current (mA)	Voltage drop (mV)	σ (S/cm)	Average σ (S/cm)
PPy/B (3)	08/20/00	463	6.20E-03 (1.08E-03)	26.5	60	0.6	25.85	140	7.45E+00	7.68E+00 (2.34E-01)
						0.9	31.45	170	7.46E+00	
						1.4	44.15	230	7.74E+00	
						1.8	53.05	275	7.78E+00	
						2.2	61.50	310	8.00E+00	
PPy/B (4)	08/31/99	828	5.78E-03 (1.58E-03)	26.5	60	2.0	64.80	203	1.38E+01	1.40E+01 (2.05E-01)
						2.3	75.10	232	1.40E+01	
						2.5	87.10	265	1.42E+01	
PPy/B (5)	01/19/00	689	5.69E-03 (8.83E-04)	25.8	57	1.0	47.10	143	1.45E+01	1.47E+01 (1.94E-01)
						1.3	59.15	178	1.46E+01	
						1.4	68.05	202	1.48E+01	
						1.6	78.35	231	1.49E+01	
PPy/C (1)	01/12/00	681	6.93E-03 (6.24E-04)	26	59	8.7	8.70	1235	2.54E-01	2.62E-01 (7.79E-03)
						10.7	10.90	1540	2.55E-01	
						13.4	14.00	1930	2.62E-01	
						15.7	16.80	2280	2.66E-01	
						18.5	20.70	2735	2.73E-01	
PPy/D (1)	08/18/00	465	3.06E-03 (3.27E-04)	25.7	58	8.4	1.70	1245	1.12E-01	1.13E-01 (2.20E-03)
						10.5	2.10	1540	1.12E-01	
						15.2	3.00	2200	1.12E-01	
						19.1	3.90	2770	1.15E-01	
						23.1	4.75	3350	1.16E-01	
PPy/D (2)	03/16/00	632	6.16E-03 (5.11E-04)	25.7	58	18.4	1.78	2215	3.26E-02	3.35E-02 (8.32E-04)
						23.1	2.30	2820	3.31E-02	
						27.1	2.75	3305	3.37E-02	
						32.5	3.38	3965	3.46E-02	
PPy/D (3)	08/18/00	480	5.78E-03 (7.77E-04)	25.8	58	6.7	1.65	560	1.27E-01	1.31E-01 (3.31E-03)
						11.7	2.90	961	1.30E-01	
						16.6	4.40	1420	1.34E-01	
PPy/E (1)	01/11/00	682	6.71E-03 (6.48E-04)	25.6	57	9.2	5.50	1175	1.74E-01	1.79E-01 (4.15E-03)
						12.3	7.40	1555	1.77E-01	
						15.9	9.70	2000	1.81E-01	
						19.0	11.90	2410	1.84E-01	
PPy/E (2)	01/11/00	682	6.84E-03 (7.67E-04)	25.6	57	9.9	3.90	1020	1.40E-01	1.42E-01 (2.47E-03)
						12.1	4.85	1255	1.41E-01	
						14.9	6.10	1555	1.43E-01	
						17.7	7.30	1835	1.45E-01	
PPy/P (1)	01/10/00	683	6.46E-03 (2.37E-04)	25.6	57	5.4	5.90	875	2.61E-01	2.67E-01 (5.86E-03)
						7.3	8.00	1175	2.63E-01	
						9.8	10.95	1577	2.68E-01	
						12.2	14.00	1976	2.74E-01	

Table P1 Experimental data of electrical conductivity measurement of PPy doped with various dopants at D/M of 1/12 at aging time more than 1 year (continued).

Material	Synthesis date (mm/dd/yy)	Age (day)	t (cm)	T (°C)	% RH	Applied voltage (V)	Applied current (mA)	Voltage drop (mV)	σ (S/cm)	Average σ (S/cm)
PPy/P (2)	01/10/00	683	6.84E-03 (2.57E-04)	25.8	58	9.7	6.80	801	3.10E-01	3.13E-01 (2.89E-03)
						13.1	9.30	1076	3.16E-01	
						17.1	12.30	1447	3.11E-01	
						21.4	15.65	1815	3.15E-01	
PPy/AB	08/17/00	466	5.89E-03 (4.65E-04)	25.5	58	33.4	0.35	400	3.71E-05	3.71E-05 (4.52E-08)
						43.0	0.45	515	3.71E-05	
						58.2	0.60	685	3.72E-05	

Table P2 Experimental conditions and data of electrical conductivity measurement of PPy/A with various D/M ratios at aging time more than 1 year.

D/M	Synthesis date (mm/dd/yy)	Age (day)	t (cm)	T (°C)	% RH	Applied voltage (V)	Applied current (mA)	Voltage drop (mV)	σ (S/cm)	Average σ (S/cm)
1/96 (1)	07/24/00	504	5.66E-03 (1.50E-04)	25	54	0.91	11.90	109	4.82E+00	4.81E+00 (3.69E-01)
						2.94	36.25	341	4.70E+00	
						4.05	52.30	470	4.92E+00	
1/96 (2)	07/24/00	504	5.28E-03 (1.06E-04)	25	54	1.84	19.10	221	4.09E+00	4.14E+00 (6.78E-02)
						2.88	30.25	342	4.19E+00	
1/48	10/28/99	755	5.39E-03 (4.91E-04)	25.7	58	1.08	37.25	126	1.37E+01	1.40E+01 (2.12E-01)
						1.37	47.70	159	1.39E+01	
						1.66	58.25	192	1.41E+01	
						1.87	66.45	217	1.42E+01	
1/24 (1)	09/06/99	807	5.53E-03 (4.37E-04)	25.5	57	1.83	57.80	213	1.23E+01	1.24E+01 (9.35E-02)
						2.08	65.95	241	1.24E+01	
						2.22	70.80	257	1.25E+01	
1/6	07/25/00	503	5.91E-03 (7.69E-04)	26.5	60	1.50	54.10	547	4.19E+00	4.21E+00 (2.18E-02)
						1.67	64.60	650	4.21E+00	
						1.85	72.15	722	4.23E+00	
1/3	07/27/00	501	5.28E-03 (4.44E-04)	26.5	60	4.27	28.10	211	6.31E+00	6.42E+00 (9.30E-02)
						6.09	38.90	285	6.47E+00	
						7.19	51.45	376.5	6.47E+00	
1/2 (1)	09/02/99	811	5.14E-03 (2.77E-04)	25.5	57	1.90	23.55	265	4.32E+00	4.38E+00 (4.64E-02)
						2.40	28.30	316	4.36E+00	
						3.00	35.20	390	4.39E+00	
						3.70	42.45	466	4.43E+00	

Table P2 Experimental conditions and data of electrical conductivity measurement of PPy/A with various D/M ratios at aging time more than 1 year (continued).

D/M	Synthesis date (mm/dd/yy)	Age (day)	t (cm)	T (°C)	% RH	Applied voltage (V)	Applied current (mA)	Voltage drop (mV)	σ (S/cm)	Average σ (S/cm)
1/2 (2)	09/03/99	810	5.65E-03 (8.59E-04)	25.5	57	0.59	7.40	100	3.27E+00	2.99E+00 (3.40E-01)
						1.17	14.40	188.5	3.38E+00	
						2.26	27.10	372.5	3.22E+00	
						3.18	31.50	516	2.70E+00	
						4.13	38.75	650.5	2.64E+00	
						6.00	61.30	1004.5	2.70E+00	
1/2 (3)	07/26/00	502	5.48E-03 (4.00E-04)	25.8	58	2.02	33.55	243.5	6.28E+00	6.34E+00 (5.68E-02)
						2.37	39.65	285	6.34E+00	
						2.90	46.85	334	6.40E+00	
2/3	09/02/99	811	5.14E-03 (2.83E-04)	25.5	57	1.50	29.90	220	6.61E+00	6.80E+00 (1.57E-01)
						1.80	35.25	257	6.67E+00	
						2.50	46.45	335	6.75E+00	
						3.00	55.85	398	6.83E+00	
						3.50	66.05	464	6.93E+00	
						4.00	75.85	525	7.03E+00	
1/1	09/02/99	811	1.18E-02 (1.16E-03)	26	57	4.96	52.95	557	2.02E+00	2.06E+00 (5.15E-02)
						5.70	62.60	646.5	2.05E+00	
						6.49	73.35	734.5	2.12E+00	
1/1	09/02/99	303	1.29E-02 (2.22E-03)	25	50	N/A	22.10	73	5.88E+00	5.79E+00 (1.30E-01)
						N/A	87.55	298.5	5.70E+00	

Appendix Q Experimental data of electrical conductivity response measurement of PPy toward acetone vapor at 16.7 vol.% in N₂

Table Q1 Experimental data of electrical conductivity response study of PPy toward acetone vapor at 16.7 vol.% in N₂, 1 atm and at 23-26 °C, sample thickness values are shown with their standard derivations in parentheses (data of PPy/B are excluded; they are shown only in Table Q3 due to the different data format).

Material	Thickness (cm)	Applied current (mA)	Voltage drop (mV)	σ (S/cm)	Acetone exposure	
					$\Delta\sigma$ (S/cm)	$\Delta\sigma/\sigma_i \times 100$ (%)
PPy/U (3)	1.05E-02 (3.46E-02)	2.15	43.90	3.16E+00	-7.10E-03	-0.23
PPy/U (4)	1.09E-02 (3.35E-02)	1.17	23.24	3.12E+00	-8.03E-03	-0.26
PPy/A (5)	6.47E-03 (3.02E-04)	22.42	92.86	2.52E+01	-3.75E-01	-1.49
PPy/A (3)	1.80E-02 (2.52E-03)	28.41	49.95	2.14E+01	-3.86E-01	-1.81
PPy/C (1)	9.22E-03 (1.49E-03)	22.20	482.98	3.36E+00	-2.88E-02	-0.86
PPy/C (1)	9.22E-03 (1.49E-03)	24.40	535.11	3.34E+00	-2.10E-02	-0.63
PPy/C (2)	8.94E-03 (1.13E-03)	21.61	518.39	3.15E+00	-1.99E-02	-0.63
PPy/D	1.34E-02 (1.16E-03)	1.17	561.13	1.05E-01	-1.69E-02	-16.13
PPy/E (1)	9.60E-03 (1.33E-03)	23.00	543.14	2.98E+00	-3.74E-02	-1.26
PPy/E (1)	9.60E-03 (1.33E-03)	21.60	517.85	2.93E+00	-6.35E-02	-2.17
PPy/E (2)	9.10E-03 (5.94E-04)	4.29	107.24	2.97E+00	-6.41E-02	-2.16
PPy/E (2)	9.10E-03 (5.94E-04)	4.85	118.69	3.03E+00	-7.56E-02	-2.50
PPy/P (1)	1.03E-02 (9.31E-04)	2.45	185.82	8.66E-01	-2.89E-02	-3.34
PPy/P (1)	1.03E-02 (9.31E-04)	2.61	209.59	8.19E-01	-1.62E-02	-1.97
PPy/AB (2B)	9.21E-03 (2.99E-03)	0.05	3013.00	1.20E-03	-3.00E-04	-24.99

Table Q2 Experimental data of electrical conductivity response study of PPy/A with various D/M ratios toward acetone vapor at 16.7 vol.% in N₂, 1 atm and at 25 ± 1 °C (excluding data of PPy/A with D/M ratio of 1/12 which is shown in Table Q1).

Material	Thickness (cm)	Applied current (mA)	Voltage drop (mV)	σ (S/cm)	Acetone exposure	
					$\Delta\sigma$ (S/cm)	$\Delta\sigma/\sigma_i \times 100$ (%)
1/96	1.10E-02 (1.16E-03)	20.07	57.33	1.89E+01	-4.33E-02	-0.23
1/48	9.66E-03 (1.50E-03)	20.57	48.89	2.60E+01	-1.45E-01	-0.56
1/24	9.44E-03 (4.30E-04)	20.26	51.25	2.50E+01	-3.50E-01	-1.40
1/6	1.03E-02 (5.45E-04)	20.07	72.76	1.60E+01	-3.81E-01	-2.38
1/6	1.03E-02 (5.45E-04)	20.09	56.05	2.08E+01	-4.20E-01	-2.02
1/3 (1)	9.75E-03 (1.23E-03)	20.77	179.15	7.10E+00	-1.48E-01	-2.08
1/3 (1)	9.75E-03 (1.23E-03)	20.78	113.58	1.12E+01	-3.50E-01	-3.13
1/3 (2)	1.09E-02 (1.63E-03)	20.41	123.50	9.04E+00	-2.80E-01	-3.10
1/2 (1)	1.10E-02 (2.26E-03)	20.96	128.88	8.80E+00	-4.09E-01	-4.65
1/2 (1)	1.10E-02 (2.26E-03)	21.21	88.28	1.30E+01	-2.67E-01	-2.05
1/2 (1)	1.10E-02 (2.26E-03)	21.29	159.11	7.24E+00	-2.81E-01	-3.88
1/2 (2)	8.99E-03 (6.52E-04)	20.72	91.13	1.51E+01	-5.51E-01	-3.65
2/3	1.01E-02 (1.36E-03)	21.75	132.04	9.70E+00	-2.90E-01	-2.99
2/3	1.01E-02 (1.36E-03)	21.20	91.13	1.37E+01	-4.00E-01	-2.92
1/1 (1A)	9.16E-03 (1.68E-03)	20.72	198.62	6.80E+00	-2.20E-01	-3.24
1/1 (1A)	9.16E-03 (1.68E-03)	24.96	162.67	1.00E+01	-2.70E-01	-2.70
1/1 (1B)	8.66E-03 (3.34E-04)	23.93	103.12	1.60E+01	-3.20E-01	-2.00

Appendix R Experimental Data of Electrical Conductivity Response

Measurement of PPy toward Acetone Vapor at Various Concentration in N₂

Table R1 Experimental data of electrical conductivity response study of PPy/U toward acetone vapor at various concentrations in N₂, 1 atm and at 23-25 °C, sample thickness values are shown with their standard derivations in parentheses.

Material	Thickness (cm)	Applied current (mA)	Voltage drop (mV)	σ (S/cm)	Acetone exposure		
					Acetone vapor conc. (vol.%)	$\Delta\sigma$ (S/cm)	$\Delta\sigma/\sigma_i \times 100$ (%)
PPy/U (1)	1.15E-02 (1.59E-03)	1.37	32.92	2.45E+00	0.00	3.91E-04	0.02
PPy/U (1)	1.15E-02 (1.59E-03)	1.37	32.88	2.45E+00	0.00	-1.16E-04	0.00
PPy/U (1)	1.15E-02 (1.59E-03)	2.05	48.11	2.51E+00	3.33	-2.46E-03	-0.10
PPy/U (2)	1.27E-02 (2.38E-03)	1.22	28.21	2.29E+00	3.33	-2.81E-03	-0.12
PPy/U (1)	1.15E-02 (1.59E-03)	1.31	31.44	2.45E+00	8.32	-4.70E-03	-0.19
PPy/U (3)	1.05E-02 (3.46E-02)	2.15	43.90	3.16E+00	16.65	-7.10E-03	-0.23
PPy/U (4)	1.09E-02 (3.35E-02)	1.17	23.24	3.12E+00	16.65	-8.03E-03	-0.26
PPy/U (1)	1.15E-02 (1.59E-03)	1.37	32.89	2.45E+00	24.97	-1.17E-02	-0.48
PPy/U (1)	1.15E-02 (1.59E-03)	1.38	33.20	2.44E+00	24.97	-8.54E-03	-0.35
PPy/U (1)	1.15E-02 (1.59E-03)	2.04	48.36	2.48E+00	33.30	-8.47E-03	-0.34
PPy/U (1)	1.15E-02 (1.59E-03)	1.37	33.13	2.44E+00	33.30	-9.65E-03	-0.40
PPy/U (2)	1.27E-02 (2.38E-03)	1.22	27.92	2.31E+00	33.30	-1.01E-02	-0.44

Table R2 Experimental data of electrical conductivity response study of PPy/A toward acetone vapor at various concentrations in N₂, 1 atm and at 23-25 °C.

Material	Thickness (cm)		Applied current (mA)	Voltage drop (mV)	σ (S/cm)	Acetone exposure		
						Acetone vapor conc. (vol.%)	$\Delta\sigma$ (S/cm)	$\Delta\sigma/\sigma_i \times 100$ (%)
PPy/A (1)	9.48E-03	(6.17E-04)	21.81	48.83	3.18E+01	0.025	-1.68E-02	-0.05
PPy/A (2A)	8.08E-03	(7.65E-04)	21.68	83.60	2.17E+01	0.025	-9.94E-03	-0.05
PPy/A (3)	1.80E-02	(2.52E-03)	27.25	42.86	2.39E+01	0.25	-1.45E-02	-0.06
PPy/A (1)	9.48E-03	(6.17E-04)	21.29	47.46	3.19E+01	0.25	-1.19E-02	-0.04
PPy/A (1)	9.48E-03	(6.17E-04)	21.66	48.94	3.15E+01	1.05	-1.16E-01	-0.37
PPy/A (3)	1.80E-02	(2.52E-03)	27.81	44.28	2.36E+01	1.05	-1.04E-01	-0.44
PPy/A (4A)	9.30E-03	(2.67E-03)	21.82	78.13	2.03E+01	1.05	-7.82E-02	-0.39
PPy/A (3)	1.80E-02	(2.52E-03)	29.84	48.83	2.29E+01	2.51	-1.87E-01	-0.81
PPy/A (4A)	9.30E-03	(2.67E-03)	27.25	94.87	2.08E+01	2.51	-1.52E-01	-0.73
PPy/A (4B)	1.12E-02	(1.95E-03)	20.55	45.60	2.71E+01	2.51	-2.00E-01	-0.74
PPy/A (4C)	9.10E-03	(8.65E-03)	22.42	73.50	2.26E+01	2.51	-1.49E-01	-0.66
PPy/A (5)	6.47E-03	(3.02E-04)	27.25	117.19	2.43E+01	4.18	-1.84E-01	-0.76
PPy/A (2B)	9.23E-03	(1.64E-03)	22.46	68.95	2.38E+01	8.37	-2.49E-01	-1.05
PPy/A (6)	9.96E-03	(1.27E-03)	21.90	58.59	2.53E+01	8.37	-3.15E-01	-1.24
PPy/A (5)	6.47E-03	(3.02E-04)	21.82	78.13	2.91E+01	12.55	-3.60E-01	-1.24
PPy/A (3)	1.80E-02	(2.52E-03)	26.38	44.49	2.23E+01	12.55	-3.59E-01	-1.61
PPy/A (4B)	1.12E-02	(1.95E-03)	20.13	44.28	2.74E+01	12.55	-3.39E-01	-1.24
PPy/A (5)	6.47E-03	(3.02E-04)	22.42	92.86	2.52E+01	16.70	-3.75E-01	-1.49
PPy/A (3)	1.80E-02	(2.52E-03)	28.41	49.95	2.14E+01	16.70	-3.86E-01	-1.81
PPy/A (4B)	1.12E-02	(1.95E-03)	21.76	48.90	2.68E+01	25.02	-4.07E-01	-1.52
PPy/A (4B)	1.12E-02	(1.95E-03)	21.95	48.92	2.70E+01	37.65	-4.09E-01	-1.51
PPy/A (2B)	9.23E-03	(1.64E-03)	20.85	73.92	2.06E+01	37.65	-4.05E-01	-1.96

Table R3 Experimental data of electrical conductivity response study of PPy/B toward acetone vapor at various concentrations in N₂, 1 atm and at 23-25 °C.

Material	Thickness (cm)	Applied current (mA)	Voltage drop (mV)	σ (S/cm)	Acetone exposure		
					Acetone vapor conc. (vol.%)	$\Delta\sigma$ (S/cm)	$\Delta\sigma/\sigma_i \times 100$ (%)
PPy/B (1)	8.96E-03 (1.55E-03)	N/A	N/A	3.52E+01 (1.1E-02)	0.25	-3.43E-02	-0.13
PPy/B (2)	8.25E-03 (5.40E-03)	N/A	N/A	2.82E+01 (7.9E-03)	0.25	-2.99E-02	-0.11
PPy/B (1)	8.96E-03 (1.55E-03)	N/A	N/A	3.42E+01 (4.3E-03)	0.33	-3.42E-02	-0.10
PPy/B (3A)	1.02E-02 (1.16E-02)	19.50	36.33	3.56E+01	0.33	-3.48E-02	-0.10
PPy/B (1)	8.96E-03 (1.55E-03)	N/A	N/A	3.43E+01 (2.0E-02)	1.05	-3.23E-02	-0.10
PPy/B (2)	8.25E-03 (5.40E-03)	N/A	N/A	2.93E+01 (2.1E-03)	1.05	-3.21E-02	-0.11
PPy/B (3B)	8.92E-03 (7.28E-03)	14.60	33.63	3.28E+01	3.33	-8.53E-02	-0.26
PPy/B (4A)	7.92E-03 (1.24E-03)	N/A	N/A	2.62E+01 (1.3E-01)	8.37	-1.45E-01	-0.55
PPy/B (4B)	8.42E-03 (4.26E-03)	N/A	N/A	2.68E+01 (1.7E-01)	8.37	-1.52E-01	-0.57
PPy/B (5)	1.52E-02 (2.37E-03)	16.81	25.06	2.97E+01	12.55	-1.68E-01	-0.57
PPy/B (1)	8.96E-03 (1.55E-03)	N/A	N/A	2.88E+01 (4.0E-03)	16.65	-1.99E-01	-0.69
PPy/B (5)	1.52E-02 (2.37E-03)	16.85	23.68	3.15E+01	16.65	-1.91E-01	-0.61
PPy/B (5)	1.52E-02 (2.37E-03)	16.90	25.62	2.92E+01	25.02	-2.10E-01	-0.72
PPy/B (3A)	1.02E-02 (1.16E-02)	18.86	35.40	3.54E+01	37.65	-1.90E-01	-0.75

Table R4 Experimental data of electrical conductivity response study of PPy/AB toward acetone vapor at various concentrations in N₂, 1 atm and at 23-25 °C.

Material	Thickness (cm)	Applied current (mA)	Voltage drop (mV)	σ (S/cm)	Acetone exposure		
					Acetone vapor conc. (vol.%)	$\Delta\sigma$ (S/cm)	$\Delta\sigma/\sigma_i \times 100$ (%)
PPy/AB (1A)	7.71E-03 (5.30E-03)	0.0241	1869.0	1.13E-03	0.17	-1.05E-18	0.00
PPy/AB (1A)	7.71E-03 (5.30E-03)	0.0237	1926.0	1.07E-03	0.33	-4.65E-05	-4.33
PPy/AB (1B)	7.41E-03 (5.93E-03)	0.0723	3100.0	2.12E-03	0.33	-3.42E-05	-1.61
PPy/AB (1A)	7.71E-03 (5.30E-03)	0.0227	1875.0	1.06E-03	0.83	-1.04E-04	-9.80
PPy/AB (1B)	7.41E-03 (5.93E-03)	0.0691	3250.0	1.94E-03	1.65	-1.25E-04	-6.48
PPy/AB (2A)	9.10E-03 (1.04E-02)	0.0610	2637.5	1.71E-03	1.65	-2.24E-04	-13.05
PPy/AB (1B)	7.41E-03 (5.93E-03)	0.0637	3115.0	1.86E-03	3.33	-2.40E-04	-12.88
PPy/AB (2A)	9.10E-03 (1.04E-02)	0.0630	3025.0	1.54E-03	3.33	-3.00E-04	-19.43
PPy/AB (1A)	7.71E-03 (5.30E-03)	0.0273	2260.0	1.06E-03	8.37	-2.83E-04	-26.72
PPy/AB (2B)	9.21E-03 (2.99E-03)	0.0494	3013.0	1.20E-03	16.60	-3.00E-04	-24.99
PPy/AB (1A)	7.71E-03 (5.30E-03)	0.0233	1910.0	1.07E-03	37.65	-2.66E-04	-24.91

Appendix S Comparison of Electrical Responses of PPy/A5 in Chapter IV and PPy/A in Chapter V

As referred in the introduction part of Chapter V, the electrical responses of PPy/A in Chapter V ($D/M = 1/12$) toward toluene, acetone, and acetic acid are similar to those of PPy/A in Chapter IV ($D/M = 1/5$), whereas their electrical responses toward water are different. Note that PPy/A, which has a higher moisture content, shows a smaller response to water than PPy/A5.

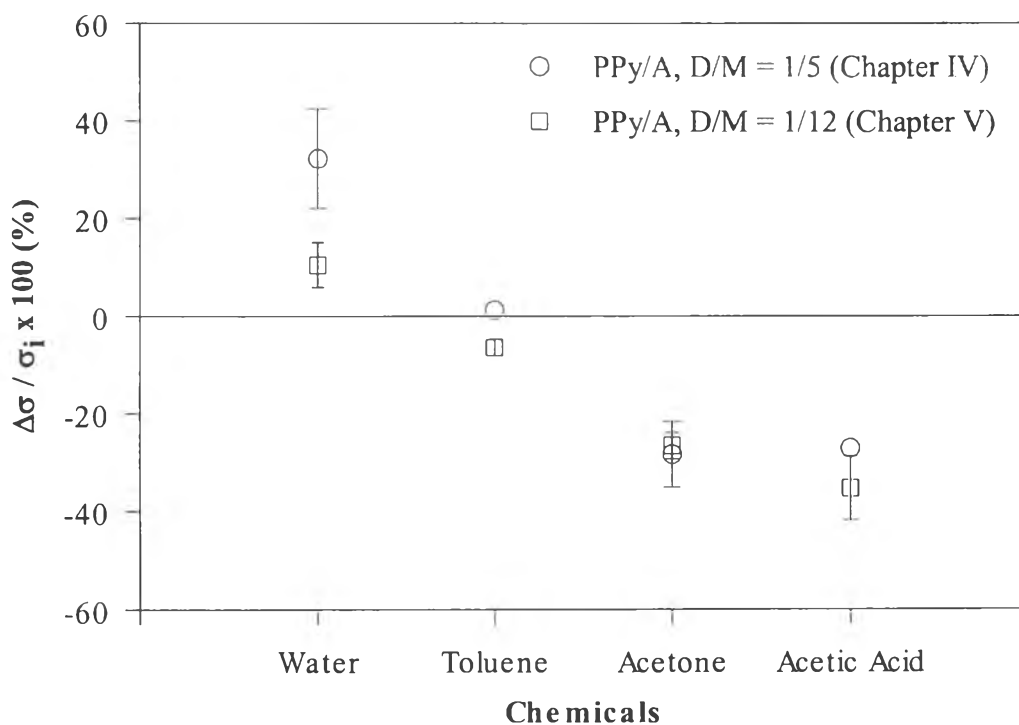


Figure S1 Comparison of electrical responses of: (O) PPy/A5 in Chapter IV and (□) PPy/A in Chapter V upon exposures to chemical liquids.

Appendix T Effect of Acetone Exposures on Charge Carrier Species of PPy

Upon exposure to the saturated acetone vapor, the absorbance peak in the visible spectrum of PPy/B film cast from m-cresol solution evidently decreased in magnitude, as shown in Figure T1. This corresponds to the change observed by Blackwood and Josowicz (1991) upon methanol vapor exposure. It was claimed to be the reduction in polaron and bipolaron species in the PPy/TCNQ film because methanol acts as a reducing agent toward PPy. The same reason is also applicable for the acetone exposure. In addition, suggesting acetone as a reducing agent corresponds to the fact that acetone reduces the conductivity of PPy. The decreases in bipolaron were found to be more dominant than those of polaron, as clarified in Table T1. There was no significant change in the transition energies observed.

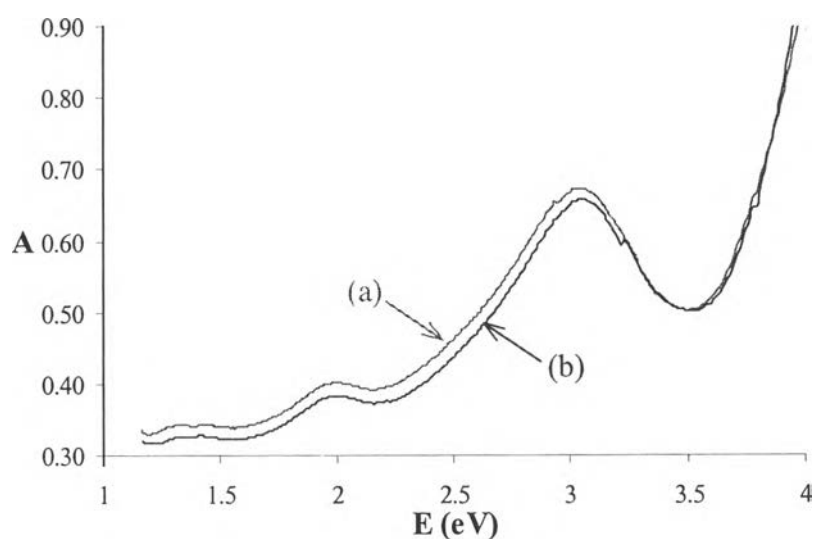


Figure T1 The visible spectra of a) the fresh PPy/B film, and b) the same film upon exposure to saturated acetone vapor.

Table T1 Transition energies in the fresh PPy/B film and the film under saturated acetone vapor.

Sample \ Transition	ω_3 or ω'_3		ω'_4		ω''_1		ω''_3	
	(eV)	(%)	(eV)	(%)	(eV)	(%)	(eV)	(%)
Fresh PPy/B (1)	3.04	67.6	1.97	10.2	1.40	2.8	2.52	19.3
	(0.01)	(2.77)	(0.00)	(0.44)	(0.00)	(0.21)	(0.02)	(3.06)
PPy/B (1) in saturate acetone vapor	3.06	75.5	1.98	7.5	1.41	0.5	2.53	16.5
	(0.01)	(0.36)	(0.00)	(0.19)	(0.00)	(0.00)	(0.03)	(0.16)
% Change in energy (1)	0.47	-	0.29	-	0.36	-	0.31	-
% Change in percentage (1)	-	11.62	-	-26.74	-	-82.15	-	-14.48
Fresh PPy/B (2)	3.04	69.0	1.98	11.7	1.37	2.1	2.52	17.2
	(0.00)	(0.22)	(0.00)	(0.08)	(0.00)	(0.09)	(0.00)	(0.34)
PPy/B (2) in saturate acetone vapor	3.07	75.6	1.99	7.0	1.43	0.1	2.54	17.3
	(0.00)	(0.69)	(0.00)	(0.37)	(0.01)	(0.01)	(0.01)	(1.08)
% Change in energy (2)	0.75	-	0.13	-	4.24	-	0.52	-
% Change in percentage (2)	-	9.53	-	-40.15	-	-95.01	-	0.38

Appendix U Effect of Chemical Exposures on Chemical Structure of PPy

Figures U1a – f show X-ray photoelectron spectrum of the fresh PPy/A at D/M ratio of 1/12 and the ones treated with chemical vapors. The changes caused by the chemicals are described in Chapter IV.

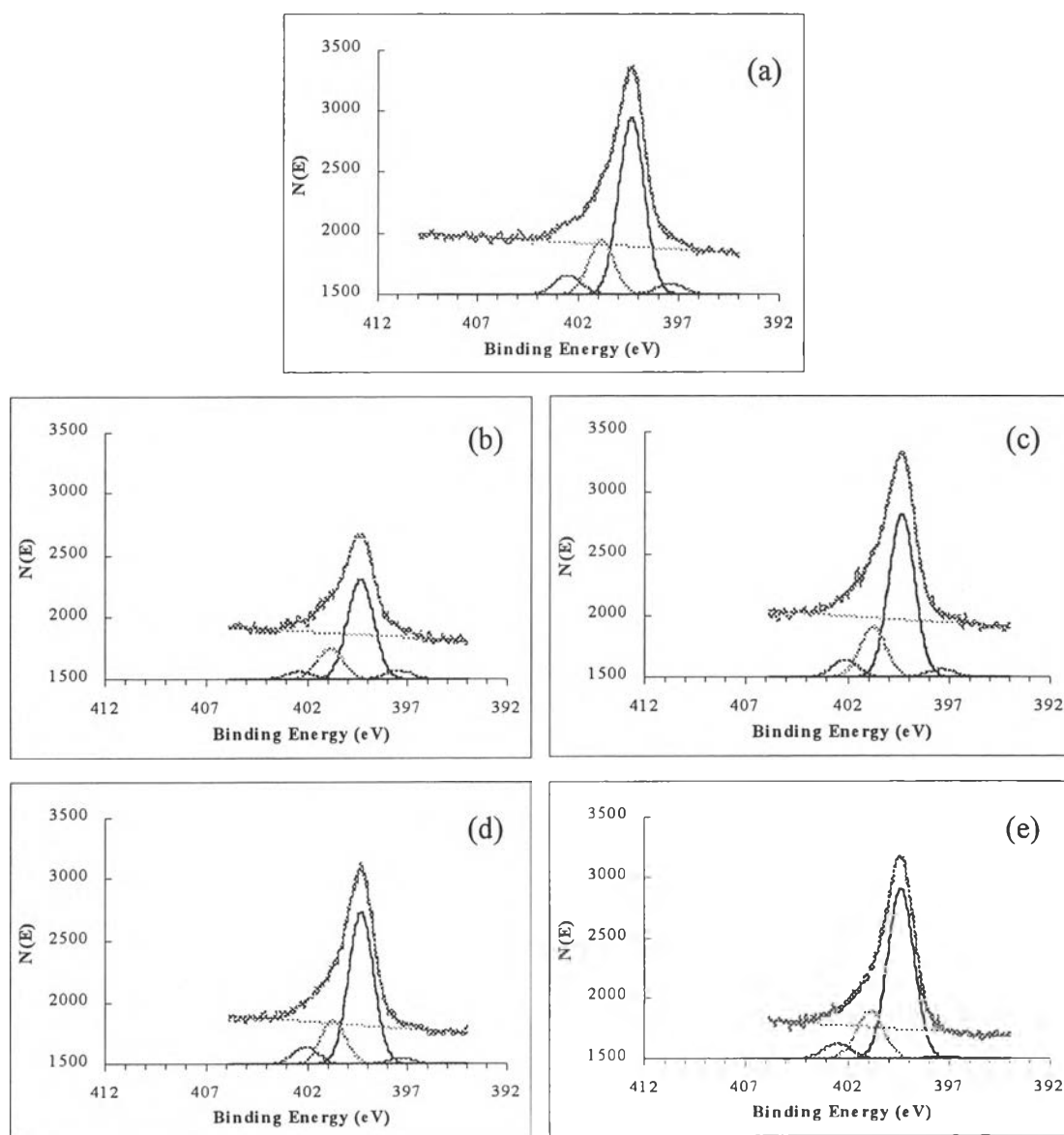


Figure U1 XPS spectra with deconvoluted results of the pellets of: a) fresh PPy/A; b) PPy/A after exposure to saturated water vapor; c) PPy/A after exposure to saturated toluene vapor; d) PPy/A after exposure to saturated acetone vapor; and e) PPy/A after exposure to saturated acetic acid vapor.

Table U1 FWHM, percentages of =N-, -NH-, -NH⁺-, and =NH⁺- of the fresh PPy/A at D/M of 1/12 and the ones treaded with saturated chemical vapors, and the percentage of change as compared with the fresh PPy/A.

Material	FWHM (eV)	% -N= (imine-like N)	% -NH- (neutral N)	% -NH ⁺ - (polaron)	% =NH ⁺ - (bipolaron)
Fresh PPy/A (1)	1.47	4.07	67.67	20.80	7.46
Fresh PPy/A (2)	1.50	3.01	69.78	20.55	6.66
Fresh PPy/A (3)	1.44	4.11	68.20	21.05	6.64
Average	1.47	3.73	68.55	20.80	6.92
SD	(0.03)	(0.63)	(1.10)	(0.25)	(0.47)
Water-treated PPy/A (4)	1.51	5.74	67.97	20.87	5.42
Water-treated PPy/A (5)	1.51	5.84	67.92	20.89	5.36
Average	1.51	5.79	67.95	20.88	5.39
SD	(0.01)	(0.07)	(0.04)	(0.01)	(0.05)
% Change	2.57	55.11	-0.88	0.36	-22.10
Toluene-treated PPy/A (6)	1.49	3.41	69.89	19.81	6.89
Toluene-treated PPy/A (7)	1.48	3.31	69.23	20.92	6.54
Average	1.49	3.36	69.56	20.37	6.71
SD	(0.01)	(0.07)	(0.47)	(0.79)	(0.25)
% Change	0.94	-9.90	1.47	-2.09	-2.97
Acetone-treated PPy/A (8)	1.47	2.95	70.67	19.82	6.56
Acetone-treated PPy/A (9)	1.47	2.83	70.40	21.23	5.54
Average	1.47	2.89	70.53	20.52	6.05
SD	(0.00)	(0.08)	(0.19)	(1.00)	(0.73)
% Change	-0.06	-22.47	2.90	-1.34	-12.55
Acetic acid-treated PPy/A (10)	1.48	1.48	72.87	19.55	6.10
Acetic acid-treated PPy/A (11)	1.49	0.85	72.52	20.36	6.27
Average	1.49	1.16	72.70	19.95	6.19
SD	(0.01)	(0.45)	(0.25)	(0.57)	(0.12)
% Change	1.01	-68.80	6.05	-4.08	-10.60

Appendix V Effect of Chemical Exposures on Order Aggregation in PPy

Figures VIa– f show XRD patterns of the fresh PPy/A at D/M ratio of 1/12 and the ones treated with chemical vapors. Note that the effect of toluene was not studied due to the null electrical response of PPy/A to toluene and its toxicity.

Due to H^+ abstraction at $-NH-$ of pyrrole ring by the water molecule, as discussed in Chapter IV, intensities of line-broadenings #2 (Py–Py order aggregation connected by single bond) and #3 (Py–Py order aggregation connected by double bond) decrease, corresponding to an increment in $-N=$ species (see Appendix U). At the same time, line-broadenings #4 and #5 (van der Waals–induced order aggregation) increase in intensity. This could be explained by the reduction in amount of charge from H^+ abstraction which enhances van der Waals force.

Effect of an acetone exposure on order aggregation are discussed in Chapter III. Note that a decrease in area of the line-broadening #3 and an increase in area of the line-broadening #2 corresponds to an increase in the neutral form of PPy ($-NH-$) as observed by XPS (see Appendix U).

Upon exposure to saturated acetic acid vapor, the line-broadening #5 of PPy/A tremendously increases in intensity. Protonation caused by acetic acid, as revealed by XPS, reduces order aggregations extensively.

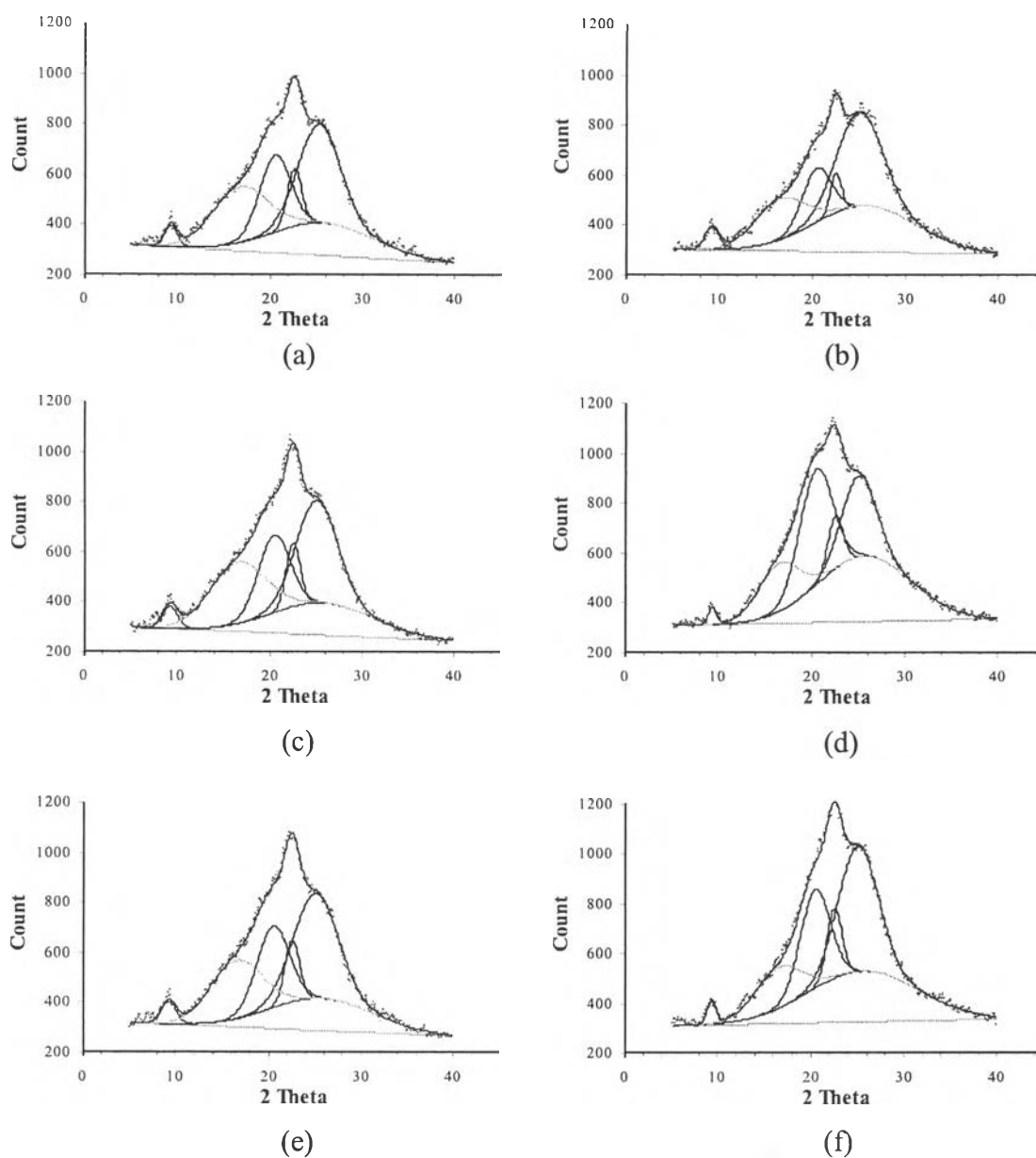


Figure V1 XRD patterns with deconvoluted results of: a) the fresh PPy/A pellet; b) the same pellet after exposure to saturated water vapor; c) the fresh PPy/A pellet; d) the same pellet after exposure to saturated acetone vapor; e) the fresh PPy/A pellet; and f) the same pellet after exposure to saturated acetic acid vapor.

Table V1 Diffraction peaks (2θ), d-spacing (D), order aggregation extent (t), and area of diffraction peaks of the fresh PPy/A at D/M of 1/12 and the ones treated with saturated chemical vapors, and the percentage of change in area as compared with XRD patterns of the fresh PPy/A (see the line-broadening assignments in Appendix E).

Material	Line-broadening #1					Line-broadening #2				
	2θ (deg.)	D (Å)	t (Å)	Area (count)	% Change	2θ (deg.)	D (Å)	t (Å)	Area (count)	% Change
Air	16.6 (0.1)	5.3 (0.0)	24.1 (0.9)	1.7E+03 (1.3E+02)	0.0	20.5 (0.0)	4.3 (0.0)	41.1 (1.0)	1.3E+03 (7.0E+01)	0.0
Water	17.0 (0.7)	5.2 (0.2)	28.0 (0.0)	1.3E+03 (3.2E+02)	-24.9	20.6 (0.3)	4.3 (0.1)	39.8 (0.0)	8.2E+02 (9.8E+01)	-39.2
Acetone	16.3 (0.5)	5.4 (0.2)	27.9 (0.0)	9.7E+02 (1.2E+02)	-42.1	20.5 (0.0)	4.3 (0.0)	39.8 (0.0)	2.0E+03 (3.6E+02)	49.6
Acetic Acid	17.3 (1.1)	5.1 (0.3)	28.0 (0.0)	1.3E+03 (3.5E+02)	-23.6	20.8 (0.5)	4.3 (0.1)	39.8 (0.0)	1.6E+03 (2.9E+01)	19.4

Material	Line-broadening #3					Line-broadening #4				
	2θ (deg.)	D (Å)	t (Å)	Area (count)	% Change	2θ (deg.)	D (Å)	t (Å)	Area (count)	% Change
Air	22.6 (0.0)	3.9 (0.0)	90.4 (1.4)	4.7E+02 (2.3E+01)	0.0	25.1 (0.1)	3.5 (0.0)	30.7 (1.1)	2.3E+03 (1.6E+02)	0.0
Water	22.6 (0.1)	3.9 (0.0)	88.6 (0.0)	3.7E+02 (1.7E+02)	-21.8	25.4 (0.3)	3.5 (0.0)	35.4 (0.0)	2.5E+03 (4.0E+02)	6.4
Acetone	22.5 (0.1)	3.9 (0.0)	88.6 (0.0)	3.0E+02 (9.4E+01)	-36.0	25.1 (0.2)	3.5 (0.0)	35.4 (0.0)	1.9E+03 (5.3E+02)	-16.6
Acetic Acid	22.6 (0.1)	3.9 (0.0)	88.6 (0.0)	4.7E+02 (1.2E+02)	1.6	25.3 (0.2)	3.5 (0.0)	35.4 (0.0)	2.7E+03 (2.9E+01)	15.0

Material	Line-broadening #5				
	2θ (deg.)	D (Å)	t (Å)	Area (count)	% Change
Air	25.7 (0.0)	3.5 (0.0)	13.0 (0.1)	1.8E+03 (1.8E+01)	0.0
Water	25.8 (0.3)	3.4 (0.0)	12.4 (1.2)	2.3E+03 (4.3E+02)	28.0
Acetone	26.6 (1.2)	3.4 (0.1)	11.5 (2.7)	3.3E+03 (8.3E+02)	88.2
Acetic Acid	26.5 (1.1)	3.4 (0.1)	10.4 (2.3)	3.5E+03 (7.3E+02)	100.8

Appendix W Determination of the Surface Degradation of PPy/A by an X-ray Photoelectron Spectroscopy

Table W1 Deconvoluted results from XP spectra of C 1s in PPy/A at different accumulated X-ray exposure times.

Accumulated X-ray exposure time (min)	C 1s									
	C/N	FWHM ³	C hydrocarbon [†]		C-OH & H ₂ O [§]		C=O [°]		π - π^*	
			BE [‡] (eV)	C / N	BE (eV)	C / N	BE (eV)	C / N	BE (eV)	π - π^* / N
150	7.87	1.9	284.02	5.49	286.25	1.48	288.08	0.65	290.15	0.25
150	7.71	1.9	284.06	5.56	286.25	1.33	288.08	0.59	290.32	0.23
450	9.25	1.9	284.38	7.64	286.38	1.06	288.27	0.44	290.23	0.12
450	8.31	1.9	284.28	6.65	286.39	1.07	288.27	0.44	290.24	0.15
600	7.76	1.9	284.28	6.08	286.13	1.05	288.00	0.45	290.28	0.17
750	7.69	1.9	284.28	6.05	286.12	1.03	287.98	0.44	290.19	0.16
900	7.74	1.9	284.28	6.10	286.12	1.03	287.98	0.44	290.20	0.16
1050	7.75	1.9	284.28	6.12	286.14	1.03	288.00	0.44	290.23	0.16
1150	7.79	1.9	284.28	6.15	286.13	1.03	287.98	0.45	290.20	0.17
1150	7.79	1.8	284.28	6.15	286.21	1.03	287.98	0.45	290.20	0.17
1500	8.51	1.8	284.31	6.90	286.23	1.03	288.15	0.42	290.27	0.16
1500	8.51	1.8	284.31	6.90	286.23	1.03	288.15	0.42	290.27	0.16
1500	8.30	1.8	284.31	6.73	286.23	1.00	288.15	0.41	290.27	0.16
1800	7.40	1.8	284.31	6.00	286.00	0.83	287.60	0.39	289.37	0.19
1800	7.40	1.8	284.31	6.00	286.00	0.83	287.60	0.39	289.37	0.19
1800	7.29	1.8	284.31	5.91	286.00	0.81	287.60	0.38	289.37	0.19
2100	9.29	1.8	284.38	7.77	286.25	0.97	288.08	0.38	290.15	0.16
2400	9.10	1.8	284.39	7.60	286.38	0.96	288.30	0.36	290.29	0.18
2400	9.00	1.8	284.39	7.51	286.38	0.95	288.30	0.35	290.29	0.18
2550	10.18	1.8	284.38	8.51	286.22	1.07	288.04	0.42	290.15	0.18
2550	10.18	1.8	284.38	8.51	286.22	1.07	288.04	0.42	290.15	0.18
2850	8.80	1.8	284.62	7.22	286.24	0.98	288.04	0.45	290.20	0.15

³ Full width at half-maximum, FWHM

[†] C α and C β of pyrrole rings and contaminant hydrocarbon

[‡] Binding energy, BE

[§] Excluding C of dopant, C at polaron, and C=N-

[°] Excluding C at bipolaron

Table W2 Deconvoluted results from XP spectra of N 1s in PPy/A at different accumulated X-ray exposure times.

Accumulated X-ray exposure time (min)	N 1s									
	C/N	FWHM	=N-		-NH-		-NH ⁺ - (polaron)		=NH ⁺ - (bipolaron)	
			BE (eV)	=N-/N	BE (eV)	-NH-/N	BE (eV)	-NH ⁺ /N	BE (eV)	=NH ⁺ /N
150	1.00	1.5	397.32	0.02	399.32	0.74	400.83	0.20	402.43	0.04
150	1.00	1.5	397.33	0.02	399.33	0.74	400.84	0.19	402.44	0.05
450	1.00	1.5	397.42	0.04	399.42	0.73	400.93	0.19	402.53	0.04
450	1.00	1.5	397.42	0.02	399.42	0.73	400.93	0.19	402.53	0.06
600	1.00	1.5	397.47	0.04	399.47	0.74	400.98	0.19	402.58	0.03
750	1.00	1.5	397.47	0.04	399.47	0.73	400.98	0.19	402.58	0.04
900	1.00	1.6	397.47	0.04	399.47	0.73	400.98	0.18	402.58	0.04
1050	1.00	1.5	397.47	0.04	399.47	0.74	400.98	0.18	402.58	0.04
1150	1.00	1.5	397.47	0.04	399.47	0.74	400.98	0.18	402.58	0.04
1150	1.00	1.4	397.47	0.04	399.47	0.74	400.98	0.18	402.58	0.04
1500	1.00	1.5	397.77	0.07	399.48	0.74	400.99	0.16	402.59	0.03
1500	1.00	1.5	397.77	0.07	399.48	0.74	400.99	0.16	402.59	0.03
1500	1.00	1.5	397.47	0.06	399.47	0.74	400.98	0.15	402.58	0.05
1800	1.00	1.5	397.92	0.08	399.52	0.75	401.03	0.14	402.63	0.03
1800	1.00	1.5	397.93	0.08	399.52	0.76	401.03	0.14	402.63	0.02
1800	1.00	1.6	397.50	0.06	399.50	0.77	401.01	0.13	402.61	0.04
2100	1.00	1.6	398.00	0.10	399.57	0.75	401.08	0.12	402.68	0.03
2400	1.00	1.5	397.82	0.09	399.56	0.75	401.07	0.13	402.67	0.03
2400	1.00	1.6	397.55	0.08	399.55	0.77	401.06	0.12	402.66	0.03
2550	1.00	1.5	397.69	0.08	399.53	0.76	401.04	0.13	402.64	0.03
2550	1.00	1.5	397.69	0.08	399.53	0.76	401.04	0.13	402.64	0.03
2850	1.00	1.6	397.75	0.08	399.75	0.76	401.26	0.11	402.86	0.05

Table W3 Deconvoluted results from XP spectra of O 1s and S 2p in PPy/A at different accumulated X-ray exposure times.

Accumulated X-ray exposure time (min)	O 1s						S 2p					
	O/N	FWHM (eV)	O=C		O-H		S/N	FWHM (eV)	S IV		S VI	
			BE (eV)	O=C/N	BE (eV)	O-H/N			BE (eV)	S IV/N	BE (eV)	S VI/N
150	1.76	2.1	530.90	1.28	532.90	0.48	0.26	1.45	166.29	0.18	167.58	0.08
150	1.62	2.2	530.91	1.17	532.83	0.45	0.26	1.54	166.35	0.19	167.71	0.07
450	1.79	2.3	531.20	1.26	533.03	0.54	0.21	1.44	166.46	0.15	167.77	0.07
450	1.59	2.3	531.15	1.14	533.00	0.45	0.25	1.52	166.55	0.19	168.10	0.06
600	1.39	2.3	531.19	1.07	533.15	0.32	0.21	1.33	166.49	0.15	167.86	0.06
750	1.38	2.3	531.19	1.07	533.13	0.31	0.21	1.41	166.48	0.15	167.77	0.06
900	1.38	2.3	531.18	1.07	533.14	0.31	0.21	1.44	166.50	0.15	167.74	0.06
1050	1.39	2.3	531.18	1.08	533.16	0.31	0.21	1.39	166.50	0.14	167.70	0.06
1150	1.39	2.2	531.18	1.07	533.15	0.31	0.21	1.42	166.45	0.14	167.66	0.07
1150	1.39	2.1	531.18	1.07	533.15	0.31	0.21	1.40	166.46	0.14	167.68	0.07
1500	1.28	2.1	531.09	0.93	532.94	0.35	0.18	1.38	166.62	0.15	168.00	0.02
1500	1.28	2.1	531.09	0.93	532.94	0.35	0.18	1.37	166.55	0.14	167.72	0.04
1500	1.25	2.1	531.09	0.91	532.94	0.35	0.17	1.40	166.62	0.15	168.00	0.02
1800	1.12	2.2	531.19	0.84	533.11	0.28	0.15	1.63	166.50	0.13	168.00	0.02
1800	1.12	2.1	531.19	0.84	533.11	0.28	0.15	1.68	166.50	0.13	168.00	0.03
1800	1.11	2.2	531.19	0.83	533.11	0.27	0.15	1.64	166.50	0.13	168.00	0.02
2100	1.25	2.1	531.24	0.96	533.18	0.29	0.16	1.73	166.54	0.13	167.98	0.03
2400	1.21	2.1	531.19	0.91	533.05	0.30	0.17	1.36	166.44	0.13	167.57	0.04
2400	1.19	2.1	531.19	0.90	533.05	0.30	0.17	1.36	166.44	0.12	167.57	0.04
2550	1.27	2.1	531.20	0.91	532.95	0.36	0.14	1.33	166.60	0.12	167.84	0.02
2550	1.27	2.1	531.20	0.91	532.95	0.36	0.14	1.33	166.62	0.12	168.01	0.02
2850	1.06	2.3	531.47	0.81	533.24	0.26	0.11	1.34	166.73	0.10	168.16	0.02

Table W4 Deconvoluted results from XP spectra of C 1s in PPy/A at different accumulated X-ray exposure times when there was no liquid nitrogen cooling kit used.

Accumulated X-ray exposure time (min)	C 1s									
	C/N	FWHM	C hydrocarbon		C-OH & H ₂ O		C=O		π - π^*	
			BE (eV)	C/N	BE (eV)	C/N	BE (eV)	C/N	BE (eV)	π - π^*/N
150	8.45	1.8	284.23	6.61	286.11	1.14	287.96	0.50	290.24	0.21
150	7.68	1.9	283.85	5.43	285.63	1.39	287.62	0.64	289.77	0.22
150	7.75	1.9	283.85	5.48	285.63	1.40	287.62	0.65	289.77	0.22
300	9.05	1.9	284.23	6.69	285.96	1.45	287.78	0.63	289.78	0.28
300	9.21	1.9	284.23	6.81	285.96	1.48	287.78	0.64	289.78	0.28
300	7.87	1.9	283.94	5.76	285.72	1.28	287.60	0.60	289.69	0.23
300	8.04	1.9	283.94	5.88	285.72	1.31	287.60	0.61	289.69	0.23
450	8.29	1.8	284.28	6.38	286.10	1.26	288.05	0.48	290.17	0.17
450	8.74	1.8	284.28	6.72	286.10	1.33	288.05	0.51	290.17	0.18
450	7.71	1.9	283.98	5.76	285.82	1.21	287.75	0.53	289.84	0.20
450	7.87	1.9	283.98	5.88	285.82	1.24	287.75	0.54	289.84	0.21
600	8.95	1.9	284.30	7.03	286.22	1.26	288.25	0.49	290.59	0.17
600	7.87	1.9	284.01	5.99	285.85	1.16	287.76	0.52	289.99	0.19
600	8.04	1.9	284.01	6.12	285.85	1.19	287.76	0.54	289.99	0.20
750	8.02	1.9	284.02	6.18	285.88	1.12	287.76	0.51	289.86	0.20
750	8.17	1.9	284.02	6.29	285.88	1.14	287.76	0.52	289.86	0.21
750	8.02	1.9	284.02	6.18	285.88	1.12	287.76	0.51	289.86	0.20
900	10.21	1.8	284.40	8.14	286.22	1.33	288.09	0.54	289.99	0.20
900	10.21	1.8	284.40	8.14	286.22	1.33	288.09	0.54	289.99	0.20
900	10.59	1.8	284.40	8.44	286.22	1.38	288.09	0.56	289.99	0.21
900	10.59	1.8	284.40	8.44	286.22	1.38	288.09	0.56	289.99	0.21
900	8.23	1.9	284.05	6.46	285.96	1.09	287.79	0.49	289.92	0.20
1050	11.01	1.8	284.41	8.94	286.32	1.34	288.26	0.55	290.25	0.18
1050	10.62	1.8	284.41	8.63	286.32	1.29	288.26	0.53	290.25	0.18

Table W5 Deconvoluted results from XP spectra of N 1s in PPy/A at different accumulated X-ray exposure times when there was no liquid nitrogen cooling kit used.

Accumulated X-ray exposure time (min)	N 1s									
	C/N	FWHM	=N-		-NH-		-NH ⁺ - (polaron)		=NH ⁺ - (bipolaron)	
			BE (eV)	=N-/N	BE (eV)	-NH-/N	BE (eV)	-NH ⁺ /N	BE (eV)	=NH ⁺ /N
150	1.00	1.5	397.42	0.01	399.42	0.77	400.93	0.17	402.50	0.05
150	1.00	1.5	397.08	0.03	399.08	0.70	400.59	0.20	402.19	0.07
150	1.00	1.5	397.10	0.03	399.07	0.69	400.51	0.20	402.01	0.08
300	1.00	1.4	397.38	0.04	399.38	0.70	400.89	0.20	402.49	0.06
300	1.00	1.4	397.34	0.04	399.35	0.69	400.74	0.20	402.12	0.07
300	1.00	1.5	397.15	0.03	399.15	0.73	400.66	0.18	402.26	0.06
300	1.00	1.4	397.49	0.04	399.10	0.67	400.36	0.21	401.88	0.08
450	1.00	1.5	397.38	0.05	399.38	0.69	400.89	0.19	402.49	0.07
450	1.00	1.3	397.79	0.05	399.36	0.66	400.69	0.21	402.33	0.08
450	1.00	1.5	397.18	0.04	399.18	0.72	400.69	0.19	402.29	0.06
450	1.00	1.4	397.44	0.04	399.14	0.67	400.43	0.21	401.91	0.08
600	1.00	1.5	397.41	0.04	399.41	0.70	400.92	0.19	402.52	0.06
600	1.00	1.5	397.21	0.03	399.21	0.74	400.72	0.17	402.32	0.05
600	1.00	1.4	397.70	0.04	399.18	0.68	400.45	0.20	401.99	0.07
750	1.00	1.5	397.25	0.04	399.25	0.76	400.76	0.15	402.36	0.05
750	1.00	1.4	397.48	0.04	399.20	0.70	400.44	0.18	401.97	0.07
750	1.00	1.5	397.25	0.04	399.25	0.76	400.76	0.15	402.36	0.05
900	1.00	1.5	397.50	0.04	399.50	0.74	401.01	0.18	402.61	0.05
900	1.00	1.5	397.50	0.04	399.50	0.74	401.01	0.18	402.61	0.05
900	1.00	1.4	397.76	0.04	399.47	0.71	400.77	0.19	402.18	0.06
900	1.00	1.4	397.76	0.04	399.47	0.71	400.77	0.19	402.18	0.06
900	1.00	1.4	397.77	0.05	399.19	0.67	400.40	0.21	401.91	0.07
1050	1.00	1.4	397.97	0.04	399.47	0.70	400.68	0.20	402.03	0.06
1050	1.00	1.6	397.52	0.03	399.52	0.76	401.03	0.17	402.63	0.04

Table W6 Deconvoluted results from XP spectra of O 1s and S 2p in PPy/A at different accumulated X-ray exposure times when there was no liquid nitrogen cooling kit used.

Accumulated X-ray exposure time (min)	O 1s						S 2p							
	O/N	FWHM (eV)	O=C		O-H		S/N	FWHM (eV)	S IV		S VI		S new	
			BE (eV)	O=C/N	BE (eV)	O-H/N			BE* (eV)	S IV/N†	BE* (eV)	S VI/N†	BE* (eV)	S _{new} /N†
150	1.64	2.1	531.14	1.27	533.10	0.37	0.29	1.44	166.67	0.19	168.02	0.06	-	0.00
150	1.86	2.2	530.85	1.28	532.73	0.58	0.27	1.52	166.09	0.20	167.46	0.06	-	0.00
150	1.88	2.2	530.85	1.29	532.73	0.59	0.27	1.52	166.09	0.20	167.46	0.06	-	0.00
300	1.98	2.2	531.32	1.40	533.20	0.58	0.31	1.58	166.45	0.21	167.54	0.10	-	0.00
300	2.02	2.2	531.32	1.42	533.20	0.59	0.32	1.58	166.45	0.21	167.54	0.11	-	0.00
300	1.79	2.2	530.93	1.23	532.78	0.56	0.27	1.60	166.20	0.20	167.53	0.06	-	0.00
300	1.83	2.2	530.93	1.26	532.78	0.57	0.27	1.60	166.20	0.21	167.53	0.06	-	0.00
450	1.75	2.2	531.29	1.18	533.04	0.57	0.25	1.23	166.61	0.12	167.59	0.09	165.50	0.05
450	1.84	2.2	531.29	1.24	533.04	0.60	0.26	1.23	166.61	0.12	167.59	0.10	165.50	0.05
450	1.70	2.1	530.96	1.16	532.81	0.54	0.24	1.41	166.43	0.14	167.64	0.05	165.50	0.06
450	1.74	2.1	530.96	1.19	532.81	0.55	0.25	1.41	166.43	0.15	167.64	0.06	165.50	0.06
600	1.79	2.2	531.38	1.26	533.15	0.53	0.24	1.22	166.48	0.13	167.51	0.09	165.50	0.03
600	1.65	2.1	531.00	1.14	532.80	0.51	0.25	1.63	166.54	0.16	167.93	0.04	165.50	0.06
600	1.69	2.1	531.00	1.16	532.80	0.52	0.25	1.63	166.54	0.17	167.93	0.04	165.50	0.06
750	1.63	2.1	531.00	1.11	532.82	0.51	0.23	1.44	166.35	0.14	167.52	0.06	165.50	0.03
750	1.66	2.1	531.00	1.13	532.82	0.52	0.24	1.42	166.31	0.15	167.50	0.06	165.50	0.03
750	1.63	2.1	531.00	1.11	532.82	0.51	0.23	1.42	166.31	0.15	167.50	0.06	165.50	0.03
900	2.01	2.2	531.49	1.36	533.18	0.65	0.26	1.61	166.62	0.18	167.78	0.08	-	0.00
900	2.01	2.2	531.49	1.36	533.18	0.65	0.25	1.32	166.70	0.14	167.77	0.08	165.50	0.04
900	2.08	2.2	531.49	1.41	533.18	0.67	0.27	1.61	166.62	0.19	167.78	0.08	-	0.00
900	2.08	2.2	531.49	1.41	533.18	0.67	0.26	1.32	166.70	0.15	167.77	0.08	165.50	0.04
900	1.62	2.1	531.03	1.14	532.84	0.48	0.24	1.48	166.32	0.18	167.73	0.05	165.50	0.01
1050	2.10	2.3	531.49	1.41	533.13	0.69	0.26	1.57	166.53	0.17	167.73	0.09	-	0.00
1050	2.02	2.3	531.49	1.36	533.13	0.66	0.25	1.44	166.59	0.15	167.75	0.09	165.50	0.02

* Represents BEs of S 2p 1/2; whereas those of 2p 3/2 are ~1.28 eV (SD = 0.6 eV) lower

† Represents areas of S 2p (S 2p 1/2 and 2p 3/2)

CURRICULUM VITAE



Name: Ms. Ladawan Ruangchuay Wannatong

Date of Birth: July 7, 1976

Nationality: Thai

University Education:

1993-1996 Bachelor Degree of Science in Chemistry, Faculty of Science,
King Mongkut's Institute of Technology Thonburi, Thailand

Publications:

1. Prissanaroon, W., Ruangchuay, L., Sirivat, A., and Schwank, J. (2000) Electrical Conductivity Response of Dodecylbenzene Sulfonic Acid-Doped Polypyrrole to SO₂-N₂ Mixtures. Synthetic Metals, 114(1), 65-72.
2. Ruangchuay, L. Schwank, J., and Sirivat, A. (2002) Surface Degradation of α -Naphthalene Sulfonate Doped Polypyrrole during XPS Characterization, Applied Surface Science, in press.
3. Tarachiwin, L., Kiattibutr, P., Ruangchuay, L., Sirivat, A., and Schwank, J. (2002) Electrical Conductivity Response of Polyaniline Films to Ethanol-Water Mixtures. Synthetic Metals, 129(3), 303-308.
4. Kiattibutr, P., Tarachiwin, L., Ruangchuay, L., Sirivat, A., and Schwank, J. (2002) Electrical Conductivity Response of Polyaniline Films to SO₂-N₂ Mixtures: Effect of Dopant Type and Doping Level. Reactive and Functional Polymers, in press.
5. Ruangchuay, L., Sirivat, A., and Schwank, J., Electrical Response of Polypyrrole to Acetone Vapor: Effect of Dopant Anions and Interaction Mechanism, Synthetic Metals, submitted.
6. Ruangchuay, L., Sirivat, A., and Schwank, J., Selectivity Improvement of a Polypyrrole-Based Sensor for Flammable Chemicals in Lacquer, Talanta, submitted.
7. Ruangchuay, L., Sirivat, A., and Schwank, J., Polypyrrole/Poly(Methyl Methacrylate) Blend as Selective Sensor for Acetone in Lacquer, Talanta, submitted.

Proceedings:

1. Effect of Dopants on Acetone Vapor Response of Polypyrroles, the 1st Thailand Materials Science and Technology Conference, Bangkok, Thailand, July 2000.
2. Effect of Dopant Anions on Acetone Vapor Response of Polypyrroles, the 221st ACS National Meeting, San Diego, California, USA, Apr 2001.
3. Selectivity Improvement for Flammable Chemical Sensor based on Polypyrrole, the 223rd ACS National Meeting, Orlando, Florida, USA, Apr 2002.

Presentations:

1. The Synthesis and Characterization of Polypyrrole for Chemical Vapor Sensor Application, presented at The Princess Chulabhorn International Science Congress, the Fourth, Bangkok, Thailand, Dec 1999.
2. Effect of Dopants on Acetone Vapor Response of Polypyrroles, presented at The First Thailand Materials Science and Technology Conference, Bangkok, Thailand, July 2000.
3. Effect of Dopants Anions on the Electrical Response of Polypyrroles toward Acetone Vapor, presented at the 26th Congress on Science and Technology of Thailand, Bangkok, Thailand, Oct 2000.
4. Effect of Dopants Anions on Acetone Vapor Response of Polypyrroles, presented at the POLY Millennium 2000, Waikoloa, Hawaii, USA, Dec 2000.
5. Effect of Dopants Anions on Acetone Vapor Response of Polypyrroles, presented at the 221st ACS National Meeting, California, USA, Apr 2001.
6. The Surface Degradation of α -naphthalene Sulfonate Doped Polypyrrole Induced by X-ray Flux in XPS Experiment, presented at the 27th Congress on Science and Technology of Thailand, Songkla, Thailand, Oct 2001.
7. Selectivity Improvement for Flammable Chemical Sensor based on Polypyrrole, presented at the 223rd ACS National Meeting, Orlando, Florida, USA, Apr 2002.
8. Selectivity Improvement of the Sensor based on α -Naphthalene Sulfonate doped Polypyrrole toward Flammable Chemicals in Lacquer, presented at the 28th Congress on Science and Technology of Thailand, Bangkok, Thailand, Oct 2002.